ISSN 1948-0210 (online)

World Journal of *Stem Cells*

World J Stem Cells 2022 December 26; 14(12): 815-867

Published by Baishideng Publishing Group Inc

WJSC

World Journal of Stem Cells

Contents

Monthly Volume 14 Number 12 December 26, 2022

World Journal of Stem Cells

Monthly Volume 14 Number 12 December 26, 2022

Contents

NAME OF JOURNAL
World Journal of Stem Cells

ISSN
ISSN 1948-0210 (online)

LAUNCH DATE
December 31, 2009

FREQUENCY
Monthly

EDITORS-IN-CHIEF
Carlo Ventura, Shengwen Calvin Li

EDITORIAL BOARD MEMBERS
https://www.wjgnet.com/1948-0210/editorialboard.htm

PUBLICATION DATE
December 26, 2022

INSTRUCTIONS TO AUTHORS
https://www.wjgnet.com/bpg/gerinfo/204

GUIDELINES FOR ETHICS DOCUMENTS
https://www.wjgnet.com/bpg/GerInfo/287

GUIDELINES FOR NON-NATIVE SPEAKERS OF ENGLISH
https://www.wjgnet.com/bpg/gerinfo/240

PUBLICATION ETHICS
https://www.wjgnet.com/bpg/GerInfo/288

PUBLICATION MISCONDUCT
https://www.wjgnet.com/bpg/gerinfo/208

ARTICLE PROCESSING CHARGE
https://www.wjgnet.com/bpg/gerinfo/242

STEPS FOR SUBMITTING MANUSCRIPTS
https://www.wjgnet.com/bpg/GerInfo/239

ONLINE SUBMISSION
https://www.f6publishing.com

World Journal of Stem Cells

Submit a Manuscript: https://www.f6publishing.com

World J Stem Cells 2022 December 26; 14(12): 815-821

DOI: 10.4252/wjsc.v14.i12.815

ISSN 1948-0210 (online)

EDITORIAL

Barriers to mesenchymal stromal cells for low back pain

Bao-Gan Peng, Xiu-Jie Yan

Specialty type: Cell and tissue engineering

Provenance and peer review: Unsolicited article; Externally peer reviewed.

Peer-review model: Single blind

Peer-review report's scientific quality classification

Grade A (Excellent): 0
Grade B (Very good): B
Grade C (Good): C, C
Grade D (Fair): 0
Grade E (Poor): 0

P-Reviewer: Galderisi U, Italy; Shen C, China; Tanabe S, Japan

Received: September 27, 2022
Peer-review started: September 27, 2022
First decision: October 24, 2022
Revised: October 30, 2022
Accepted: November 30, 2022
Article in press: November 30, 2022
Published online: December 26, 2022

Bao-Gan Peng, Xiu-Jie Yan, Department of Orthopaedics, The Third Medical Center, General Hospital of the Chinese People's Liberation Army, Beijing 100039, China

Corresponding author: Bao-Gan Peng, MD, PhD, Professor, Department of Orthopaedics, The Third Medical Center, General Hospital of the Chinese People's Liberation Army, No. 69 Yongding Road, Beijing 100039, China. pengbaogan@163.com

Abstract

Intervertebral disc degeneration is the main cause of low back pain. In the past 20 years, the injection of mesenchymal stromal cells (MSCs) into the nucleus pulposus of the degenerative disc has become the main approach for the treatment of low back pain. Despite the progress made in this field, there are still many barriers to overcome. First, intervertebral disc is a highly complex load-bearing composite tissue composed of annulus fibrosus, nucleus pulposus and cartilaginous endplates. Any structural damage will change its overall biomechanical function, thereby causing progressive degeneration of the entire intervertebral disc. Therefore, MSC-based treatment strategies should not only target the degenerated nucleus pulposus but also include degenerated annulus fibrosus or cartilaginous endplates. Second, to date, there has been relatively little research on the basic biology of annulus fibrosus and cartilaginous endplates, although their pathological changes such as annular tears or fissures, Modic changes, or Schmorl's nodes are more commonly associated with low back pain. Given the high complexity of the structure and composition of the annulus fibrosus and cartilaginous endplates, it remains an open question whether any regeneration techniques are available to achieve their restorative regeneration. Finally, due to the harsh microenvironment of the degenerated intervertebral disc, the delivered MSCs die quickly. Taken together, current MSC-based regenerative medicine therapies to regenerate the entire disc complex by targeting the degenerated nucleus pulposus alone are unlikely to be successful.

Key Words: Intervertebral disc degeneration; Low back pain; Mesenchymal stromal cells; Regenerative medicine; Nucleus pulposus; Editorial

Core Tip: Intervertebral disc is a highly complex weight-bearing tissue, and its degeneration is a major cause of low back pain. Current mesenchymal stromal cell-based clinical trials are difficult to succeed because the repair only targets the degenerated nucleus pulposus, and the transplanted cells die rapidly.

Citation: Peng BG, Yan XJ. Barriers to mesenchymal stromal cells for low back pain. *World J Stem Cells* 2022; 14(12): 815-821
URL: https://www.wjgnet.com/1948-0210/full/v14/i12/815.htm
DOI: https://dx.doi.org/10.4252/wjsc.v14.i12.815

INTRODUCTION

Low back pain is extremely common, affecting about 40% of the world's population, and is the most common cause of years lived with a disability[1]. Its main cause is considered to be intervertebral disc degeneration (IDD), a chronic progressive process characterized by the loss of viable cells and the breakdown of the extracellular matrix within the disc, especially in its innermost region, the nucleus pulposus[2]. Therefore, the idea of transplanting living cells from patients or unrelated donors to supplement the nucleus pulposus cell population may be a possible solution to regenerate degenerate disc *in vivo*[3]. Many cell types, such as notochordal cells[4], nucleus pulposus cells[5-7], annulus fibrosus cells[8], chondrocytes[9,10], adult mesenchymal stromal cells (MSCs) from bone marrow[11,12], adipose[13], or umbilical cord[14], embryonic stem cells[15,16], or induced pluripotent stem cells [17-19], have been used for regenerative therapy of degenerate discs. Among these cell types, MSCs, which exist in most stroma tissues, are heterogeneous populations containing pluripotent stem cells, progenitor cells and differentiated cells[20]. They provide an almost unlimited cell source with self-renewal ability and multilineage differentiation potential, and have become the most popular transplanted cells for intervertebral disc regeneration. Recently, various clinical trials have reported the application of MSCs, to repair and regenerate degenerate discs, whether alone or in combination with biomaterial scaffolds or carriers[2,3]. Despite the progress made in the field, much work remains to be done before MSC therapy can become an effective new treatment.

IDD PATHOPHYSIOLOGY

Both physiologically aged disc and pathologically painful disc show decreased signal intensity on magnetic resonance imaging T2-weighted images (black discs). The former is due to the increase in age, the activity of nucleus pulposus cells declines or the number decreases, resulting in the reduction of extracellular matrix, especially proteoglycan synthesis; the latter is the failure of the intervertebral disc structure, showing degenerative changes[21]. Pain provocation tests have demonstrated that painful intervertebral discs are always structurally ruptured[21,22]. Painful degenerative discs are characterized by the formation of vascularized granulation tissue that extends along a tear in the annulus fibrosus or a defective endplate into the nucleus pulposus, with extensive nociceptive innervation[22,23]. Once the disc ruptures, no matter in the annulus fibrosus or the endplate, the mechanical environment of the disc changes immediately, resulting in decompression of the nucleus pulposus and increased annulus fibrosus loading[21]. Different animal models of disc degeneration reveal that annular or endplate disruption inevitably leads to degenerative changes throughout the disc[24]. As the disc gradually degenerates, the nucleus pulposus shrinks and its hydrostatic pressure continues to drop, so more of the mechanical loading is borne by the annulus fibrosus[21]. In this case, attempts at cellular repair either in the annulus fibrosus or in the nucleus pulposus, become impossible, not because the cells are defective, but because their local mechanical environment is altered.

FEASIBILITY OF MSCS FOR IDD

The proteoglycan-rich gelatinous nucleus pulposus is sealed by the annulus fibrosus and cartilaginous endplates. The nucleus pulposus can perform its physiological function only when the annulus fibrosus and cartilaginous endplates are intact. Currently, treatment of IDD using MSCs refers to the delivery of MSCs to the nucleus pulposus region, thereby potentially repopulating the nucleus pulposus cells to repair the damaged disc or at least modulate the degenerative microenvironment[2,3]. Is this treatment strategy feasible? First, we have to make it clear that the disc that needs MSC therapy is a painful disc, not an aging asymptomatic disc. Second, painful discs are always structurally defective, either in the annulus fibrosus or in the cartilaginous endplate. Discs with intact annulus fibrosus and cartilaginous

endplates are always painless. Third, structural defects initiate degeneration of the entire disc including the nucleus pulposus, which is secondary. Even if the proteoglycan synthesis in the nucleus pulposus is increased by MSC injection, the mechanical environment of the nucleus pulposus is not restored because the defect of the annulus fibrosus or cartilaginous endplates is not repaired, and the partially regenerated nucleus pulposus will eventually degenerate further. Therefore, the treatment strategy should not only target the degenerated nucleus pulposus, but also include the defective annulus fibrosus or cartilaginous endplate.

The torn annulus fibrosus heals defectively, possibly because of not only the inability of the sparse cell population to break down the large collagen fiber bundles of the annulus fibrosus and replace them with new ones, but also the poor blood supply[21]. The highly complex structure and composition of the annulus fibrosus endow it with excellent mechanical properties (Figure 1), making it challenging for tissue regeneration[25]. To date, little information is available on the basic cell biology of the annulus fibrosus, particularly regarding the origin of distinct cell populations and their functional roles, as well as phenotypic changes following injury or disease. Whether there are any regenerative techniques that can overcome the high load and harsh disc microenvironment to achieve reparative regeneration of the annulus fibrosus remains an open question[26].

The cartilaginous endplate is a thin layer of hyaline cartilage that is structurally similar to articular cartilage. The research history of articular cartilage repair is much longer than that of intervertebral disc. Many attempts to regenerate cartilage have produced hyaline-like tissue in vitro. In these techniques, a variety of cells are capable of producing large amounts of proteoglycans and type II collagen. However, when tested *in vivo* in large animal models, none of these techniques restored the structure of the collagen network, but instead formed fibrocartilage repair tissue, explaining their functional failure. The lack of progress in cartilage regeneration may be attributed to a limited understanding of the basic biology and biomechanics of articular cartilage[27]. Given the importance of cartilaginous endplates in low back pain and the nutrient supply to the disc, strategies aimed at restoring healthy cartilaginous endplate structures will prove crucial. However, due to the complexity of cartilaginous endplate repair and limited understanding of its cell biology and biomechanics, current treatment strategies have not considered targeting cartilaginous endplates for low back pain.

MECHANISM OF ACTION OF MSCS FOR IDD

It was originally envisioned that delivery of MSCs to the nucleus pulposus region within the degenerative disc will allow the cells to become nucleus pulposus cells under the influence of local signals and to replenish or regenerate the disc. Further research showed that the idea of MSCs as cell replacement therapy was almost entirely incorrect[28]. Several tracing studies involving intra-articular injection of labeled MSCs into rat and rabbit knee joints have shown that the number of cells delivered in the joints decreases rapidly after injection, and cells cannot be detected in the joints after several weeks. Similar to the ischemic microenvironment of the infarcted heart, more than 99% of transplanted bone marrow MSCs cannot survive and die within 4 d after injection[29]. Thus, a large part of MSCs will die or apoptosis soon after transplantation to a degenerate disc.

Without an accurate understanding of the molecular mechanisms underlying the therapeutic effects of MSCs, it is impossible to consider the development of new medicinal products. According to the extensive literature over the past 20 years, 3 main mechanisms of action mediate the beneficial effects of MSCs after transplantation into recipients (Figure 2), including: (1) Paracrine effects through soluble factors and extracellular vesicles (EVs); (2) Mesodermal differentiation; and (3) Efferocytosis[28-30]. In most models tested, MSCs showed low levels of engraftment (usually 3% or less), accompanied by rapid clearance in large populations, but still had positive therapeutic results, which seems to be related to the other two mechanisms. EVs are membrane-enclosed nanoparticles that are capable of delivering biomolecules, including proteins, lipids, and coding and noncoding RNAs, and it is now believed that MSC-derived EVs are the major players that induce biological changes in the target tissues[31]. The best-studied EVs can be classified into exosomes and microvesicles according to their respective sizes, shapes, biogenesis, origins, and composition. Exosomes are small lipid membrane EVs formed by endocytosis, integration, and efflux; they are 30–150 nm in diameter. Mediating cellular communication is the primary role of exosomes, as they can be released by one cell and captured by neighboring cells *via* ligand-receptor or direct binding. MSC research has focused on MSC-derived exosomes (MSC-Exos). MSC-Exos have similar biological functions to MSCs, but are smaller in size, can penetrate biofilms, have low immunogenicity, and can be stored[32,33]. Microvesicles, also known as ectosomes, are heterogeneous membrane-bound vesicles with a diameter of 50-1000 nm that play an important role in cell-cell communication, tissue homeostasis, cell differentiation, and organ development and remodeling. Functionally impaired, apoptotic, or dying MSCs may trigger phagocytosis by resident tissue macrophages, a process known as efferocytosis. This phenomenon is attributed to the polarization of macrophages towards an anti-inflammatory phenotype and the release of soluble mediators such as interleukin-10, indoleamine 2,3-dioxygenase (IDO) and transforming growth factor-β, which ultimately leads to suppression or tolerance of immune effector cells[29,30].

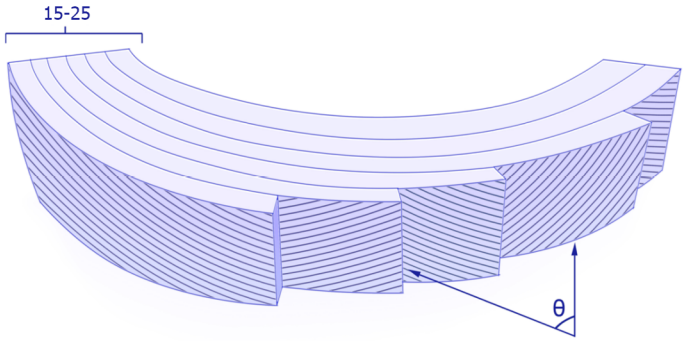

DOI: 10.4252/wjsc.v14.i12.815 **Copyright** ©The Author(s) 2022.

Figure 1 Annulus fibrosus structure. Annulus fibrosus (AF) is composed of 15-25 concentric lamellar layers with oblique collagen fibers in alternating directions lying parallel within each lamella. From the edge of the disc inward through the annulus, the angle-ply fiber orientation (θ) decreases from ± 62° from the vertical axis to ± 45° in a linear manner. From the outer to inner AF regions, glycosaminoglycan increases from 3% to 8% *per* wet weight, while the ratio of type I collagen to type II collagen decreases. The inner AF mainly contains rounded fibrocartilage cells, and the outer AF mainly contains elongated fibroblast-like cells, while other cell types located in or near the AF include peripheral cells, interlamellar cells, and stem/progenitor cells.

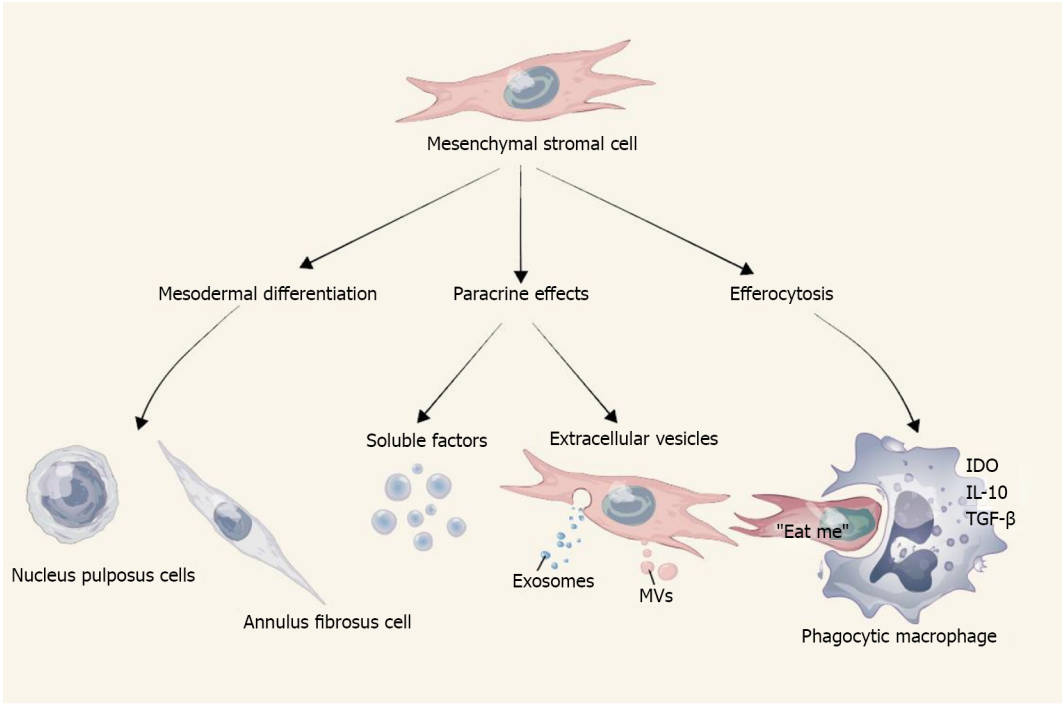

DOI: 10.4252/wjsc.v14.i12.815 **Copyright** ©The Author(s) 2022.

Figure 2 Action mechanisms underlying mesenchymal stromal cell-mediated disc repair. IDO: Indoleamine 2,3-dioxygenase; IL: Interleukin; MVs: Microvesicles; TGF-: Transforming growth factor-beta.

MSC therapies have been a hot topic in clinical trials for more than a generation, and the results of advanced clinical trials have failed to meet the expectations of encouraging preclinical animal data in various disease models[29]. In the field of MSC therapy, there is a contradiction between the effects of MSC manufactured by industrial MSCs and academic centers. Potential variables affecting MSCs based cell therapy include donor variance, *ex vivo* expansion and senescence, immunogenicity and cryopreservation[34]. Culture-expanded human MSCs showed potent immune T-, B-, and dendritic cell-targeted inhibitory properties through the expression of IDO and other effector molecules, many of which were enhanced by interferon (IFN)-γ stimulation[34]. It is now well established that human MSCs licensed with IFN-γ significantly enhance their immunosuppressive properties *in vitro* and that IFN-γ responsiveness *in vivo* is essential for their suppressive function. Because IFN-γ activates otherwise indistinguishable MSCs preparations from normal human donors, the magnitude of the IDO response varies considerably[35]. Patients who receive MSCs from normal volunteers with low IFN-γ response levels may have poorer results than patients who receive donor cells with high IFN-γ response levels. A mechanistically defined, ideal MSCs immunoplastic profile could provide a scientific rationale for the

selection of voluntary donors whose MSCs donation provides maximum veto function and avoids the pitfalls of injecting low-potency products into subjects participating in critical clinical trials[34]. In addition, culture-expanded human MSCs have been shown to experience telomere shortening and other phenotypic alterations that may play a role in modifying their regenerative and immunosuppressive properties[34,36,37].

In many countries, a large number of unregulated clinics provide for-profit services with little or no oversight. These clinics often exaggerate the efficacy, but lack objective evidence[30]. Furthermore, industrial sponsors have led advanced phase III trials for nearly all MSC therapy, and the field as a whole has been heavily criticized for its ill-informed and irrational exuberance. Such criticism often reflects anxiety caused by the heavily predatory commercial activity of unregulated stem cell clinics around the world, leveraging the promise of unproven regenerative therapies, including MSCs, as a panacea[29].

Most clinical trials of MSC therapy for low back pain published now show efficacy, including pain reduction and functional improvement, but insufficient evidence of improvement in disc structure[2]. Injected cells die rapidly due to immune-mediated damage and lack of nutrients and oxygen. The efficacy is likely to be related to the paracrine mechanism of MSCs. However, due to the short half-life of paracrine-produced soluble factors and mediators, the therapeutic effect of MSCs on IDD cannot be long-term or sustained. Intervertebral discs are prone to degeneration due to their avascular nature and low cell density. Human disc repair, including restoring disc height, is unlikely to be faster than in animals. The half-life of proteoglycans in human intervertebral disc is 3-6 years, whereas the half-life of fibrous proteins such as collagen and elastin is over 50 years, reflecting the low rate of matrix synthesis and degradation in this tissue[38]. As mentioned earlier, the development of cell therapy regimens should target both the nucleus pulposus and the annulus fibrosus or cartilaginous endplates, but all cell-based clinical trials to date have focused on the nucleus pulposus, which is clearly flawed in terms of regenerative strategies. Furthermore, all cell treatments are unlikely to be successful until the biomechanical recovery of the degenerative disc[39].

CONCLUSION

The disc is a highly complex load-bearing mechanical device composed of three different cartilage structures, and any structural damage or degeneration of it alters its overall biomechanical function, so the repair strategy cannot only target the degenerated nucleus pulposus. To date, relatively few basic biological studies have been performed on the annulus fibrosus and cartilaginous endplates, although their pathological changes such as annular tears or fissures, Modic changes, or Schmorl's nodes are more commonly associated with low back pain. Taken together, current MSC based regenerative medicine therapies to regenerate the entire disc complex by targeting the degenerated nucleus pulposus alone are unlikely to succeed. The success of disc repair depends on a comprehensive understanding of the basic cellular biology of the disc, and the pathophysiology and biomechanics following disc injury or degeneration, in order to develop more targeted regeneration techniques that anatomically and functionally replicate healthy native tissue.

FOOTNOTES

Author contributions: Peng BG and Yan XJ conceived the idea for the manuscript and reviewed the manuscript; Both authors contributed equally.

Conflict-of-interest statement: All the authors report having no relevant conflicts of interest for this article.

Country/Territory of origin: China

ORCID number: Bao-Gan Peng 0000-0002-7767-9424.

S-Editor: Fan JR
L-Editor: Filipodia
P-Editor: Fan JR

REFERENCES

1 **Vlaeyen JWS**, Maher CG, Wiech K, Van Zundert J, Meloto CB, Diatchenko L, Battié MC, Goossens M, Koes B, Linton SJ. Low back pain. *Nat Rev Dis Primers* 2018; **4**: 52 [PMID: 30546064 DOI: 10.1038/s41572-018-0052-1]

2 **Binch ALA**, Fitzgerald JC, Growney EA, Barry F. Cell-based strategies for IVD repair: clinical progress and translational obstacles. *Nat Rev Rheumatol* 2021; **17**: 158-175 [PMID: 33526926 DOI: 10.1038/s41584-020-00568-w]

3 **Williams RJ**, Tryfonidou MA, Snuggs JW, Le Maitre CL. Cell sources proposed for nucleus pulposus regeneration. *JOR Spine* 2021; **4**: e1175 [PMID: 35005441 DOI: 10.1002/jsp2.1175]

4 **Bach FC**, Tellegen AR, Beukers M, Miranda-Bedate A, Teunissen M, de Jong WAM, de Vries SAH, Creemers LB, Benz K, Meij BP, Ito K, Tryfonidou MA. Biologic canine and human intervertebral disc repair by notochordal cell-derived matrix: from bench towards bedside. *Oncotarget* 2018; **9**: 26507-26526 [PMID: 29899873 DOI: 10.18632/oncotarget.25476]

5 **Huang B**, Zhuang Y, Li CQ, Liu LT, Zhou Y. Regeneration of the intervertebral disc with nucleus pulposus cell-seeded collagen II/hyaluronan/chondroitin-6-sulfate tri-copolymer constructs in a rabbit disc degeneration model. *Spine (Phila Pa 1976)* 2011; **36**: 2252-2259 [PMID: 21358466 DOI: 10.1097/BRS.0b013e318209fd85]

6 **Iwashina T**, Mochida J, Sakai D, Yamamoto Y, Miyazaki T, Ando K, Hotta T. Feasibility of using a human nucleus pulposus cell line as a cell source in cell transplantation therapy for intervertebral disc degeneration. *Spine (Phila Pa 1976)* 2006; **31**: 1177-1186 [PMID: 16688029 DOI: 10.1097/01.brs.0000217687.36874.c4]

7 **Gorensek M**, Jaksimović C, Kregar-Velikonja N, Gorensek M, Knezevic M, Jeras M, Pavlovcic V, Cör A. Nucleus pulposus repair with cultured autologous elastic cartilage derived chondrocytes. *Cell Mol Biol Lett* 2004; **9**: 363-373 [PMID: 15213815]

8 **Gao C**, Ning B, Sang C, Zhang Y. Rapamycin prevents the intervertebral disc degeneration *via* inhibiting differentiation and senescence of annulus fibrosus cells. *Aging (Albany NY)* 2018; **10**: 131-143 [PMID: 29348392 DOI: 10.18632/aging.101364]

9 **Ganey T**, Libera J, Moos V, Alasevic O, Fritsch KG, Meisel HJ, Hutton WC. Disc chondrocyte transplantation in a canine model: a treatment for degenerated or damaged intervertebral disc. *Spine (Phila Pa 1976)* 2003; **28**: 2609-2620 [PMID: 14652478 DOI: 10.1097/01.BRS.0000097891.63063.78]

10 **Acosta FL Jr**, Metz L, Adkisson HD, Liu J, Carruthers-Liebenberg E, Milliman C, Maloney M, Lotz JC. Porcine intervertebral disc repair using allogeneic juvenile articular chondrocytes or mesenchymal stem cells. *Tissue Eng Part A* 2011; **17**: 3045-3055 [PMID: 21910592 DOI: 10.1089/ten.tea.2011.0229]

11 **Noriega DC**, Ardura F, Hernández-Ramajo R, Martín-Ferrero MÁ, Sánchez-Lite I, Toribio B, Alberca M, García V, Moraleda JM, Sánchez A, García-Sancho J. Intervertebral Disc Repair by Allogeneic Mesenchymal Bone Marrow Cells: A Randomized Controlled Trial. *Transplantation* 2017; **101**: 1945-1951 [PMID: 27661661 DOI: 10.1097/TP.0000000000001484]

12 **Omlor GW**, Lorenz S, Nerlich AG, Guehring T, Richter W. Disc cell therapy with bone-marrow-derived autologous mesenchymal stromal cells in a large porcine disc degeneration model. *Eur Spine J* 2018; **27**: 2639-2649 [PMID: 30141058 DOI: 10.1007/s00586-018-5728-4]

13 **Hoogendoorn RJ**, Lu ZF, Kroeze RJ, Bank RA, Wuisman PI, Helder MN. Adipose stem cells for intervertebral disc regeneration: current status and concepts for the future. *J Cell Mol Med* 2008; **12**: 2205-2216 [PMID: 18298653 DOI: 10.1111/j.1582-4934.2008.00291.x]

14 **Pang X**, Yang H, Peng B. Human umbilical cord mesenchymal stem cell transplantation for the treatment of chronic discogenic low back pain. *Pain Physician* 2014; **17**: E525-E530 [PMID: 25054402]

15 **Ma W**, Tavakoli T, Derby E, Serebryakova Y, Rao MS, Mattson MP. Cell-extracellular matrix interactions regulate neural differentiation of human embryonic stem cells. *BMC Dev Biol* 2008; **8**: 90 [PMID: 18808690 DOI: 10.1186/1471-213X-8-90]

16 **Vadalà G**, Russo F, Ambrosio L, Loppini M, Denaro V. Stem cells sources for intervertebral disc regeneration. *World J Stem Cells* 2016; **8**: 185-201 [PMID: 27247704 DOI: 10.4252/wjsc.v8.i5.185]

17 **Zhu Y**, Liang Y, Zhu H, Lian C, Wang L, Wang Y, Gu H, Zhou G, Yu X. The generation and functional characterization of induced pluripotent stem cells from human intervertebral disc nucleus pulposus cells. *Oncotarget* 2017; **8**: 42700-42711 [PMID: 28498811 DOI: 10.18632/oncotarget.17446]

18 **Sheyn D**, Ben-David S, Tawackoli W, Zhou Z, Salehi K, Bez M, De Mel S, Chan V, Roth J, Avalos P, Giaconi JC, Yameen H, Hazanov L, Seliktar D, Li D, Gazit D, Gazit Z. Human iPSCs can be differentiated into notochordal cells that reduce intervertebral disc degeneration in a porcine model. *Theranostics* 2019; **9**: 7506-7524 [PMID: 31695783 DOI: 10.7150/thno.34898]

19 **Xia K**, Zhu J, Hua J, Gong Z, Yu C, Zhou X, Wang J, Huang X, Yu W, Li L, Gao J, Chen Q, Li F, Liang C. Intradiscal Injection of Induced Pluripotent Stem Cell-Derived Nucleus Pulposus-Like Cell-Seeded Polymeric Microspheres Promotes Rat Disc Regeneration. *Stem Cells Int* 2019; **2019**: 6806540 [PMID: 31191679 DOI: 10.1155/2019/6806540]

20 **Galderisi U**, Peluso G, Di Bernardo G. Clinical Trials Based on Mesenchymal Stromal Cells are Exponentially Increasing: Where are We in Recent Years? *Stem Cell Rev Rep* 2022; **18**: 23-36 [PMID: 34398443 DOI: 10.1007/s12015-021-10231-w]

21 **Adams MA**, Roughley PJ. What is intervertebral disc degeneration, and what causes it? *Spine (Phila Pa 1976)* 2006; **31**: 2151-2161 [PMID: 16915105 DOI: 10.1097/01.brs.0000231761.73859.2c]

22 **Peng B**, Hao J, Hou S, Wu W, Jiang D, Fu X, Yang Y. Possible pathogenesis of painful intervertebral disc degeneration. *Spine (Phila Pa 1976)* 2006; **31**: 560-566 [PMID: 16508552 DOI: 10.1097/01.brs.0000201324.45537.46]

23 **Freemont AJ**, Watkins A, Le Maitre C, Baird P, Jeziorska M, Knight MT, Ross ER, O'Brien JP, Hoyland JA. Nerve growth factor expression and innervation of the painful intervertebral disc. *J Pathol* 2002; **197**: 286-292 [PMID: 12115873 DOI: 10.1002/path.1108]

24 **Daly C**, Ghosh P, Jenkin G, Oehme D, Goldschlager T. A Review of Animal Models of Intervertebral Disc Degeneration: Pathophysiology, Regeneration, and Translation to the Clinic. *Biomed Res Int* 2016; **2016**: 5952165 [PMID: 27314030

DOI: 10.1155/2016/5952165]
25 **Peredo AP**, Gullbrand SE, Smith HE, Mauck RL. Putting the Pieces in Place: Mobilizing Cellular Players to Improve Annulus Fibrosus Repair. *Tissue Eng Part B Rev* 2021; **27**: 295-312 [PMID: 32907498 DOI: 10.1089/ten.TEB.2020.0196]
26 **Torre OM**, Mroz V, Bartelstein MK, Huang AH, Iatridis JC. Annulus fibrosus cell phenotypes in homeostasis and injury: implications for regenerative strategies. *Ann N Y Acad Sci* 2019; **1442**: 61-78 [PMID: 30604562 DOI: 10.1111/nyas.13964]
27 **Malda J**, Groll J, van Weeren PR. Rethinking articular cartilage regeneration based on a 250-year-old statement. *Nat Rev Rheumatol* 2019; **15**: 571-572 [PMID: 31367006 DOI: 10.1038/s41584-019-0278-7]
28 **Barry F**. MSC Therapy for Osteoarthritis: An Unfinished Story. *J Orthop Res* 2019; **37**: 1229-1235 [PMID: 31081558 DOI: 10.1002/jor.24343]
29 **Galipeau J**, Sensébé L. Mesenchymal Stromal Cells: Clinical Challenges and Therapeutic Opportunities. *Cell Stem Cell* 2018; **22**: 824-833 [PMID: 29859173 DOI: 10.1016/j.stem.2018.05.004]
30 **Krampera M**, Le Blanc K. Mesenchymal stromal cells: Putative microenvironmental modulators become cell therapy. *Cell Stem Cell* 2021; **28**: 1708-1725 [PMID: 34624232 DOI: 10.1016/j.stem.2021.09.006]
31 **Seo Y**, Kim HS, Hong IS. Stem Cell-Derived Extracellular Vesicles as Immunomodulatory Therapeutics. *Stem Cells Int* 2019; **2019**: 5126156 [PMID: 30936922 DOI: 10.1155/2019/5126156]
32 **Du T**, Ju G, Zhou J, Zhong L, Rong L, Chen W, Zhang X, Zhou R, Ding D, Ji T. Microvesicles derived from human umbilical cord mesenchyme promote M2 macrophage polarization and ameliorate renal fibrosis following partial nephrectomy *via* hepatocyte growth factor. *Hum Cell* 2021; **34**: 1103-1113 [PMID: 33860459 DOI: 10.1007/s13577-021-00525-z]
33 **Chang X**, Ma Z, Zhu G, Lu Y, Yang J. New perspective into mesenchymal stem cells: Molecular mechanisms regulating osteosarcoma. *J Bone Oncol* 2021; **29**: 100372 [PMID: 34258182 DOI: 10.1016/j.jbo.2021.100372]
34 **Galipeau J**. The mesenchymal stromal cells dilemma--does a negative phase III trial of random donor mesenchymal stromal cells in steroid-resistant graft-versus-host disease represent a death knell or a bump in the road? *Cytotherapy* 2013; **15**: 2-8 [PMID: 23260081 DOI: 10.1016/j.jcyt.2012.10.002]
35 **François M**, Romieu-Mourez R, Li M, Galipeau J. Human MSC suppression correlates with cytokine induction of indoleamine 2,3-dioxygenase and bystander M2 macrophage differentiation. *Mol Ther* 2012; **20**: 187-195 [PMID: 21934657 DOI: 10.1038/mt.2011.189]
36 **Digirolamo CM**, Stokes D, Colter D, Phinney DG, Class R, Prockop DJ. Propagation and senescence of human marrow stromal cells in culture: a simple colony-forming assay identifies samples with the greatest potential to propagate and differentiate. *Br J Haematol* 1999; **107**: 275-281 [PMID: 10583212 DOI: 10.1046/j.1365-2141.1999.01715.x]
37 **Bork S**, Pfister S, Witt H, Horn P, Korn B, Ho AD, Wagner W. DNA methylation pattern changes upon long-term culture and aging of human mesenchymal stromal cells. *Aging Cell* 2010; **9**: 54-63 [PMID: 19895632 DOI: 10.1111/j.1474-9726.2009.00535.x]
38 **Sivan SS**, Hayes AJ, Wachtel E, Caterson B, Merkher Y, Maroudas A, Brown S, Roberts S. Biochemical composition and turnover of the extracellular matrix of the normal and degenerate intervertebral disc. *Eur Spine J* 2014; **23** Suppl 3: S344-S353 [PMID: 23591805 DOI: 10.1007/s00586-013-2767-8]
39 **Vergroesen PP**, Kingma I, Emanuel KS, Hoogendoorn RJ, Welting TJ, van Royen BJ, van Dieën JH, Smit TH. Mechanics and biology in intervertebral disc degeneration: a vicious circle. *Osteoarthritis Cartilage* 2015; **23**: 1057-1070 [PMID: 25827971 DOI: 10.1016/j.joca.2015.03.028]

World Journal of Stem Cells

Submit a Manuscript: https://www.f6publishing.com

World J Stem Cells 2022 December 26; 14(12): 822-838

DOI: 10.4252/wjsc.v14.i12.822

ISSN 1948-0210 (online)

ORIGINAL ARTICLE

Basic Study

SPOC domain-containing protein 1 regulates the proliferation and apoptosis of human spermatogonial stem cells through adenylate kinase 4

Dai Zhou, Fang Zhu, Zeng-Hui Huang, Huan Zhang, Li-Qing Fan, Jing-Yu Fan

Specialty type: Reproductive biology

Provenance and peer review: Unsolicited article; Externally peer reviewed.

Peer-review model: Single blind

Peer-review report's scientific quality classification

Grade A (Excellent): 0
Grade B (Very good): B, B
Grade C (Good): C
Grade D (Fair): 0
Grade E (Poor): 0

P-Reviewer: Abu Yousuf M, Bangladesh; Lomperta K, Poland

Received: August 4, 2022
Peer-review started: August 4, 2022
First decision: September 29, 2022
Revised: October 7, 2022
Accepted: November 30, 2022
Article in press: November 30, 2022
Published online: December 26, 2022

Dai Zhou, Fang Zhu, Zeng-Hui Huang, Huan Zhang, Li-Qing Fan, Jing-Yu Fan, Institute of Reproduction and Stem Cell Engineering, School of Basic Medicine Science, Central South University, Changsha 410000, Hunan Province, China

Dai Zhou, Zeng-Hui Huang, Huan Zhang, Li-Qing Fan, Reproductive and Genetic Hospital of CITIC-Xiangya, Changsha 410000, Hunan Province, China

Dai Zhou, College of Life Sciences, Hunan Normal University, Changsha 410000, Hunan Province, China

Dai Zhou, Zeng-Hui Huang, Huan Zhang, Li-Qing Fan, Clinical Research Center for Reproduction and Genetics in Hunan Province, Changsha 410000, Hunan Province, China

Jing-Yu Fan, Department of Chemistry and Biochemistry, University of South Carolina, Columbia, SC 29208, United States

Corresponding author: Jing-Yu Fan, MD, PhD, Researcher, Department of Chemistry and Biochemistry, University of South Carolina, 631 Sumter St, GSRC 109, Columbia, SC 29208, United States. jingyu@email.sc.edu

Abstract

BACKGROUND

Spermatogonial stem cells (SSCs) are the origin of male spermatogenesis, which can reconstruct germ cell lineage in mice. However, the application of SSCs for male fertility restoration is hindered due to the unclear mechanisms of proliferation and self-renewal in humans.

AIM

To investigate the role and mechanism of SPOC domain-containing protein 1 (SPOCD1) in human SSC proliferation.

METHODS

We analyzed publicly available human testis single-cell RNA sequencing (RNA-seq) data and found that SPOCD1 is predominantly expressed in SSCs in the early developmental stages. Small interfering RNA was applied to suppress SPOCD1 expression to detect the impacts of SPOCD1 inhibition on SSC proliferation and

apoptosis. Subsequently, we explored the target genes of SPOCD1 using RNA-seq and confirmed their role by restoring the expression of the target genes. In addition, we examined SPOCD1 expression in some non-obstructive azoospermia (NOA) patients to explore the correlation between SPOCD1 and NOA.

RESULTS

The uniform manifold approximation and projection clustering and pseudotime analysis showed that SPOCD1 was highly expressed in the early stages of SSC, and immunohistological results showed that SPOCD1 was mainly localized in glial cell line-derived neurotrophic factor family receptor alpha-1 positive SSCs. SPOCD1 knockdown significantly inhibited cell proliferation and promoted apoptosis. RNA-seq results showed that SPOCD1 knockdown significantly downregulated genes such as adenylate kinase 4 (AK4). Overexpression of AK4 in SPOCD1 knockdown cells partially reversed the phenotypic changes, indicating that AK4 is a functional target gene of SPOCD1. In addition, we found a significant downregulation of SPOCD1 expression in some NOA patients, suggesting that the downregulation of SPOCD1 may be relevant for NOA.

CONCLUSION

Our study broadens the understanding of human SSC fate determination and may offer new theories on the etiology of male infertility.

Key Words: Human; Testis; Spermatogonial stem cells; SPOC domain-containing protein 1; Adenylate kinase 4; Proliferation

Core Tip: In this study, we reported the dominant expression of SPOC domain-containing protein 1 (SPOCD1) in human spermatogonial stem cells (SSCs). Knockdown of SPOCD1 in SSC caused a significant decrease in proliferation and self-renewal, and the induction of apoptosis. RNA sequencing showed that SPOCD1 knockdown caused significant downregulation of genes such as adenylate kinase 4 (AK4), and overexpression of AK4 in SPOCD1-knockdown cells reversed the phenotypic alterations induced by SPOCD knockdown. Additionally, we found significant downregulation of SPOCD1 in non-obstructive azoospermia patients. These results broaden our understanding of human SSC fate determination and provide new theories on the etiology of male infertility.

Citation: Zhou D, Zhu F, Huang ZH, Zhang H, Fan LQ, Fan JY. SPOC domain-containing protein 1 regulates the proliferation and apoptosis of human spermatogonial stem cells through adenylate kinase 4. *World J Stem Cells* 2022; 14(12): 822-838

URL: https://www.wjgnet.com/1948-0210/full/v14/i12/822.htm

DOI: https://dx.doi.org/10.4252/wjsc.v14.i12.822

INTRODUCTION

Infertility affects about 15% of couples worldwide, and about 50% of these cases are due to male factors [1]. Non-obstructive azoospermia (NOA) is the most severe cause of male infertility, for which there is a lack of effective treatment[2]. Thus, solving the fertility issues associated with NOA has been an important research direction in reproductive medicine.

Spermatogonial stem cells (SSCs) are responsible for initiating and maintaining adult spermatogenesis throughout life, which produces mature sperm through constant self-renewal and differentiation[3]. In rodents, long-term *in vitro* culture of mouse SSCs has been achieved, with reports showing the restoration of testicular transplantation in recipient mouse germline reconstitution[4,5]. However, the mouse SSC culture system is unsuitable for humans, and insufficient proliferation capacity *in vitro* is currently a significant problem encountered during human SSC culture[6]. Therefore, exploring the mechanism of human SSC proliferation and self-renewal is key to solving the long-term *in vitro* culture of human SSCs and the basis for using SSCs in treating male infertility.

Glial cell line-derived neurotrophic factor (GDNF) is a crucial growth factor for maintaining SSC proliferation and self-renewal[7]. GDNF binds to the GDNF family receptor alpha-1 (GFRA1)/c-Ret; activates downstream RAS, AKT, and mitogen-activated protein kinase (MAPK) pathways; and regulates the transcription of ETS variant transcription factor 5, B-cell CLL/lymphoma 6 member B protein, and LIM homeobox 1 to promote the self-renewal of SSCs[8]. Another essential growth factor is

fibroblast growth factor 2, which regulates SSC self-renewal by activating the MAPK pathway[9]. Due to differences in species, sample sources, and ethical issues, only a few studies have been performed to investigate the regulations of human SSCs. Recently, microRNA-1908-3p (miR-1908-3p) was shown to enhance SSC proliferation by mediating the degradation of Krüppel-like factor 2 (KLF2) in humans[10]. miR-122-5p[11] and miR-663a[12] are also involved in the regulation of SSC proliferation. Calcium-responsive transcription factor (CARF) affects SSC functions in mice through the WNT pathway, and mutations in human CARF also cause male infertility[13]. Human SSCs have also been modulated by RNF144B through the Fc epsilon receptor II/neurogenic locus notch homolog protein 2/HES1 pathway [14]. In addition, we previously reported that transcription factor 3 is specifically localized in the nucleus of human SSCs, and promotes human SSC proliferation by regulating podocalyxin-like protein 1 expression[15]. However, the regulatory mechanisms of SSCs are poorly understood.

To further explore the developmental process of human SSCs, GSE149512[16] and GSE112013[17] databases containing adult testis single-cell data were analyzed. We found that SPOC domain-containing protein 1 (SPOCD1) was specifically expressed in a subpopulation of SSCs, and the result was validated by immunohistochemistry. SPOCD1 knockdown decreased the proliferation of immortalized human SSCs, with numerous genes downregulated, including adenylate kinase 4 (*AK4*), *KLF8*, and vesicular, overexpressed in cancer, prosurvival protein 1 (*VOPP1*). AK4 re-expression reversed the cell proliferation and apoptotic changes caused by SPOCD1 knockdown. Furthermore, the expression of SPOCD1 was significantly reduced in some NOA patients. Overall, these results describe a role for SPOCD1 in SSC proliferation and expand our understanding of SSC fate determination.

MATERIALS AND METHODS

Ethics statement

Our study was approved by the ethics committee of the Reproductive and Genetic Hospital of CITIC-Xiangya (LL-SC-2021-025). The overview of our research is illustrated in Figure 1. Each participant provided signed informed consent. Testicular tissues of 18 patients (6 OA and 12 NOA), aged between 28-years-old and 48-years-old who underwent testicular biopsy were collected, with approximately 25 mg each. Sterile phosphate-buffered saline (PBS) was used to wash the samples at least three times to remove blood cells. Subsequently, the tissues were frozen in liquid nitrogen or fixed in 40 g/L paraformaldehyde (PFA).

Single-cell RNA sequencing data analysis

To analyze single-cell RNA sequencing (scRNA-seq) datasets (GSE149512 and GSE112013) of the normal adult testis, Seurat 4.2 (https://github.com/satijalab/seurat/) program in R was employed. In the first step, we used the Read.10X function to load the expression matrix data in R and created the Seurat object. Cells with gene expression numbers between 500 and 4000 and with less than 15% of mitochondrial genes were retained. Then, each Seurat object was processed using the NormalizeData and FindVariableFeatures functions. Next, all Seurat objects were merged using the FindIntegration-Anchors and IntegrateData functions. The combined data were clustered using the uniform manifold approximation and projection (UMAP) method set by default, and subsequently, cell types were identified based on the expression of cellular markers. The data of SSC cell populations were extracted using the Subset function and re-clustered using UMAP. Monocle 3 (https://github.com/cole-trapnell-lab/monocle3) in R was used to perform pseudotime analysis of SSCs. The cell developmental trajectory begins in Subpopulation State 2. Dot, line, and violin plots were created and modified using ggplot2 (https://github.com/tidyverse/ggplot2) in R.

Culture of immortalized human SSCs

By transfecting Large T antigen into G protein-coupled receptor 125 (GPR125)-positive human undifferentiated spermatogonia, immortalized human SSC lines were established[18]. Immortalized human SSCs maintained many properties of their primary cells and expressed many markers of primary SSCs including GFRA1, RET, and promyelocytic leukemia zinc finger (PLZF). They did not express testicular endosomal cell markers such as SRY-box transcription factor 9[15]. The immortalized human SSCs were grown at 34 °C with 50 mL/L CO_2 in an incubator, and the culture medium consisted of Dulbecco's modified Eagle's medium (DMEM)/F12 (Gibco, Grand Island, NY, United States) supplemented with 100 mL/L fetal bovine serum (FBS; Gibco). The cells were subcultured every 2 d or 3 d (0.5 g/L trypsin and 0.53 mmol/L Ethylenediaminetetraacetic acid (EDTA); Invitrogen, Carlsbad, CA, United States).

Total RNA extraction, reverse transcription PCR, and quantitative PCR

The total RNA of cells was isolated using RNAiso Plus reagent (Takara, Kusatsu, Japan) following the manufacturer's instructions. Nanodrop (Thermo Fisher Scientific, Waltham, MA, United States) was employed to detect the quality and concentration of the extracted RNA. Then the reverse transcription of cDNA was conducted using commercial kits (Roche, Mannheim, Germany).

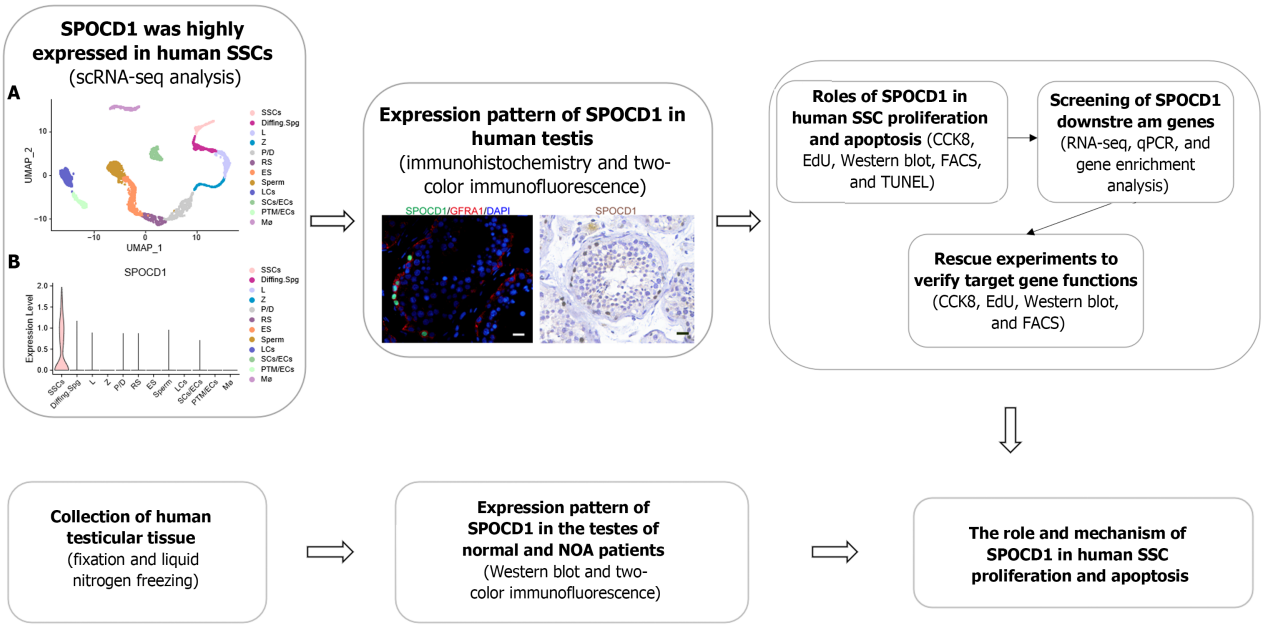

DOI: 10.4252/wjsc.v14.i12.822

Figure 1 Flow chart of this study's design. NOA: Non-obstructive azoospermia; scRNA-seq: Single-cell RNA sequencing; SPOCD1: SPOC domain-containing protein 1; SSCs: Spermatogonial stem cells.

According to the manufacturer's instructions, quantitative PCR (qPCR) was performed using the ABI Prism 7700 system (Applied Biosystems, Foster City, CA, United States). The $2^{-\Delta\Delta(Ct)}$ method was chosen to measure the relative levels of mRNAs, and actin beta was selected as an internal reference. Each sample was analyzed three times, and the results were averaged. All primer sequences were designed and listed in Supplementary Table 1.

Immunohistochemistry and immunofluorescence for tissue sections

Testis sections were deparaffinized with xylene and rehydrated with graded ethanol for immunohistochemistry. Then the heat-induced antigen retrieval method was conducted in 0.01 mol/L sodium citrate buffer at 98 °C for 18 min. After cooling and washing, the sections were incubated with 30 mL/L hydrogen peroxidase (Zsbio, Beijing, China) to block the endogenous peroxidase activity. After three washes with PBS, the tissue sections were permeated for 15 min with 2.5 mL/L Triton X-100 (Sigma, St. Louis, MO, United States), and 50 mL/L bovine serum albumin was applied to block nonspecific antigens for 1 h at room temperature (RT). Subsequently, sections were incubated with primary antibodies listed in Supplementary Table 2 at 4 °C overnight. After three washes with PBS, the sections were incubated with horseradish peroxidase-conjugated goat anti-rabbit secondary antibody for 1 h at RT, and the 3,3'-diaminobenzidine chromogen kit (Dako, Glostrup, Denmark) was used for color development. Hematoxylin was used to stain the nucleus for 7 min at RT. For immunofluorescence, after incubation of the primary antibody for 16h at 4 °C, chromogenic development was performed using Alexa Fluor-conjugated secondary antibody, and 4,6-diamidino-2-phenylindole was used to counterstain the cell nuclei. The microscopic images of testicular sections were captured and analyzed using a Zeiss microscope (Zeiss, Jena, Germany).

Protein extraction and Western blotting

For total protein extraction, testicular tissue and cells were lysed using RIPA (Thermo Fisher Scientific) or 15 min on ice, followed by centrifugation at 12000 g for 15 min and the collection of supernatants. According to the operating manual, the BCA Kit was utilized to detect total protein concentration. Twenty micrograms of total protein were taken from each sample for sodium dodecyl sulfate-polyacrylamide gel electrophoresis and Western blot analysis, as previously described[15]. Detailed antibody information is listed in Supplementary Table 2. Enhanced chemiluminescent chromogenic solution (Thermo Fisher Scientific) was used to visualize the protein band, and the chemiluminescent signal of bands was captured and analyzed with Fusion FX (Vilber Lourmat, Marne-la-Vallée, France). All samples were analyzed three times, and the results were averaged.

Gene silencing

All small interfering RNAs (siRNAs) were designed and synthesized by Ribobio (Guangzhou, China), and the sequence of siRNAs was listed in Supplementary Table 3. Immortalized human SSCs were transfected with siRNAs (100 nmol/L) using Lipofectamine 3000 (Life Technologies, Carlsbad, CA,

United States) according to the manufacturer's instructions. After transfection for 48 h, cells were collected to extract protein and RNA for PCR and Western blot analysis.

Cell Counting Kit-8 assay

The Cell Counting Kit-8 (CCK-8) Kit (Dojindo, Kumamoto, Japan) was used to detect SSC viability according to the manufacturer's instructions. Cells were cultured for 3 h using the culture medium supplemented with 100 mL/L CCK-8 reagents. Then a microplate reader (Thermo Fisher Scientific) was used to detect the absorbance at 450 nm.

5-ethynyl-2'-deoxyuridine assay

For the 5-ethynyl-2'-deoxyuridine (EdU) incorporation assay, DNA synthesis was detected with an EdU labeling kit (RiboBio). According to the manufacturer's protocol, human SSCs were seeded into 96-well plates (5000 cells per well) in culture medium supplemented with 50 μmol/L EdU. After 12 h of incubation, cells were washed with DMEM and fixed in 40 g/L PFA. Next, cells were neutralized with glycine (2 mg/mL) and permeabilized with 5 mL/L Triton X-100 for 10 min at RT. Apollo staining reaction buffer was used for EdU visualization, and DAPI was employed for labeling cell nuclei. The microscopic images of EdU-positive cells were captured and analyzed using the Zeiss fluorescence microscope. A minimum of 500 cells per sample were assessed.

Flow cytometry with annexin V-APC/propidium iodide staining

After transfection with SPOCD1-siRNA for 48 h, cells were digested using trypsin/EDTA and washed twice with ice-cold PBS. Next, according to the manufacturer's instructions, at least 10^6 cells were resuspended in Annexin V binding buffer (BD Biosciences, Franklin Lakes, NJ, United States). The cells were incubated with 5 μL APC-labeled Annexin V for 15 min at RT. Before the assay, cells were incubated with 10 μL PI for 10 min. Cell apoptosis was evaluated on the C6 flow cytometer (BD Biosciences).

Terminal deoxynucleotidyl transferase dUTP nick end labeling assay

After transfection in human SSCs with SPOCD1-siRNA, an *in situ* cell death detection kit (Roche) was used to evaluate cell apoptosis according to the manufacturer's instructions. Cells were fixed in PFA, and then incubated with proteinase K (20 mg/mL) for 15 min at RT. After washing, the cells were incubated with 50 μL terminal deoxynucleotidyl transferase (TdT) reaction buffer for 1 h away from light, and DAPI was used to label the cell nucleus. PBS free of TdT enzyme was utilized to treat the cells of the negative control group. At least 500 cells were counted per group using fluorescence microscopy (Zeiss).

RNA-seq

The total RNA of cells was isolated using the Trizol Reagent Kit (Invitrogen). RNA quality was measured using the Agilent 2100 Bioanalyzer (Agilent Technologies, Santa Clara, CA, United States). To enrich eukaryotic mRNA, oligo (dT) beads were used, and ribosomal RNA (rRNA) was removed using a Magnetic Kit (Epicentre, Madison, WI, United States). Following this, the enriched mRNA was fragmented using the fragmentation buffer, and reverse transcription was performed using random hexamers. Subsequently, the cDNA was synthesized and purified using a commercial purification kit (Qiagen, Venlo, The Netherlands), followed by their end repair, poly (A) introduction, and ligation. Next, we utilized agarose electrophoresis to separate the ligation products, and after amplifying them using PCR, sequencing was performed on the Illumina HiSeq2500 system. Fastp (version 0.18.0) was used to filter the reads obtained from the sequencing machine. Bowtie2 (version 2.2.8) was applied to remove the rRNA-mapped reads. The remaining clean reads were used to assemble transcripts and determine gene abundance and mapped to the reference genome. Then the mapped reads were assembled using StringTie (version 1.3.1) in a reference-based strategy. DESeq2 software was used to assess differentially expressed genes (DEGs). ClusterProfiler in R was used to perform Gene Ontology and Kyoto Encyclopedia of Genes and Genomes enrichment analysis on DEGs.

Statistical analysis

GraphPad Prism version 8.0 (GraphPad Software, La Jolla, CA, United States) was used for the data analyses. All assays were performed at least in triplicate. Data are shown as the mean ± SD. Differences between groups were evaluated using the *t*-test. $P < 0.05$ indicated statistical significance.

RESULTS

Human SSC profiling based on scRNA-seq analysis

To explore the molecular mechanisms underlying the proliferation and self-renewal of human SSCs, we performed bioinformatics analysis on scRNA-seq datasets of normal adult testis from GSE149512 and

GSE112013. By screening and integrating the data, 5176 testis cells and 23152 genes were identified. All cells were divided into 12 clusters using the Seurat package on R and identified according to the expression levels of a series of testicular cell marker genes including SSC markers (inhibitor of DNA binding 4, HLH protein), differentiating markers (*KIT* and stimulated by retinoic acid 8), meiosis markers (synaptonemal complex protein 3, *SPO11*, ovo-like zinc finger 2, and *NME8*), spermatid structure proteins (transition protein 2 and protamine 2), and some somatic markers and their respective cell clusters were identified. The 12 cell populations were SSCs, differentiating spermatogonia (Diffing. Spg), leptotene spermatocytes (L), zygotene spermatocytes (Z), pachytene/diplotene spermatocytes (P/D), round spermatids (RS), elongated spermatocytes (ES), sperm, Leydig cells (LCs), Sertoli cells/endothelial cells (SCs/ECs), peritubular myoid cells (PTM)/ECs, and macrophages (Mø) (Figure 2A). To further analyze the regulation of SSCs, reclustering of SSCs was performed using the Seurat package on R, and all SSCs were subdivided into three states, namely states 0, 1, and 2 (Figure 2B). Then, a monocle-based pseudotime analysis on SSCs was performed to create a developmental trajectory. According to the level of PIWI-like RNA-mediated gene silencing 4 and Nanos C2HC-type zinc finger 3, we assumed that State 2 was the developmental starting point, State 0 was late in development, and State 1 was the transitional period of development (Figure 2C). Differential gene expression analysis identified various genes including *SPOCD1*, ankyrin repeat and SOCS box containing 9, and chromosome 19 open reading frame 84 (Figure 2D). We also observed the distribution of these genes in all testicular cells using a Violin plot. Among these DEGs, *SPOCD1* was specifically expressed in SSCs and progressively decreased with developmental trajectory (Figure 2E), indicating that *SPOCD1* is associated with the SSC self-renewal and proliferation ability.

Validation of SPOCD1 distribution pattern in human testis

To validate the results of scRNA-seq analysis, we investigated the expression pattern of SPOCD1 in normal adult testicular tissue. Western blot analysis showed that SPOCD1 protein was moderately expressed in the testes of three OA patients with normal spermatogenesis (Figure 3A). Furthermore, we examined the localization of SPOCD1 in the normal testis using immunohistochemistry. The results demonstrated that the positive signal appeared in the nucleus of cells near the basal membrane of the seminal tubules, indicating that SPOCD1 is mainly expressed in spermatogonia (Figure 3B and C). Thus, we further analyzed the cell subtypes in which SPOCD1 was expressed using double immunofluorescence. The results showed that 91.11% ± 4.65% of SPOCD1-positive cells expressed glial cell derived neurotrophic factor family receptor alpha 1 (a marker of SSCs), and only 3.38% ± 1.54% of SPOCD1-positive cells weakly expressed KIT, a marker of differentiating spermatogonia. It should be noted that 84.60% ± 2.79% of SPOCD1-positive cells expressed proliferating cell nuclear antigen (PCNA), a feature of proliferating cells (Figure 3D and E). These data validated the results from bioinformatics analysis, showing that SPOCD1 was mainly localized to SSCs and may play roles in human SSC proliferation and self-renewal.

The role of SPOCD1 in the proliferation of human SSC lines

To examine the roles of SPOCD1 in SSC proliferation, an immortalized human SSC cell line was used. We used several siRNAs to repress SPOCD1 expression in cells and verified the knockdown efficiency of each siRNA by qPCR (Figure 4A) and Western blot analysis (Figure 4B and C). These results indicated that all three siRNAs inhibited the expression of SPOCD1, of which SPOCD1-siRNA2 had the best knockdown efficiency. Then, a CCK-8 assay was performed to investigate the proliferation of SPOCD1 siRNA2-transfected cells (Figure 4D). The results showed that SPOCD1 knockdown suppressed cell proliferation from Day 3 to Day 5 after transduction. We also examined the levels of various proteins associated with SSC proliferation, including promyelocytic leukemia zinc finger, cyclin D1, PCNA, and Thy-1 cell surface antigen, and found that all were significantly downregulated after the knockdown of SPOCD1 (Figure 4E and F). Likewise, 48 h after cell transfection, EdU incorporation assays were used to detect cell DNA synthesis. SPOCD1 inhibition induced a significant decrease in cellular DNA synthesis compared to the control group (34.73% ± 4.02% *vs* 21.56% ± 1.56%, $P < 0.05$) (Figure 4G and H).

The influence of SPOCD1 in the apoptosis of human SSC lines

Following transfection with SPOCD1-siRNA2 for 48 h, we observed a significant increase in suspended cells and debris, so we examined cell apoptosis using Annexin V/propidium iodide staining and flow cytometry. The analysis showed that SPOCD1 knockdown led to a significant increase in early and late apoptosis compared to the control group (early apoptosis: 4.39% ± 0.40% *vs* 1.81% ± 0.29%, $P < 0.05$; late apoptosis: 11.43% ± 0.24% *vs* 6.24% ± 0.02%, $P < 0.05$, Figure 5A and B). Similar results were obtained with the TdT dUTP nick end labeling (TUNEL) assay, which showed a significant increase in the cellular DNA fragmentation rate (Figure 5C and D). These results suggest that inhibition of SPOCD1 expression triggers apoptosis in human SSC lines.

Screening of SPOCD1 downstream target genes

To explore the mechanisms of SPOCD1 in the proliferation and apoptosis of the SSC lines, we

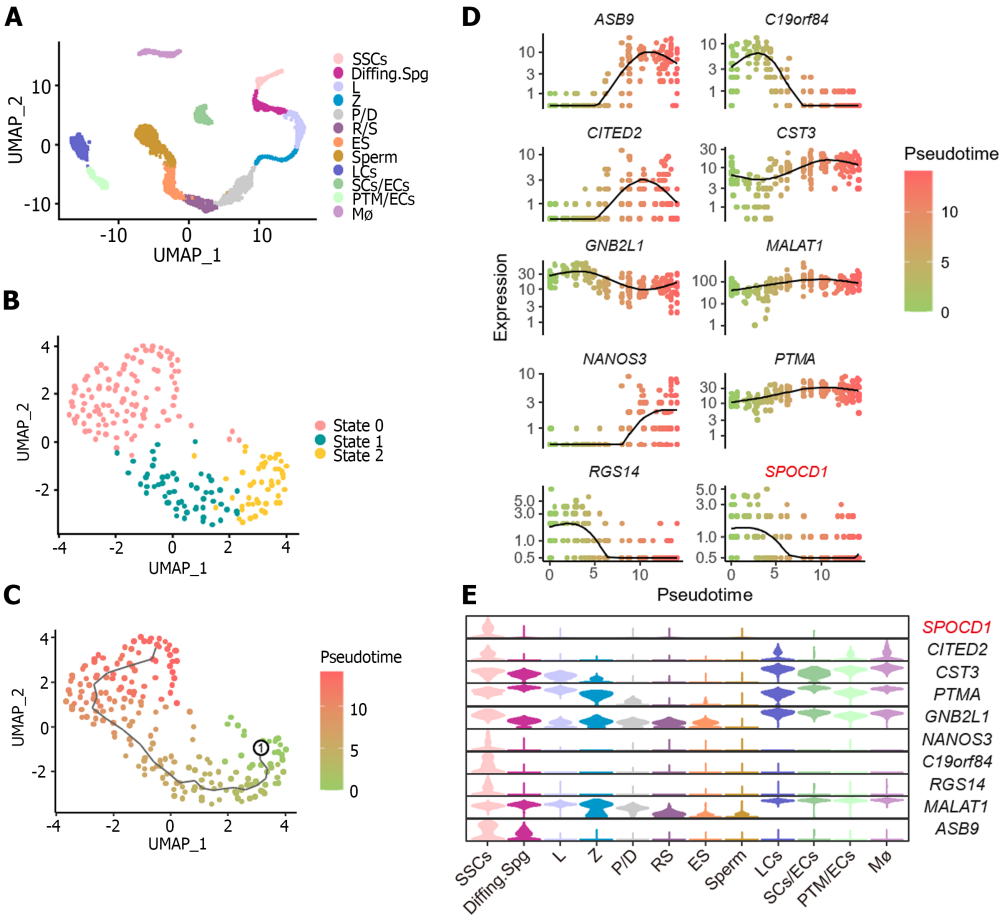

DOI: 10.4252/wjsc.v14.i12.822 **Copyright** ©The Author(s) 2022.

Figure 2 Integrated analysis of human testes single-cell sequencing datasets (GSE149512 and GSE112013). A: Uniform manifold approximation and projection (UMAP) and clustering analyses of combined single-cell transcriptomic data from human testes; B: UMAP and re-clustering analysis of spermatogonial stem cell (SSC) clusters, each dot represents a single cell and is colored according to legends; C: Pseudo-time analysis of SSC cluster showing three discrete cellular states (states 0, 1, and 2) during SSC development, the black curve is the developmental trajectory created by the Monocle 3 package, and character 1 represents the starting point of the developmental trajectory; D: Expression levels of the top 10 differentially expressed genes (DEGs) during SSC development. The black curve is the mean level expression along with pseudotime; E: Violin plots show the expression levels of the top 10 DEGs in all testicular cells. Diffing.Spg: Differentiating spermatogonia; ES: Elongated spermatids; L: Leptotene spermatocytes; LCs: Leydig cells; Mø: Macrophages; P/D: Pachytene/diplotene spermatocytes; PTM/ECs: Peritubular myoid cells/endothelial cells; RS: Round spermatids; SCs/ECs: Sertoli cells/endothelial cells; Z: Zygotene spermatocytes.

performed RNA-seq on cells after transfection with SPOCD1-siRNA. A total of about 20000 genes were detected. After excluding unrecognized reads and genes with fragments per kilobase of exon model per million reads mapped value < 0.001, 14556 genes were included for subsequent analysis (Supplementary Table 4). The results showed that SPOCD1 knockdown caused significant changes in 212 genes compared with control groups (Figure 6A) and affected signaling pathways such as cyclic AMP and tumor necrosis factor (Supplementary Figure 1). The expression of SPOCD1 and 10 randomly selected DEGs were validated using qPCR (Figure 6B), and the results were consistent with the RNA-seq data. Then we selected the top 20 DEGs according to the fold changes and *P* value ($P < 0.05$). We found that genes such as *VOPP1*, *AK4*, and *KLF8* were significantly downregulated, and genes such as zinc finger protein 431 (*ZNF431*), copper metabolism domain containing 1 (*COMMD1*), and SP140 nuclear body protein were significantly upregulated. The expression of these genes is shown in the Volcano plot of Figure 6C and the heat map in Figure 6D. We also explored the distributions of the top 20 DEGs in the test using sc-seq data (Figure 6E) and observed that angiopoietin-related protein 7 was not detected in the scRNA data. Considering the expression level, fold change, and distribution of genes, *AK4* was predominantly expressed in SSCs, demonstrated moderate expression levels, and was downregulated about four-fold after SPOCD1 knockdown (Figure 6B). This result was also validated using Western blotting (Figure 7A). Therefore, we hypothesized that AK4 might be a potential target of SPOCD1.

AK4 is responsible for the reduced proliferation of SSC line by SPOCD1 knockdown

To verify the functions of AK4 in the SPOCD1-mediated proliferation of human SSCs, we re-expressed AK4 in SPOCD1-knockdown cells. Western blot analysis confirmed the transfection efficiency of SPOCD1-siRNA and AK4 expression plasmid (Figure 7A and B). CCK-8 (Figure 7C) and EdU (Figure 7D and E) results showed that the re-expression of AK4 significantly attenuated the growth

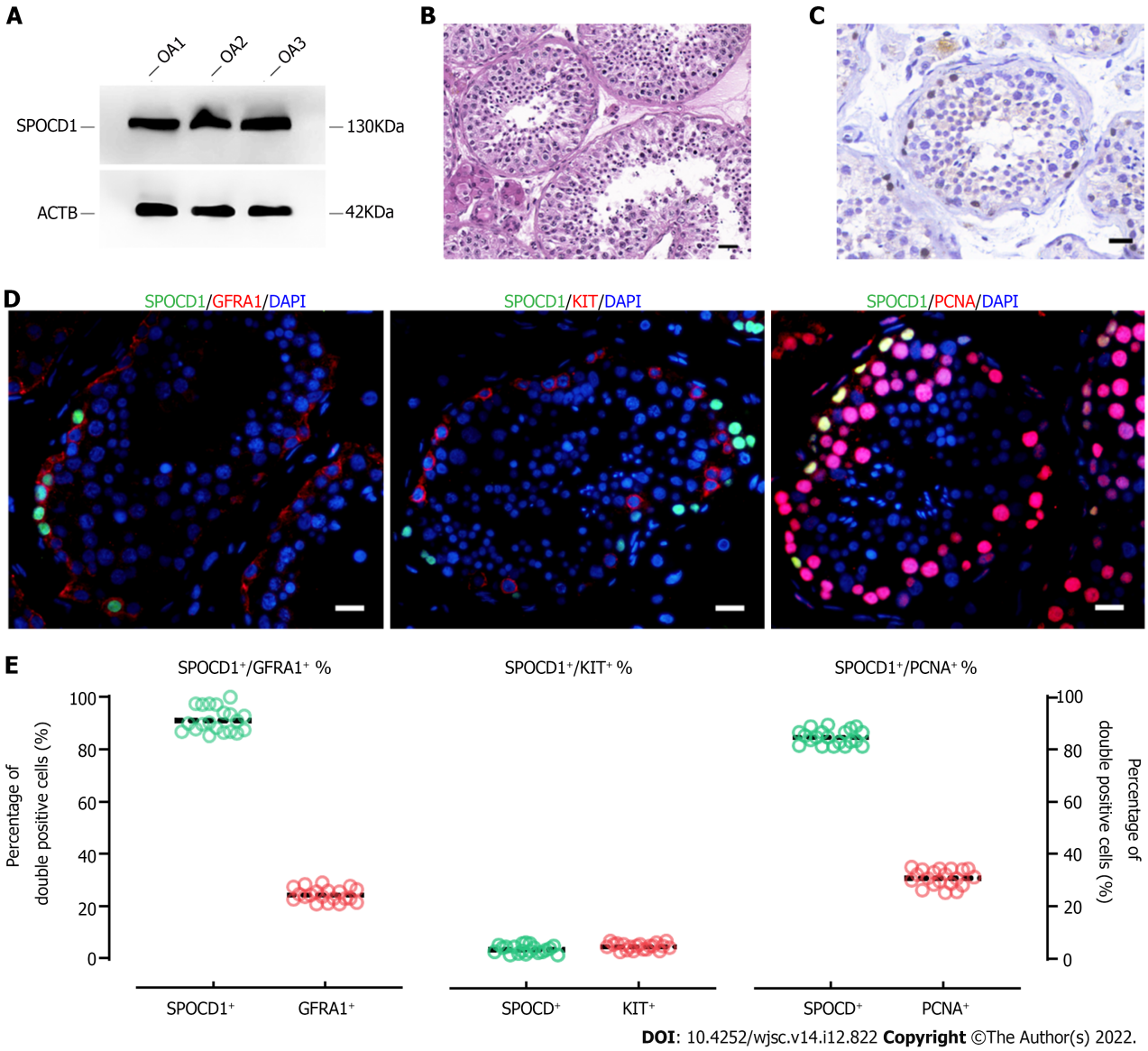

DOI: 10.4252/wjsc.v14.i12.822

Figure 3 Expression pattern of SPOC domain-containing protein 1 in normal adult testis. A: Western blotting show SPOC domain-containing protein 1 (SPOCD1) levels in three obstructive azoospermia (OA) samples with normal spermatogenesis; B: Representative hematoxylin and eosin-stained image of OA testicular tissues; C: Immunohistochemistry images for cell distribution of SPOCD1 in OA samples with normal spermatogenesis; D: Double immunostaining shows co-expression of SPOCD1 with glial cell line-derived neurotrophic factor family receptor alpha-1 (GFRA1), KIT, and proliferating cell nuclear antigen (PCNA) in testes with normal spermatogenesis; E: The abundance of SPOCD1+ cells co-expressing GFRA1, KIT, and PCNA. Each circle represents one count result, and at least 20 cross-sections of seminiferous tubules were assessed for each sample. Scale bars in B and D: 50 μm.

inhibition conferred by SPOCD1 knockdown in human SSCs. Western blot analysis also showed that the re-expression of AK4 significantly restored the downregulation of PLZF and PCNA proteins caused by SPOCD1 knockdown (Figure 7F and G). We further examined the apoptosis level of the SSCs using fluorescence activated cell sorting. The results showed that the re-expression of AK4 significantly reversed the increased apoptosis resulting from SPOCD1 knockdown (Figure 7H and I), suggesting that AK4 is essential for SPOCD1-induced SSC proliferation.

The abnormal expression of SPOCD1 may be associated with NOA

NOA is one of the most serious male infertility disorders without effective treatment. According to the pathological examination of testicular tissue, NOA can be categorized as spermatogonia maturation arrest (Spg MA), spermatocyte maturation arrest (Spc MA), spermatid maturation arrest (Std MA), hypo-spermatogenesis (HS) and SC only syndrome (SCOS). SSCs are responsible for initiating adult spermatogenesis, and many studies have shown that the abnormal viability of SSCs impairs spermatogenesis. To explore whether SPOCD1 affected adult testicular function *via* SSCs, we examined the level and distribution of SPOCD1 in eight adult testes (Supplementary Figure 2) and the distribution changes of SPOCD1 in tissues by immunofluorescence staining with GFRA1 (Figure 8A). These findings revealed that the percentage of SPOCD1-positive cells was significantly decreased in testes diagnosed

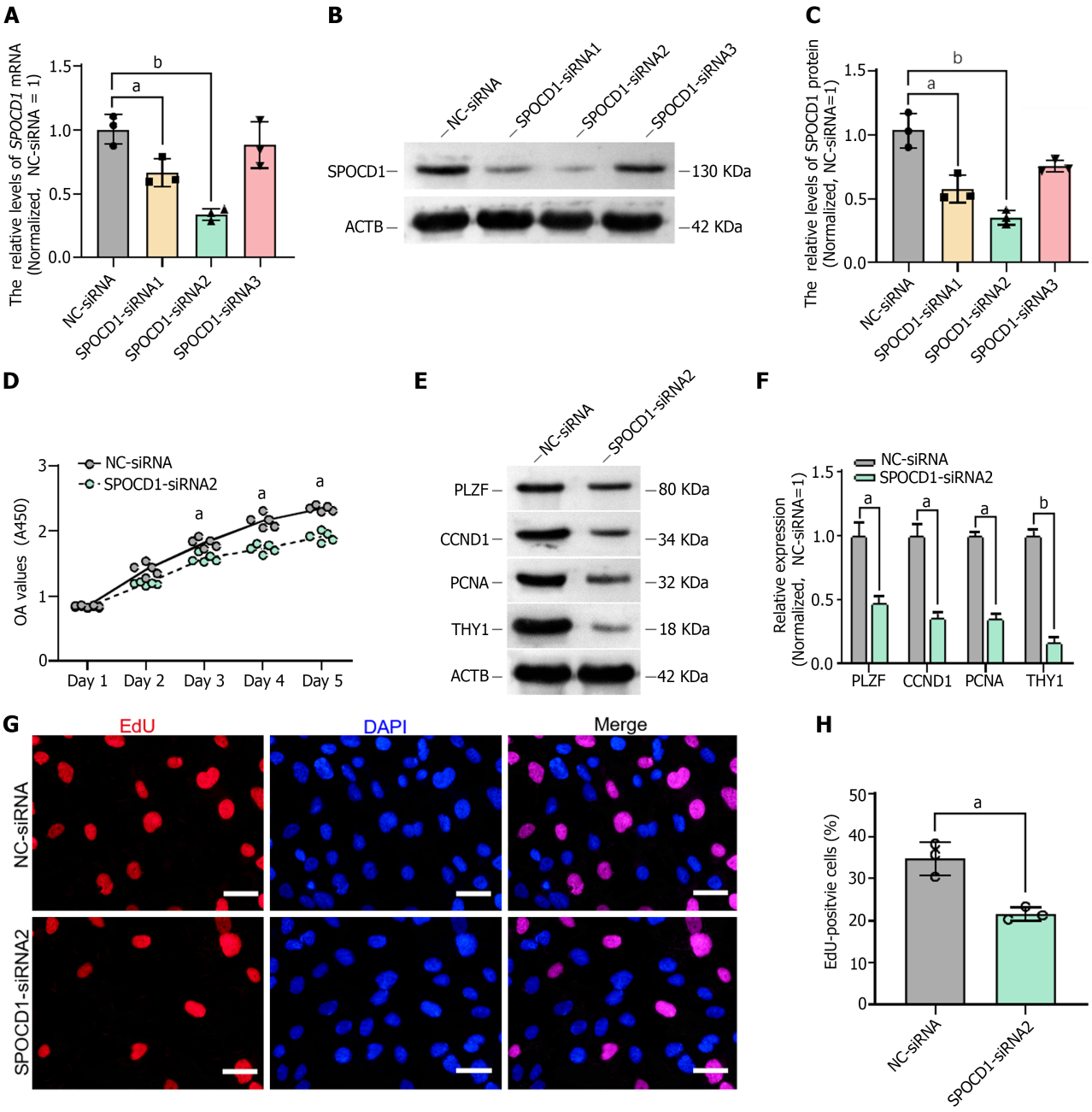

DOI: 10.4252/wjsc.v14.i12.822

Figure 4 Influence of SPOC domain-containing protein 1 knockdown on the proliferation of human spermatogonial stem cells. A: Quantitative PCR results show SPOC domain-containing protein 1 (SPOCD1) mRNA levels in a human spermatogonial stem cell line after transfection with SPOCD1-small interfering RNA (siRNA) 1-, 2-, and 3; B and C: Western blotting shows the changes of SPOCD1 protein after transfection with SPOCD1-siRNA; D: The Cell Counting Kit-8 assay shows the proliferation of human SSCs transfected with negative control (NC)-siRNA and SPOCD1-siRNA 2; E and F: Protein levels of promyelocytic leukemia zinc finger (PLZF), cyclin D1 (CCND1), proliferating cell nuclear antigen (PCNA), and Thy-1 cell surface antigen (THY1) after transfection with NC-siRNA and SPOCD1-siRNA 2; G and H: The percentage of 5-ethynyl-2'-deoxyuridine (EdU)-positive cells after transfection with NC-siRNA and SPOCD1-siRNA 2. Scale bar in G: 20 μm. $^{a}P < 0.05$; $^{b}P < 0.01$.

with Spc MA and Spg MA (Figure 8B). Additionally, there was no change in SPCOD1 intracellular localization; it remained in the nuclei. Western blot analysis showed that SPOCD1 levels were significantly downregulated in patients with Spg MA and Spc MA (Figure 8C and D). Our results indicate that SPOCD1 downregulation might be associated with spermatogenesis dysregulation in humans, but more evidence is needed to confirm these observations.

DISCUSSION

SSCs are responsible for long-term spermatogenesis by balancing self-renewal and differentiation[19].

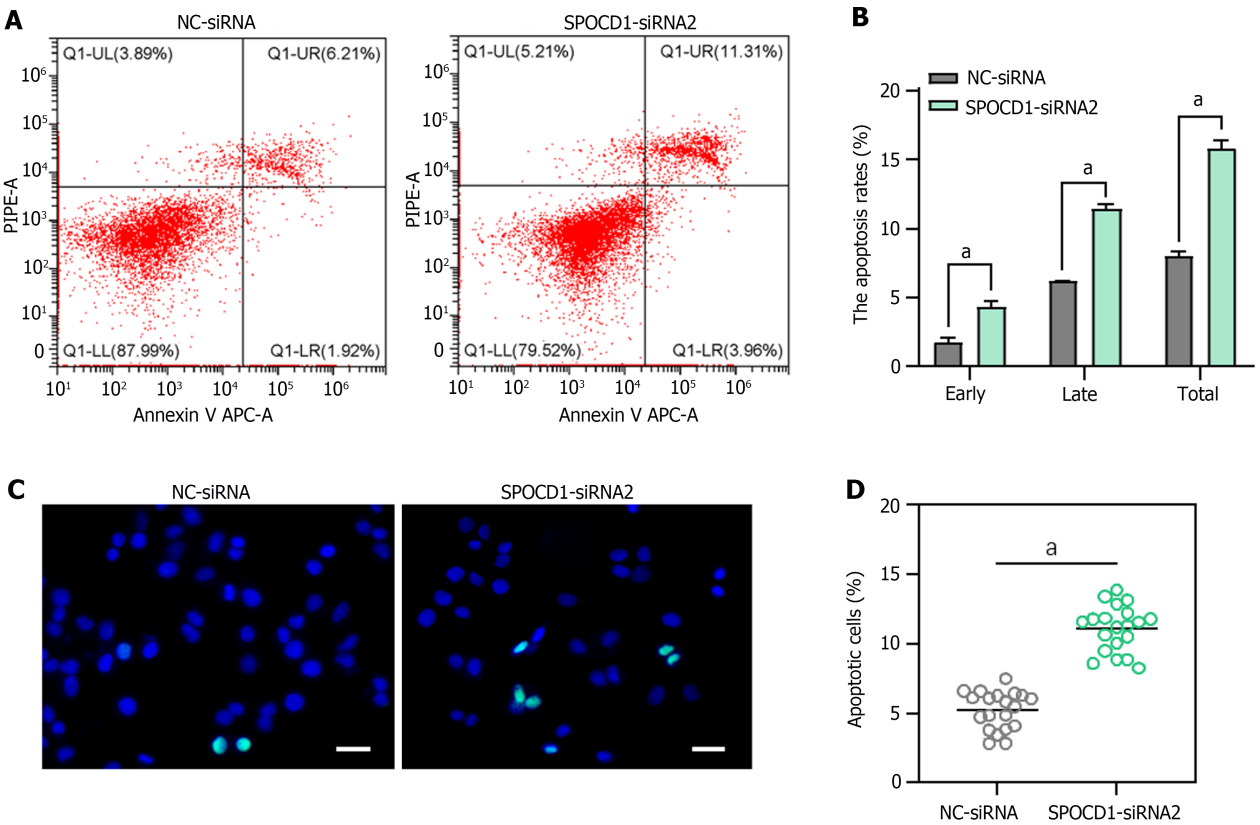

DOI: 10.4252/wjsc.v14.i12.822

Figure 5 Effects of SPOC domain-containing protein 1 inhibition on apoptosis of human spermatogonial stem cells. A and B: Flow cytometry and APC Annexin V analysis show proportions of early and late apoptotic cells in human spermatogonial stem cells (SSCs) transfected with negative control (NC)-small interfering RNA (siRNA) and SPOC domain-containing protein 1-siRNA 2; C and D: Terminal deoxynucleotidyl transferase dUTP nick end labeling (TUNEL) analysis shows proportions of TUNEL-positive cells in human SSCs transfected with NC-siRNA and forkhead box P4 (FOXP4)-siRNA 2. Scale bars in C: 20 μm. $^{a}P < 0.05$.

Although many regulatory mechanisms were revealed in mouse SSCs and restored spermatogenesis in infertile mice by SSC transplantation[20], they were not conserved in humans and mice. Therefore, the regulatory mechanisms of human SSCs remain poorly understood. scRNA-seq has provided us with a transcriptional map of human SSCs, and various potential regulatory molecules of human SSCs have been discovered[21]. By analyzing the testis scRNA data from two studies and performing histological validation, SPOCD1 was found as a molecule specifically expressed in the early developmental stage of human SSCs.

SPOCD1 was first found to interact with testis protein phosphatase 1 in 2011[22]. It is a protein belonging to the transcription factor S-II family of transcription factors. SPOCD1 contains a SPOC domain that can regulate developmental progression and is considered a tumor-associated factor in various tumors[23]. It was shown to be significantly upregulated in many tumors including gastric cancer[24], glioblastoma[25], bladder cancer[26], and ovarian cancer[27]. Knockdown of SPOCD1 significantly inhibited the proliferation, migration, and invasion of gastric cancer cells in nude mice[24]. ADP ribosylation factor 5/Rab35 axis controlled the growth and invasiveness of glioblastoma by inhibiting the levels of SPOCD1[25]. SPOCD1 promotes ovarian cancer progression and inhibits apoptosis through the phosphoinositide 3-kinase/AKT pathway[28]. Recently, it was shown that the conditional knockout of SPOCD1 in the mice testis leads to spermatogenesis arrest in the pachytene stage[29]. Although the study demonstrated the importance of SPOCD1 in male fertility, it focused on the role of SPOCD1 in PIWI-interacting-directed *de novo* DNA methylation. The functions and mechanisms of SPOCD1 in spermatogenesis, especially in SSC fate determination, remain unknown. Our study found that SPOCD1 was mainly localized to human SSCs at an early stage. It was significantly downregulated in some NOA patients. It affected the proliferation and apoptosis of the human SSC lines, consistent with the reported SPOCD1$^{-/-}$ mouse phenotype, suggesting that SPOCD1 may mediate a conserved regulatory pathway in human and mouse SSCs. Additionally, considering that the SSC line originates from primary human spermatogonia transfected with the Large T gene. It overcomes the difficulty of human spermatogonia proliferation in vitro, but it may inevitably produce some genome-scale changes. Our results were obtained from *in vitro* cultured SSC lines, which may differ from the actual situation in the testis.

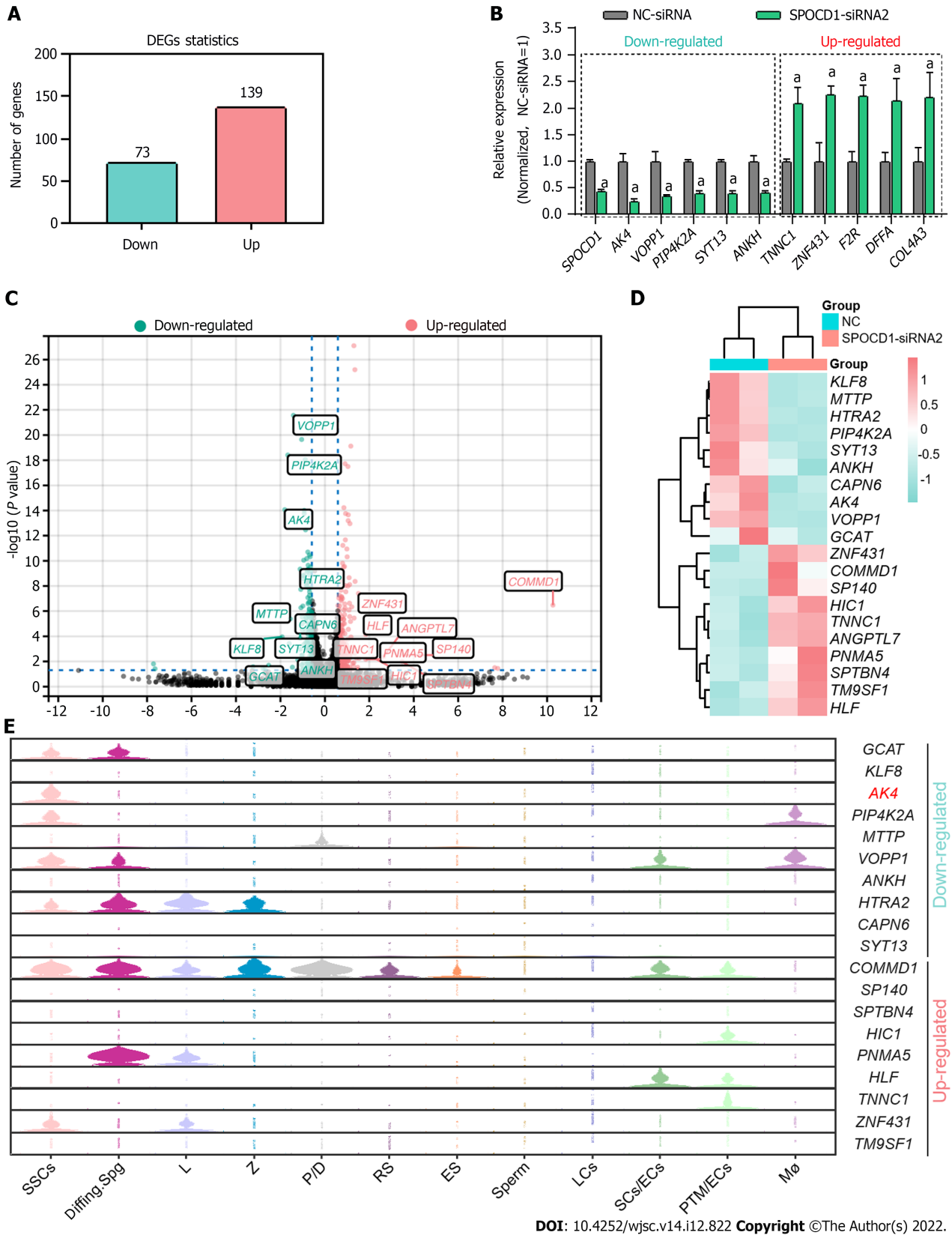

DOI: 10.4252/wjsc.v14.i12.822

Figure 6 Identification of the target genes of SPOC domain-containing protein 1. A: The number of genes was significantly affected by SPOC domain-containing protein 1 (SPOCD1) knockdown; B: Quantitative PCR validated the expression levels of SPOCD1 and 10 randomly selected genes significantly affected by SPOCD1; C: Volcano plot of differential gene expression between negative control (NC)-siRNA and SPOCD1-siRNA2 groups; D: Heatmap analysis of the top 20 differentially expressed genes (DEGs); E: Violin plots show the expression levels of the top 20 DEGs in all testicular cells. $^{a}P < 0.05$.

AK4 is an adenylate kinase family member expressed in the mitochondrial matrix[30]. It is a phosphorylation enzyme that transfers phosphate from ATP or GTP to AMP, generating two molecules of ADP, which help to keep energy homeostasis by balancing the cellular adenine nucleotide

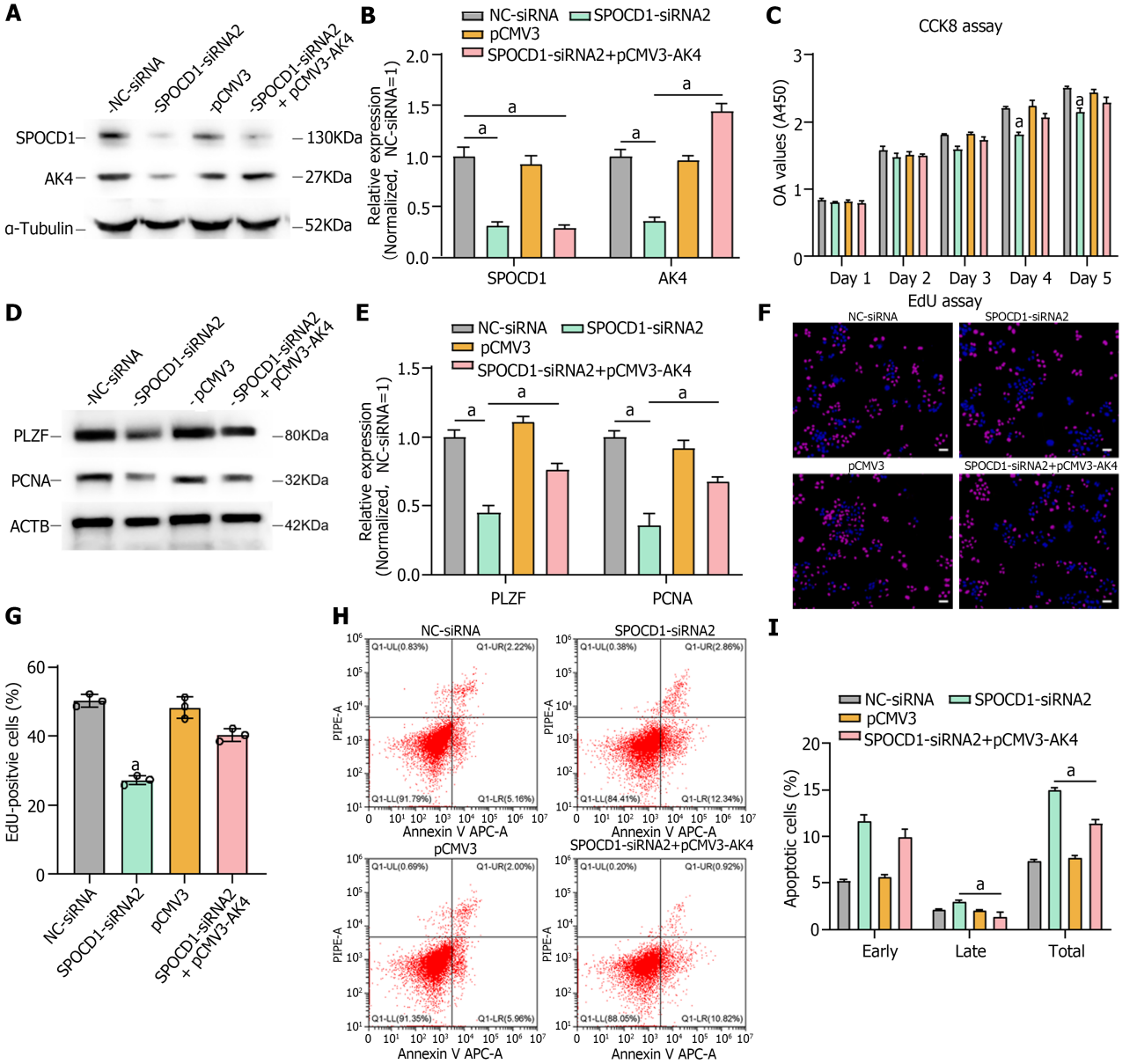

DOI: 10.4252/wjsc.v14.i12.822

Figure 7 SPOC domain-containing protein 1 promotes the proliferation of spermatogonial stem cells *via* adenylate kinase 4. A and B: Western blotting shows the level of adenylate kinase 4 (AK4) after re-expression in SPOC domain-containing protein 1 (SPOCD1) knockdown spermatogonial stem cells (SSCs); C: Cell Counting Kit-8 was used to detect cell proliferation after AK4 was overexpressed in SPOCD1-knockdown SSCs; D and E: Cellular DNA synthesis was detected by 5-ethynyl-2'-deoxyuridine (EdU) analysis; F and G: Western blotting shows the protein levels of promyelocytic leukemia zinc finger (PLZF) and proliferating cell nuclear antigen (PCNA) after transfection with AK4 expression plasmid in SPOCD1 inhibited SSC; H and I: Cell apoptosis analysis after re-expression of AK4 using flow cytometry. Scale bar in D: 20 μm. $^{a}P < 0.05$.

composition[31]. AK4 plays important roles in energy metabolism and tumorigenesis. AK4 promotes lung adenocarcinoma metastasis by modulating oxidative stress and stabilizing hypoxia-inducible 1 alpha[30]. Increased expression of AK4 is involved in tamoxifen resistance through m6A-based epitranscriptomic mechanisms[32]. In addition, AK4 is also involved in energy metabolism, especially glycolysis[33-35]. Given that glycolysis is a major process for energy metabolism in SSCs to promote SSC self-renewal in mice[36], the association of AK4 with glycolysis in SSCs and its effects on SSC proliferation should be further confirmed in more studies.

Our study found many genes affected by SPOCD1 including *AK4*, *KLF8*, *VOPP1*, *ZNF431*, and *COMMD1*. We validated the functions of AK4 in SPOCD1-knockdown cells but did not clarify whether SPOCD1 influenced cell behavior through other pathways. SPOCD1 affects the proliferation of glioma cells *via* pentraxin 3[37]. Thus, whether SPOCD1 can mediate SSC fate determination through different ways remains further investigated. In addition, we tried to detect DNA fragments directly bound by SPOCD1 using the chromatin immunoprecipitation assay. Still, the results were not credible due to the lack of appropriate antibodies. In some NOA patients, we found the significant downregulation in SPOCD1, especially in Spg MA and Spc MA patients. However, it should be noted that the sample size

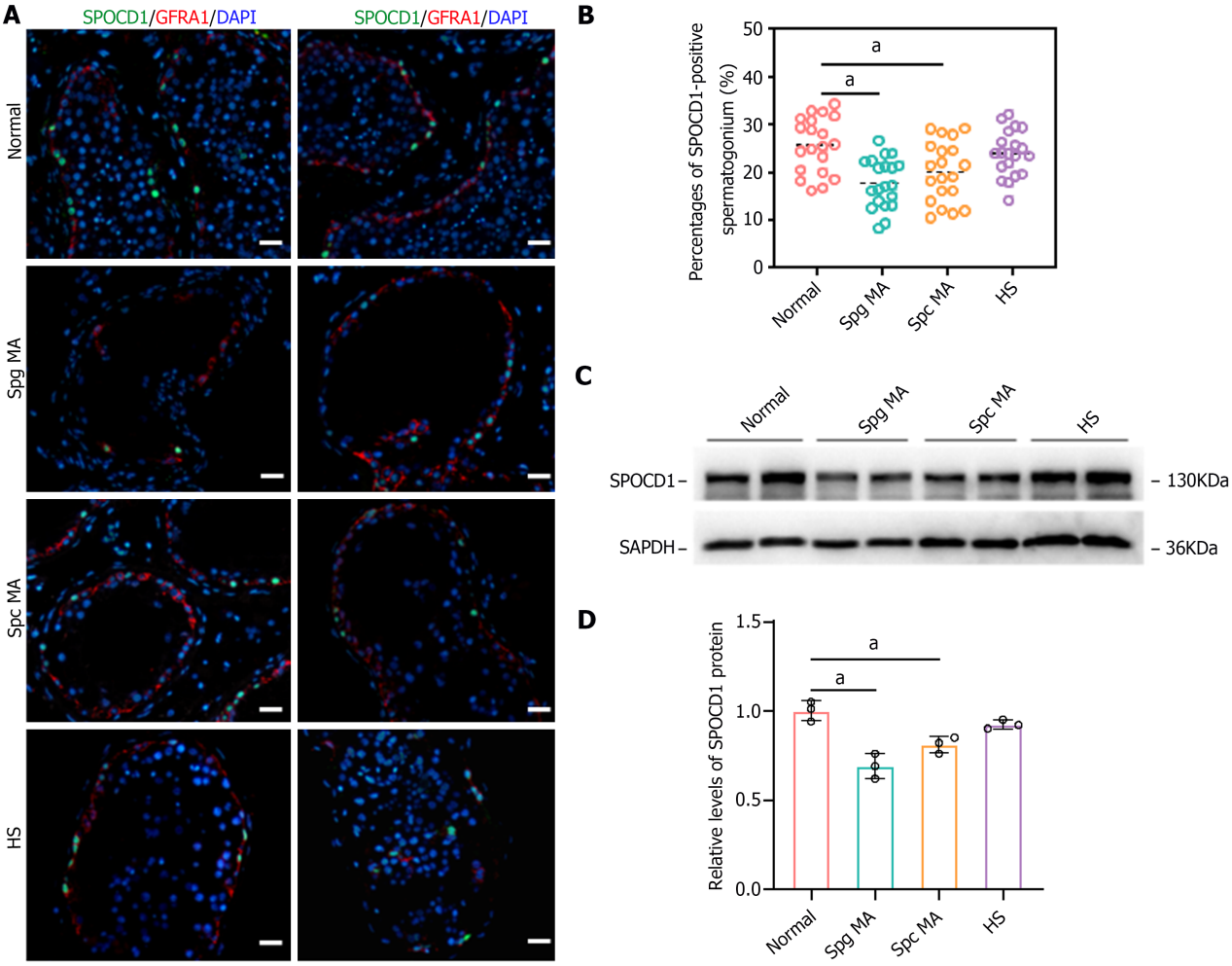

DOI: 10.4252/wjsc.v14.i12.822

Figure 8 SPOC domain-containing protein 1 expression in the testes of obstructive azoospermia and non-obstructive azoospermia patients. A and B: Proportions of glial cell line-derived neurotrophic factor family receptor alpha-1-positive spermatogonial stem cells (red) with SPOC domain-containing protein 1 (SPOCD1) expression (green) in obstructive azoospermia (OA) with normal spermatogenesis and other types of non-obstructive azoospermia (NOA) patients; C and D: Western blot analysis shows SPOCD1 protein levels in OA and NOA patients. In (A), each picture represents one testicular sample. Each group had two samples. HS: Hypospermatogenesis; Normal: Normal spermatogenesis; Spc MA: Spermatocyte maturation arrest; Spg MA: Spermatogonia maturation arrest. Scale bar in A: 50 μm. $^{a}P < 0.05$.

included in our study was limited. According to recent reports[38,39], using computerized deep learning methods may help elucidate the relationship between SPOCD1 and NOA in large samples. A recent study showed that conditional silencing of the SPOCD1 gene in mouse testes resulted in blocked spermatogenesis at the pachytene spermatocyte stage[29]. However, we did not confirm whether SPOCD1 mutations or downregulation resulted in impaired spermatogenesis in humans. Further analysis of SPOCD1 mutations in NOA patients *via* whole-exome sequencing and validating the effects of SPOCD1 mutation would help to clarify the role of SPOCD1 in male reproduction.

sc-seq analysis showed that all testicular cells could be classified into 12 populations, with showed little difference from other reports[17,40]. During data quality control, we selectively retained cells where the percentage of mitochondrial genes was less than 15%. This may have contributed to fewer testicular cells being included. Furthermore, we divided SSCs into three states, which differ from other reports. According to Guo *et al*[17], there are five subtypes of SSCs and differentiating spermatogonia. Sohni *et al*[40] categorized all spermatogonium into five types. The difference could have been related to using different resolution parameters and reduction methods to reduce dimensionality, and only SSCs were included in our re-clustering analysis.

CONCLUSION

We demonstrated that SPOCD1 was predominantly localized to the human SSCs, and its downregulation suppressed cell proliferation and induced apoptosis. Re-expression of AK4 in SPOCD1

knockdown cells reversed the changes in cell proliferation and apoptosis. In addition, we also found that SPOCD1 was significantly downregulated in some patients with NOA. Thus, our study provides new insights into regulating human SSCs and new theories on the etiology of male infertility.

ARTICLE HIGHLIGHTS

Research background

Spermatogonial stem cells (SSCs) are the origin of spermatogenesis, which continuously generates spermatozoa through self-renewal and differentiation. Although we have identified many molecules and pathways that regulate SSC function in mice, the mechanisms regulating human SSCs are not yet fully revealed.

Research motivation

To explore the regulatory mechanisms of human SSCs, we analyzed human testis single-cell RNA sequencing (scRNA-seq) data from the GSE149512 and GSE112013 datasets. We found that SPOC domain-containing protein 1 (SPOCD1) is differentially expressed in human SSCs. This study explored the role of SPOCD1 in human proliferation and apoptosis, which will help to expand the understanding of SSC regulation.

Research objectives

To investigate the functions and mechanisms of SPOCD1 in human proliferation and apoptosis, and to explore the potential effects on spermatogenesis.

Research methods

In this study, scRNA-seq was used to detect differentially expressed genes in human SSCs, in which the SPOCD1 gene is highly expressed in human SSCs. Immunohistochemistry was used to investigate the expression pattern of SPOCD1 in human testicular tissue. Subsequently, we used small interfering RNA to knockdown SPOCD1 in human SSC lines and dissected the role of SPOCD1 in human SSCs by Cell Counting Kit-8, Western blot analysis, 5-ethynyl-2′-deoxyuridine, fluorescence-activated cell sorting, and terminal deoxynucleotidyl transferase dUTP nick end labeling. RNA-seq was used to explore gene expression alterations induced by SPOCD1 downregulation. Finally, we identified the functional target genes of SPOCD1 by rescue experiments.

Research results

The scRNA-seq and immunohistochemical results showed that SPOCD1 was predominantly localized to human SSCs. Knockdown of SPOCD1 in human SSC lines resulted in a significant decrease in cell proliferation and induced apoptosis. RNA-seq results showed that SPOCD1 knockdown caused the significant downregulation of genes such as adenylate kinase 4 (AK4) and affected pathways such as tumor necrosis factor and cyclic AMP. Overexpression of AK4 in SPOCD1 knockdown cells significantly responded to the changes in cell proliferation and apoptosis caused by SPOCD1 inhibition.

Research conclusions

We demonstrated that SPOCD1 was predominantly localized to human SSCs and regulated its proliferation and apoptosis through AK4. Our study provides new insights into regulating human SSCs and potential novel targets for treating male infertility.

Research perspectives

Future studies will explore the correlation between SPOCD1 and abnormal human spermatogenesis in large samples. These include screening for potentially curative mutations of SPOCD1 in azoospermia patients and exploring the association between abnormal SPOCD1 expression and azoospermia in large samples using deep learning.

FOOTNOTES

Author contributions: Fan JY designed the study and supervised the laboratory experiments; Zhou D conducted the experiments and drafted the manuscript; Zhu F assisted in bioinformatics analysis; Huang ZH and Zhang H assisted with the experiments and sample collection; Fan LQ contributed new reagents and analytic tools; all authors read and approved the final manuscript.

Supported by the National Natural Science Foundation for Young Scholars of China, No. 82201771; National Natural Science Foundation of China, No. 32270912; Natural Science Foundation of Changsha, No. kq2202491; Research

Grant of CITIC-Xiangya, No. YNXM202109 and No. YNXM202115; and Hunan Provincial Grant for Innovative Province Construction, No. 2019SK4012.

Institutional review board statement: The study was reviewed and approved by the Reproductive & Genetic Hospital of CITIC-Xiangya, Basic Medical Science School, Central South University Institutional Review Board (Approval No. LL-SC-2021-025).

Informed consent statement: All study participants, or their legal guardian, provided informed written consent prior to study enrollment.

Conflict-of-interest statement: The authors have no conflicts of interest to declare.

Data sharing statement: All data are available from the corresponding author upon reasonable request jingyu@email.sc.edu.

Country/Territory of origin: China

ORCID number: Dai Zhou 0000-0003-4577-8898; Fang Zhu 0000-0001-6234-2901; Zeng-Hui Huang 0000-0003-3242-5946; Huan Zhang 0000-0002-2861-7067; Li-Qing Fan 0000-0001-6021-9520; Jing-Yu Fan 0000-0002-0489-8423.

S-Editor: Chen YL
L-Editor: Filipodia
P-Editor: Cai YX

REFERENCES

1 **Agarwal A**, Baskaran S, Parekh N, Cho CL, Henkel R, Vij S, Arafa M, Panner Selvam MK, Shah R. Male infertility. *Lancet* 2021; **397**: 319-333 [PMID: 33308486 DOI: 10.1016/S0140-6736(20)32667-2]
2 **Tharakan T**, Luo R, Jayasena CN, Minhas S. Non-obstructive azoospermia: current and future perspectives. *Fac Rev* 2021; **10**: 7 [PMID: 33659925 DOI: 10.12703/r/10-7]
3 **de Rooij DG**. Stem cells in the testis. *Int J Exp Pathol* 1998; **79**: 67-80 [PMID: 9709376 DOI: 10.1046/j.1365-2613.1998.00057.x]
4 **Brinster RL**, Avarbock MR. Germline transmission of donor haplotype following spermatogonial transplantation. *Proc Natl Acad Sci U S A* 1994; **91**: 11303-11307 [PMID: 7972054 DOI: 10.1073/pnas.91.24.11303]
5 **Kanatsu-Shinohara M**, Ogonuki N, Inoue K, Miki H, Ogura A, Toyokuni S, Shinohara T. Long-term proliferation in culture and germline transmission of mouse male germline stem cells. *Biol Reprod* 2003; **69**: 612-616 [PMID: 12700182 DOI: 10.1095/biolreprod.103.017012]
6 **Medrano JV**, Rombaut C, Simon C, Pellicer A, Goossens E. Human spermatogonial stem cells display limited proliferation in vitro under mouse spermatogonial stem cell culture conditions. *Fertil Steril* 2016; **106**: 1539-1549.e8 [PMID: 27490045 DOI: 10.1016/j.fertnstert.2016.07.1065]
7 **Meng X**, Lindahl M, Hyvönen ME, Parvinen M, de Rooij DG, Hess MW, Raatikainen-Ahokas A, Sainio K, Rauvala H, Lakso M, Pichel JG, Westphal H, Saarma M, Sariola H. Regulation of cell fate decision of undifferentiated spermatogonia by GDNF. *Science* 2000; **287**: 1489-1493 [PMID: 10688798 DOI: 10.1126/science.287.5457.1489]
8 **Yoshida S**. Stem cells in mammalian spermatogenesis. *Dev Growth Differ* 2010; **52**: 311-317 [PMID: 20388168 DOI: 10.1111/j.1440-169X.2010.01174.x]
9 **Ishii K**, Kanatsu-Shinohara M, Toyokuni S, Shinohara T. FGF2 mediates mouse spermatogonial stem cell self-renewal *via* upregulation of Etv5 and Bcl6b through MAP2K1 activation. *Development* 2012; **139**: 1734-1743 [PMID: 22491947 DOI: 10.1242/dev.076539]
10 **Chen W**, Cui Y, Liu B, Li C, Du L, Tang R, Qin L, Jiang Y, Li J, Yu X, He Q, He Z. Hsa-miR-1908-3p Mediates the Self-Renewal and Apoptosis of Human Spermatogonial Stem Cells *via* Targeting KLF2. *Mol Ther Nucleic Acids* 2020; **20**: 788-800 [PMID: 32438314 DOI: 10.1016/j.omtn.2020.04.016]
11 **Zhou F**, Chen W, Cui Y, Liu B, Yuan Q, Li Z, He Z. miRNA-122-5p stimulates the proliferation and DNA synthesis and inhibits the early apoptosis of human spermatogonial stem cells by targeting CBL and competing with lncRNA CASC7. *Aging (Albany NY)* 2020; **12**: 25528-25546 [PMID: 33231565 DOI: 10.18632/aging.104158]
12 **Zhou F**, Yuan Q, Zhang W, Niu M, Fu H, Qiu Q, Mao G, Wang H, Wen L, Lu M, Li Z, He Z. MiR-663a Stimulates Proliferation and Suppresses Early Apoptosis of Human Spermatogonial Stem Cells by Targeting NFIX and Regulating Cell Cycle. *Mol Ther Nucleic Acids* 2018; **12**: 319-336 [PMID: 30195770 DOI: 10.1016/j.omtn.2018.05.015]
13 **Cui W**, He X, Zhai X, Zhang H, Zhang Y, Jin F, Song X, Wu D, Shi Q, Li L. CARF promotes spermatogonial self-renewal and proliferation through Wnt signaling pathway. *Cell Discov* 2020; **6**: 85 [PMID: 33298864 DOI:

10.1038/s41421-020-00212-7]
14 **Du L**, Chen W, Li C, Cui Y, He Z. RNF144B stimulates the proliferation and inhibits the apoptosis of human spermatogonial stem cells *via* the FCER2/NOTCH2/HES1 pathway and its abnormality is associated with azoospermia. *J Cell Physiol* 2022; **237**: 3565-3577 [PMID: 35699595 DOI: 10.1002/jcp.30813]
15 **Zhou D**, Fan J, Liu Z, Tang R, Wang X, Bo H, Zhu F, Zhao X, Huang Z, Xing L, Tao K, Zhang H, Nie H, Zhu W, He Z, Fan L. TCF3 Regulates the Proliferation and Apoptosis of Human Spermatogonial Stem Cells by Targeting PODXL. *Front Cell Dev Biol* 2021; **9**: 695545 [PMID: 34422820 DOI: 10.3389/fcell.2021.695545]
16 **Hermann BP**, Cheng K, Singh A, Roa-De La Cruz L, Mutoji KN, Chen IC, Gildersleeve H, Lehle JD, Mayo M, Westernströer B, Law NC, Oatley MJ, Velte EK, Niedenberger BA, Fritze D, Silber S, Geyer CB, Oatley JM, McCarrey JR. The Mammalian Spermatogenesis Single-Cell Transcriptome, from Spermatogonial Stem Cells to Spermatids. *Cell Rep* 2018; **25**: 1650-1667.e8 [PMID: 30404016 DOI: 10.1016/j.celrep.2018.10.026]
17 **Guo J**, Grow EJ, Mlcochova H, Maher GJ, Lindskog C, Nie X, Guo Y, Takei Y, Yun J, Cai L, Kim R, Carrell DT, Goriely A, Hotaling JM, Cairns BR. The adult human testis transcriptional cell atlas. *Cell Res* 2018; **28**: 1141-1157 [PMID: 30315278 DOI: 10.1038/s41422-018-0099-2]
18 **Hou J**, Niu M, Liu L, Zhu Z, Wang X, Sun M, Yuan Q, Yang S, Zeng W, Liu Y, Li Z, He Z. Establishment and Characterization of Human Germline Stem Cell Line with Unlimited Proliferation Potentials and no Tumor Formation. *Sci Rep* 2015; **5**: 16922 [PMID: 26585066 DOI: 10.1038/srep16922]
19 **de Rooij DG**, Russell LD. All you wanted to know about spermatogonia but were afraid to ask. *J Androl* 2000; **21**: 776-798 [PMID: 11105904]
20 **Brinster RL**, Zimmermann JW. Spermatogenesis following male germ-cell transplantation. *Proc Natl Acad Sci U S A* 1994; **91**: 11298-11302 [PMID: 7972053 DOI: 10.1073/pnas.91.24.11298]
21 **Chen Y**, Zheng Y, Gao Y, Lin Z, Yang S, Wang T, Wang Q, Xie N, Hua R, Liu M, Sha J, Griswold MD, Li J, Tang F, Tong MH. Single-cell RNA-seq uncovers dynamic processes and critical regulators in mouse spermatogenesis. *Cell Res* 2018; **28**: 879-896 [PMID: 30061742 DOI: 10.1038/s41422-018-0074-y]
22 **Fardilha M**, Esteves SL, Korrodi-Gregório L, Vintém AP, Domingues SC, Rebelo S, Morrice N, Cohen PT, da Cruz e Silva OA, da Cruz e Silva EF. Identification of the human testis protein phosphatase 1 interactome. *Biochem Pharmacol* 2011; **82**: 1403-1415 [PMID: 21382349 DOI: 10.1016/j.bcp.2011.02.018]
23 **Kimura K**, Wakamatsu A, Suzuki Y, Ota T, Nishikawa T, Yamashita R, Yamamoto J, Sekine M, Tsuritani K, Wakaguri H, Ishii S, Sugiyama T, Saito K, Isono Y, Irie R, Kushida N, Yoneyama T, Otsuka R, Kanda K, Yokoi T, Kondo H, Wagatsuma M, Murakawa K, Ishida S, Ishibashi T, Takahashi-Fujii A, Tanase T, Nagai K, Kikuchi H, Nakai K, Isogai T, Sugano S. Diversification of transcriptional modulation: large-scale identification and characterization of putative alternative promoters of human genes. *Genome Res* 2006; **16**: 55-65 [PMID: 16344560 DOI: 10.1101/gr.4039406]
24 **Zhu M**, Yan C, Ren C, Huang X, Zhu X, Gu H, Wang M, Wang S, Gao Y, Ji Y, Miao X, Yang M, Chen J, Du J, Huang T, Jiang Y, Dai J, Ma H, Zhou J, Wang Z, Hu Z, Ji G, Zhang Z, Shen H, Shi Y, Jin G. Exome Array Analysis Identifies Variants in SPOCD1 and BTN3A2 That Affect Risk for Gastric Cancer. *Gastroenterology* 2017; **152**: 2011-2021 [PMID: 28246015 DOI: 10.1053/j.gastro.2017.02.017]
25 **Kulasekaran G**, Chaineau M, Piscopo VEC, Verginelli F, Fotouhi M, Girard M, Tang Y, Dali R, Lo R, Stifani S, McPherson PS. An Arf/Rab cascade controls the growth and invasiveness of glioblastoma. *J Cell Biol* 2021; **220** [PMID: 33443570 DOI: 10.1083/jcb.202004229]
26 **van der Heijden AG**, Mengual L, Lozano JJ, Ingelmo-Torres M, Ribal MJ, Fernández PL, Oosterwijk E, Schalken JA, Alcaraz A, Witjes JA. A five-gene expression signature to predict progression in T1G3 bladder cancer. *Eur J Cancer* 2016; **64**: 127-136 [PMID: 27414486 DOI: 10.1016/j.ejca.2016.06.003]
27 **Wang C**, Wang J, Shen X, Li M, Yue Y, Cheng X, Lu W, Wang X, Xie X. LncRNA SPOCD1-AS from ovarian cancer extracellular vesicles remodels mesothelial cells to promote peritoneal metastasis *via* interacting with G3BP1. *J Exp Clin Cancer Res* 2021; **40**: 101 [PMID: 33726799 DOI: 10.1186/s13046-021-01899-6]
28 **Liu D**, Yang Y, Yan A. SPOCD1 accelerates ovarian cancer progression and inhibits cell apoptosis *via* the PI3K/AKT pathway. *Onco Targets Ther* 2020; **13**: 351-359 [PMID: 32021280 DOI: 10.2147/OTT.S200317]
29 **Zoch A**, Auchynnikava T, Berrens RV, Kabayama Y, Schöpp T, Heep M, Vasiliauskaitė L, Pérez-Rico YA, Cook AG, Shkumatava A, Rappsilber J, Allshire RC, O'Carroll D. SPOCD1 is an essential executor of piRNA-directed de novo DNA methylation. *Nature* 2020; **584**: 635-639 [PMID: 32674113 DOI: 10.1038/s41586-020-2557-5]
30 **Jan YH**, Lai TC, Yang CJ, Lin YF, Huang MS, Hsiao M. Adenylate kinase 4 modulates oxidative stress and stabilizes HIF-1α to drive lung adenocarcinoma metastasis. *J Hematol Oncol* 2019; **12**: 12 [PMID: 30696468 DOI: 10.1186/s13045-019-0698-5]
31 **Jan YH**, Tsai HY, Yang CJ, Huang MS, Yang YF, Lai TC, Lee CH, Jeng YM, Huang CY, Su JL, Chuang YJ, Hsiao M. Adenylate kinase-4 is a marker of poor clinical outcomes that promotes metastasis of lung cancer by downregulating the transcription factor ATF3. *Cancer Res* 2012; **72**: 5119-5129 [PMID: 23002211 DOI: 10.1158/0008-5472.CAN-12-1842]
32 **Liu X**, Gonzalez G, Dai X, Miao W, Yuan J, Huang M, Bade D, Li L, Sun Y, Wang Y. Adenylate kinase 4 modulates the resistance of breast cancer cells to tamoxifen through an m(6)a-based epitranscriptomic mechanism. *Mol Ther* 2020; **28**: 2593-2604 [DOI: 10.1016/j.ymthe.2020.09.007]
33 **Wujak M**, Veith C, Wu CY, Wilke T, Kanbagli ZI, Novoyatleva T, Guenther A, Seeger W, Grimminger F, Sommer N, Schermuly RT, Weissmann N. Adenylate Kinase 4-A Key Regulator of Proliferation and Metabolic Shift in Human Pulmonary Arterial Smooth Muscle Cells *via* Akt and HIF-1α Signaling Pathways. *Int J Mol Sci* 2021; **22** [PMID: 34638712 DOI: 10.3390/ijms221910371]
34 **Zhang S**, Yamada S, Park S, Klepinin A, Kaambre T, Terzic A, Dzeja P. Adenylate kinase AK2 isoform integral in embryo and adult heart homeostasis. *Biochem Biophys Res Commun* 2021; **546**: 59-64 [PMID: 33571905 DOI: 10.1016/j.bbrc.2021.01.097]
35 **Chin WY**, He CY, Chow TW, Yu QY, Lai LC, Miaw SC. Adenylate Kinase 4 Promotes Inflammatory Gene Expression *via* Hif1α and AMPK in Macrophages. *Front Immunol* 2021; **12**: 630318 [PMID: 33790902 DOI: 10.3389/fimmu.2021.630318]

36 **Kanatsu-Shinohara M**, Tanaka T, Ogonuki N, Ogura A, Morimoto H, Cheng PF, Eisenman RN, Trumpp A, Shinohara T. Myc/Mycn-mediated glycolysis enhances mouse spermatogonial stem cell self-renewal. *Genes Dev* 2016; **30**: 2637-2648 [PMID: 28007786 DOI: 10.1101/gad.287045.116]

37 **Liu Q**, Wang XY, Qin YY, Yan XL, Chen HM, Huang QD, Chen JK, Zheng JM. SPOCD1 promotes the proliferation and metastasis of glioma cells by up-regulating PTX3. *Am J Cancer Res* 2018; **8**: 624-635 [PMID: 29736308]

38 **Aurna NF**, Yousuf MA, Taher KA, Azad AKM, Moni MA. A classification of MRI brain tumor based on two stage feature level ensemble of deep CNN models. *Comput Biol Med* 2022; **146**: 105539 [PMID: 35483227 DOI: 10.1016/j.compbiomed.2022.105539]

39 **Ahamed KU**, Islam M, Uddin A, Akhter A, Paul BK, Yousuf MA, Uddin S, Quinn JMW, Moni MA. A deep learning approach using effective preprocessing techniques to detect COVID-19 from chest CT-scan and X-ray images. *Comput Biol Med* 2021; **139**: 105014 [PMID: 34781234 DOI: 10.1016/j.compbiomed.2021.105014]

40 **Sohni A**, Tan K, Song HW, Burow D, de Rooij DG, Laurent L, Hsieh TC, Rabah R, Hammoud SS, Vicini E, Wilkinson MF. The Neonatal and Adult Human Testis Defined at the Single-Cell Level. *Cell Rep* 2019; **26**: 1501-1517.e4 [PMID: 30726734 DOI: 10.1016/j.celrep.2019.01.045]

World Journal of Stem Cells

Submit a Manuscript: https://www.f6publishing.com

World J Stem Cells 2022 December 26; 14(12): 839-850

DOI: 10.4252/wjsc.v14.i12.839

ISSN 1948-0210 (online)

ORIGINAL ARTICLE

Basic Study

Optimal concentration of mesenchymal stem cells for fracture healing in a rat model with long bone fracture

Myung-Seo Kim, Hyun-Ju Chung, Kang-Il Kim

Specialty type: Cell and tissue engineering

Provenance and peer review: Unsolicited article; Externally peer reviewed.

Peer-review model: Single blind

Peer-review report's scientific quality classification

Grade A (Excellent): 0
Grade B (Very good): B
Grade C (Good): C, C
Grade D (Fair): 0
Grade E (Poor): 0

P-Reviewer: Prasetyo EP, Indonesia; Ventura C, Italy

Received: September 27, 2022
Peer-review started: September 27, 2022
First decision: October 10, 2022
Revised: October 30, 2022
Accepted: December 7, 2022
Article in press: December 7, 2022
Published online: December 26, 2022

Myung-Seo Kim, Kang-Il Kim, Department of Orthopaedic Surgery, School of Medicine, Kyung Hee University and Kyung Hee University Hospital at Gangdong, Seoul 05278, South Korea

Hyun-Ju Chung, Department of Core Research Laboratory, Clinical Research Institute, Kyung Hee University Hospital at Gangdong, Seoul 05278, South Korea

Corresponding author: Kang-Il Kim, MD, PhD, Professor, Department of Orthopaedic Surgery, School of Medicine, Kyung Hee University and Kyung Hee University Hospital at Gangdong, 892, Dongnam-ro, Gangdong-gu, Seoul 05278, South Korea. khuknee@gmail.com

Abstract

BACKGROUND

There is still no consensus on which concentration of mesenchymal stem cells (MSCs) to use for promoting fracture healing in a rat model of long bone fracture.

AIM

To assess the optimal concentration of MSCs for promoting fracture healing in a rat model.

METHODS

Wistar rats were divided into four groups according to MSC concentrations: Normal saline (C), 2.5 × 10^6 (L), 5.0 × 10^6 (M), and 10.0 × 10^6 (H) groups. The MSCs were injected directly into the fracture site. The rats were sacrificed at 2 and 6 wk post-fracture. New bone formation [bone volume (BV) and percentage BV (PBV)] was evaluated using micro-computed tomography (CT). Histological analysis was performed to evaluate fracture healing score. The protein expression of factors related to MSC migration [stromal cell-derived factor 1 (SDF-1), transforming growth factor-beta 1 (TGF-β1)] and angiogenesis [vascular endothelial growth factor (VEGF)] was evaluated using western blot analysis. The expression of cytokines associated with osteogenesis [bone morphogenetic protein-2 (BMP-2), TGF-β1 and VEGF] was evaluated using real-time polymerase chain reaction.

RESULTS

Micro-CT showed that BV and PBV was significantly increased in groups M and H compared to that in group C at 6 wk post-fracture (P = 0.040, P = 0.009; P = 0.004, P = 0.001, respectively). Significantly more cartilaginous tissue and immature bone were formed in groups M and H than in group C at 2 and 6 wk post-fracture (P = 0.018, P = 0.010; P = 0.032, P = 0.050, respectively). At 2 wk post-

fracture, SDF-1, TGF-β1 and VEGF expression were significantly higher in groups M and H than in group L (P = 0.031, P = 0.014; P < 0.001, P < 0.001; P = 0.025, P < 0.001, respectively). BMP-2 and VEGF expression were significantly higher in groups M and H than in group C at 6 wk post-fracture (P = 0.037, P = 0.038; P = 0.021, P = 0.010). Compared to group L, TGF-β1 expression was significantly higher in groups H (P = 0.016). There were no significant differences in expression levels of chemokines related to MSC migration, angiogenesis and cytokines associated with osteogenesis between M and H groups at 2 and 6 wk post-fracture.

CONCLUSION

The administration of at least 5.0 × 10^6 MSCs was optimal to promote fracture healing in a rat model of long bone fractures.

Key Words: Rat model; Femoral shaft fracture; Mesenchymal stem cells; Direct injection; Optimal concentration; Fracture healing

Core Tip: This study focused on the optimal concentration of mesenchymal stem cells (MSCs) that affect fracture healing in a rat model of long bone shaft fracture. Factors related to the homing effect of MSCs, osteogenesis and angiogenesis were analyzed by *in vivo* (radiographic and histologic evaluation) as well as *in vitro* (reverse transcriptase-polymerase chain reaction and western blot analysis). Among the various concentrations used, the administration of at least 5.0 × 10^6 MSCs was optimal to promote the therapeutic effect on fracture healing.

Citation: Kim MS, Chung HJ, Kim KI. Optimal concentration of mesenchymal stem cells for fracture healing in a rat model with long bone fracture. *World J Stem Cells* 2022; 14(12): 839-850
URL: https://www.wjgnet.com/1948-0210/full/v14/i12/839.htm
DOI: https://dx.doi.org/10.4252/wjsc.v14.i12.839

INTRODUCTION

Long bone fractures, such as those of the femur, tibia, and humerus, occur mainly in working-age adults [1] and are caused by high-energy trauma[2]. Long bone fractures have a high incidence of nonunion owing to the complex and specific anatomical area of the fracture[3]. Intramedullary nailing is the treatment of choice for femoral shaft fractures[4]; however, the risk of nonunion in this procedure has been reported to be up to 13%, even after nailing[5]. As femur has a significant weight-bearing role, the fracture nonunion can cause an increase in morbidity[2]. Moreover, it may be impossible for patients to return to normal daily activities after an injury[6]. Ekegren *et al*[3] reported that among fracture healing complications, the post-operative readmission rate was highest for femoral shaft fractures, followed by tibial shaft fractures. Among these, nonunion has been reported to be the most common cause. The nonunion rate has been reported to be up to 33% after intramedullary nailing in humerus and femur shaft fractures, and a relatively high nonunion rate of approximately 5%-7% has also been reported in tibial shaft fractures[7]. Thus, when nonunion occurs in long bone fractures, significant disability occurs and quality of life deteriorates, resulting in a high socioeconomic burden during treatment[3,7]. Therefore, preventing nonunion during the initial surgery of shaft fractures in long bones is important for improving patient prognosis.

Autologous cells with regeneration potential have emerged as a novel method to replace the standard method of bone repair[8-10]. Mesenchymal stem cells (MSCs) have the potential to promote both osteoinduction and osteogenesis[11]. Stem cell therapy using this type of cell has an important effect in promoting the bone-healing process[8,10]; some animal studies have reported that MSCs improve fracture healing[12]. Wilson *et al*[12] evaluated the extent of bone defect regeneration in the ramus of swine with or without MSC injection. They reported that bone healing was accelerated in a group injected with MSCs[12,13]. Obermeyer *et al*[13] reported that the administration of MSCs increased the volume and biomechanical strength of the callus in an alcohol-induced impaired fracture healing mouse model, resulting in accelerated fracture healing. Some previous studies have reported that injection of MSCs improves fracture healing; however, no studies have specifically reported the most effective concentration of MSC. Although a concentration of 5.0 × 10^6 MSCs was mainly used in several previous studies[10-12], there was no rationale for this selection. Therefore, this study aimed to confirm the ability of MSCs and assess their optimal concentration to promote fracture healing in a rat model of long bone fracture. The authors hypothesized that administration of at least 5.0 × 10^6 MSCs would signi-

ficantly improve fracture healing.

MATERIALS AND METHODS

Animal model

Forty-eight adult male Wistar rats (8 wk old with 200-250 g weight) were obtained from the Orient Bio Institute, Seongnam City, Gyeonggi-do, Republic of Korea. All procedures and treatments involving animals in this study followed the requirements of the Institutional Animal Care and Use Committee of the Clinical Research Institute, and the final approval was obtained from the ethics committee of Kyung Hee University Hospital at Gangdong (KHNMC AP 2020-018). The rats had free access to food and water and were bred in a controlled environment at 21 ± 2 °C with a 12-h/12-h light/dark cycle.

Long bone fracture model and MSC injection

The femoral shaft, which is a representative long bone, was used as the fracture model in this study. Under general anesthesia, the right lower extremities of the rats were shaved and disinfected. First, the approach was performed using an anterior midline incision. After exposing the right knee joint by dislocating the patella medially, the intercondylar groove of the femur was exposed by flexion of the knee joint. An 18-gauge needle was retrogradely inserted into the center of the intercondylar groove to prevent significant displacement during the fracture. Since the proximal end of the needle protruding into the knee joint can affect the knee joint range of motion, we cut it and inserted the proximal end of the needle into the distal femur. Next, the femoral shaft was approached through a lateral approach, taking care to avoid damage to the periosteum. After applying an oscillating thin saw at a depth of 1 mm, a fracture was generated in the femoral shaft using the 3-point bending technique[14]. Sterile saline was injected into the fracture site to minimize the periosteal damage owing to heat when applying the saw. After inserting the needle tip into the fracture site, the muscular fascia was closed, the adipose-derived (AD)-MSCs were mixed with 0.3 mL sterile normal saline, and the cells were injected once directly into the fracture site. The muscular fascia was repaired before direct injection of the cell suspension to prevent AD-MSCs from flowing out. Other weight-bearing activities were unrestricted post operatively.

Preparation of MSCs

Human AD-MSCs (Jointstem; R-Bio, Seoul, Korea) were used in this study[15,16]. Three weeks before injection, human adipose tissue was collected by lipoaspiration using the tumescent technique. The aspirated tissue was digested with collagenase I to obtain AD-MSCs, and the digested tissue was centrifuged after removing cellular debris. The obtained pellet was resuspended in Dulbecco's modified Eagle's medium (DMEM; Invitrogen)-based medium containing 0.2 mmol/L ascorbic acid and 10% fetal bovine serum, and the cell suspension was recentrifuged. When the cells reached 90% confluence by resuspension and recentrifugation, they were passaged[16]. AD-MSCs at passage 3 were used in this study. AD-MSCs were prepared under Good Manufacturing Practice conditions at the Stem Cell Research Center of RNL BIO. The expanded cells were then tested for number, viability, purity, identity, and fungal, bacterial, endotoxin, and mycoplasma contamination, as suggested by the Code of Federal Regulations Title 21, before further use. Cultured AD-MSCs showed a survival rate of over 80% between 2 and 8 °C for 72 h[15]. Immediately before injection, 2.5×10^6, 5.0×10^6, and 10.0×10^6 AD-MSCs were counted using a hemocytometer[17]. The prepared AD-MSCs were injected into rats within one day of arrival at the animal laboratory.

Categorization according to the concentration of administered MSCs

After breeding for one week, the rats were randomly divided into four groups (n = 6 in each group): Rats injected with normal saline (C), 2.5×10^6 (L), 5.0×10^6 (M), and 10.0×10^6 (H) groups. Several studies have reported the injection of 5×10^6 MSCs into animal models[10-12]. In particular, Wilson *et al*[12] injected 5.0×10^6 MSCs based on the study by Hou *et al*[18] that concluded that > 3.0×10^6 MSCs should be injected for bone healing. Therefore, a concentration of 5.0×10^6 MSCs were used as a reference in this study. The highest concentration was set as 10.0×10^6, according to a previous study that reported that the effective dose for fracture healing was between 2.0×10^6 and 10.0×10^6 MSCs[19]. Moreover, 2.5×10^6 cells, an intermediate concentration between normal saline and 5.0×10^6 cells, was set as the lowest concentration.

At 2 and 6 wk post-fracture, the rats were sacrificed to harvest femur specimens, and the intramedullary needle was removed. Six weeks post-fracture has been reported as an important time point for fracture healing in previous studies[20-22]; hence, 6 wk after fracture was chosen in this study to evaluate the late phase of fracture healing. Wang *et al*[20] reported that the expression of transforming growth factor-beta 1 (TGF-β1), a chemokine that has an important effect on MSC migration, peaked at 2 wk post-fracture. Moreover, it is known that the renewal phase, in which MSCs proliferate and differentiate, usually occurs 7-10 d post-fracture[23]. In this study, the expression levels

Table 1 Fracture healing scores according to the histological findings

Score	Histological findings
1	Fibrous tissue
2	Predominantly fibrous tissue with small amount of cartilage
3	Equal mixture of fibrous and cartilaginous tissue
4	Predominantly cartilage with small amount of fibrous tissue
5	Cartilage
6	Predominantly cartilage with small amount of immature bone
7	Equal mixture of cartilage and immature bone
8	Predominantly immature bone with small amount of cartilage
9	Union of fracture fragments by immature bone
10	Union of fracture fragments by mature bone

of factors related to MSC migration were also analyzed. Referring to the above studies, the early phase was set at 2 wk post-fracture.

Assessment of fracture healing (in vivo studies)

Radiologic evaluation through micro-computed tomography: Micro-computed tomography (micro-CT) was used to evaluate the volume of the newly formed callus [bone volume (BV)] and the percentage of BV [(PBV), calculated as BV/tissue volume]. A 6-mm long section centered on the fracture site was analyzed. Preexisting cortical bone and medullary canal volumes were excluded according to the method described by Wang *et al*[20]. The femur specimens were scanned using three-dimensional micro-focus micro-CT (Sky-Scan 1172™, Skyscan, Kontich, Belgium) at 10 μm resolution, 440 ms exposure, 0.4° rotation step, 80 kV, and 167 μm with a 0.5 mm aluminum filter.

Histological evaluation: Decalcification was performed using a rapid decalcifier solution (RDO, Apex Engineering Products Corporation) at room temperature for three days. The RDO solution was replaced daily. The decalcification process and endpoint were assessed using a surgical blade and radiographic analysis, wherein in the opacity of the tissue suggested incomplete decalcification. The femur specimen was sagittally sectioned to a thickness of 3 μm and stained with hematoxylin and eosin (H&E) (Sigma-Aldrich) for histological analysis. The slides were visualized using an Olympus CX41 microscope (Olympus Co., Tokyo, Japan). Fracture healing was evaluated using a histological scoring tool for fracture healing[24] (Table 1).

Assessment of fracture healing (in vitro studies)

Western blot analysis: Rat femur specimens were ground in liquid nitrogen and incubated with lysis buffer containing 140 mmol/L NaCl, 50 mmol/L NaF, 1 mmol/L EDTA, 1 mmol/L Na_3VO_4, 1 mmol/L phenylmethylsulfonyl fluoride, 10 μg/mL aprotinin, and 1% (w/v) Nonidet P-40 in 20 mmol/L Tris-HCl (pH 7.4). Protein fractions were separated by sodium dodecyl sulfate-polyacrylamide gel electrophoresis on 12% polyacrylamide gels and electrotransferred onto PVDF membranes (Bio-Rad, Hercules, CA, United States). The membranes were then blocked with Tris-buffered saline buffer consisting of 1% nonfat dry milk and 1% bovine serum albumin for 1 h. Next, membranes were then incubated overnight at 4 °C with primary antibodies against stromal cell-derived factor 1 (SDF-1) (Abcam, Cat # ab18919, 1:3000), TGF-β1 (Abcam, Cat # ab215715, 1:3000), vascular endothelial growth factor (VEGF) (Santa Cruz, SC-7269, 1:2000) and β-actin (Santa Cruz Biotechnology; 1:1000). The membranes were developed for 1 h peroxidase-conjugated anti-rabbit immunoglobulin G (Santa Cruz Biotechnology). The blots were visualized using a ChemicDoc XRS system (Bio-Rad), and protein concentrations were quantified using the Quantity One imaging software (Bio-Rad). All experiments were performed in triplicates.

Real-time quantitative polymerase chain reaction: Total RNA from the rat femur specimens was extracted using an RNeasy Mini Kit (Qiagen, Hilden, Germany), according to the manufacturer's protocol. RNA was reverse transcribed using Superscript II reverse transcriptase (Life Technologies) at 42 °C *via* random hexamer priming. The quantitative polymerase chain reaction (qPCR) conditions were as follows: Pre-denaturation at 95 °C for 5 min, denaturation at 95 °C for 10 s, and annealing at 60 °C for 30 s for a total of 40 cycles, followed by fluorescence signal detection during annealing. Glyceraldehyde 3-phosphate dehydrogenase was used as an internal reference for normalization. The reactions were performed using the StepOnePlus Real-Time PCR System (Applied Biosystems, Foster City, CA, United States). The sequences of the primers used for reverse transcriptase-qPCR (RT-qPCR) are listed in Supplementary Table 1.

Statistical analysis: Based on the concentration of MSCs, one-way analysis of variance and *post hoc* analyses were performed to evaluate the differences in micro-CT, histological scores of fracture healing, and mRNA and protein expression (as evidenced by RT-qPCR and western blot results, respectively). Statistical significance was set $P = 0.05$, with 95% confidence interval. SPSS version 21.0 software (SPSS, Inc., Chicago, Illinois, United States) was used for all statistical analyses.

RESULTS

In vivo studies

Fracture healing as evaluated *via* micro-CT analysis: At 2 and 6 wk post-fracture, BV was significantly higher in group M and H than in group C ($P = 0.048$, $P = 0.040$ and $P = 0.023$, $P = 0.009$, respectively). There was no significant difference in BV between M and H groups ($P = 0.999$ and $P = 0.887$). There was no significant difference in PBV between four groups at 2 wk post-fracture. However, PBV was significantly increased in groups M and H compared to that in group C ($P = 0.004$ and $P = 0.001$, respectively) and group L ($P = 0.026$ and $P = 0.003$, respectively) at 6 wk post-fracture. There was no significant difference in the PBV between groups M and H ($P = 0.425$) (Table 2, Figures 1 and 2).

Histological scores of fracture healing evaluated using H&E staining: The formation of fibrous, cartilaginous, and immature bones was evaluated using histological scores. At 2 and 6 wk post-fracture, there was no significant difference in the fracture healing scores between groups C and L (2.8 ± 0.5 *vs* 3.8 ± 0.5, $P = 1.000$ and 5.3 ± 0.5 *vs* 6.5 ± 1.7, $P = 1.000$, respectively). Significantly more cartilaginous tissue was formed in groups M (5.5 ± 1.3) and H than in group C ($P = 0.018$ and $P = 0.010$, respectively) at 2 wk post-fracture (Figure 3). Moreover, significantly more immature bone was formed in groups M (8.8 ± 1.9) and H (8.5 ± 1.3) than in the group injected with normal saline ($P = 0.032$ and $P = 0.050$, respectively) at 6 wk post-fracture (Figure 4).

In vitro studies

Comparison of protein expression levels of chemokines related to MSC migration and angiogenesis at 2 wk post-fracture: The fold change in mRNA expression (all reported values are fold-changes relative to the comparator) of SDF-1 was significantly higher in groups L, M, and H than in group C ($P < 0.001$ all). Compared to group L, groups M and H showed significantly higher SDF-1 expression ($P = 0.031$, $P = 0.014$, respectively). There was no significant difference in SDF-1 expression between groups M and H ($P = 0.974$). TGF-β1 expression was significantly higher in groups L, M and H than in group C ($P = 0.003$, $P < 0.001$, $P < 0.001$, respectively). Compared to group L, groups M and H also showed significantly higher TGF-β1 expression at 2 wk post-fracture ($P < 0.001$, all). There was no significant difference in TGF-β1 expression between groups M and H ($P = 0.997$). VEGF expression was significantly higher in groups M and H than in group C ($P < 0.001$, all). In addition, VEGF expression was significantly higher in groups M and H than in group L ($P = 0.025$, $P < 0.001$, respectively). There was no significant difference in VEGF expression between groups M and H ($P = 0.239$) (Figures 5 and 6) (Supplementary Table 2).

Comparison of the mRNA expression levels of osteogenesis-related factors and chemokine related to angiogenesis at 6 wk post-fracture: Bone morphogenetic protein-2 (BMP-2) expression was significantly higher in groups L, M, and H than in group C ($P < 0.001$, all). Compared to group L, BMP-2 expression was significantly higher in groups M and H ($P = 0.037$, $P = 0.038$, respectively). There was no significant difference in BMP-2 expression between groups M and H ($P = 1.000$). TGF-β1 expression was significantly higher in groups L, M and H than in group C ($P = 0.002$, $P < 0.001$, $P < 0.001$, respectively). Compared to group L, TGF-β1 expression was significantly higher in groups H ($P = 0.016$). There was no significant difference in TGF-β1 expression between groups M and H ($P = 0.824$).

VEGF expression was significantly higher in groups L, M and H than in group C ($P < 0.001$, all). In addition, VEGF expression was significantly higher in groups M and H than in group L ($P = 0.021$, $P = 0.010$, respectively). There was no significant difference in VEGF expression between groups M and H ($P = 0.943$) (Figure 7) (Supplementary Table 3). The protein expression levels of BMP-2, TGF- β1 and VEGF are listed in Supplementary Table 4.

DISCUSSION

In this study, fracture healing was significantly improved in the groups injected with MSCs compared with that in the control group. In addition, after injection of MSCs at different concentrations, the mRNA and protein expression of genes related to MSC migration, angiogenesis, and osteogenesis were higher in groups injected with 5.0×10^6 and 10×10^6 MSCs than in the group injected with 2.5×10^6 MSCs. This study is meaningful as it is the first animal study to confirm that an MSC concentration of

Table 2 Radiologic evaluation of the fractures using micro-computed tomography analysis

		Normal saline	2.5 × 10^6	5.0 × 10^6	10.0 × 10^6
Two weeks post-fracture	BV (μm^3)	34.9 ± 3.1	37.3 ± 4.5	45.3 ± 2.9	45.7 ± 4.9
	Normal saline	-	0.878	0.048	0.040
	2.5 × 10^6	0.878	-	0.137	0.112
	5.0 × 10^6	0.048	0.137	-	0.999
	10.0 × 10^6	0.040	0.112	0.999	-
	PBV (TV/BV, %)	7.3 ± 0.8	9.0 ± 0.5	10.8 ± 1.2	11.0 ± 2.6
	Normal saline	-	0.517	0.079	0.067
	2.5 × 10^6	0.517	-	0.509	0.445
	5.0 × 10^6	0.079	0.509	-	0.999
	10.0 × 10^6	0.067	0.445	0.999	-
Six weeks post-fracture	BV (μm^3)	71.3 ± 8.0	78.7 ± 8.8	101.4 ± 14.0	107.2 ± 6.9
	Normal saline	-	0.798	0.023	0.009
	2.5 × 10^6	0.798	-	0.083	0.030
	5.0 × 10^6	0.023	0.083	-	0.887
	10.0 × 10^6	0.009	0.030	0.887	-
	PBV (TV/BV, %)	13.4 ± 2.2	15.0 ± 3.1	20.5 ± 2.2	23.6 ± 3.3
	Normal saline	-	0.769	0.004	0.001
	2.5 × 10^6	0.769	-	0.026	0.003
	5.0 × 10^6	0.004	0.026	-	0.425
	10.0 × 10^6	0.001	0.003	0.425	-

CT: Computed tomography; BV: Bone volume; PBV: Percentage bone volume; TV: Tissue volume.

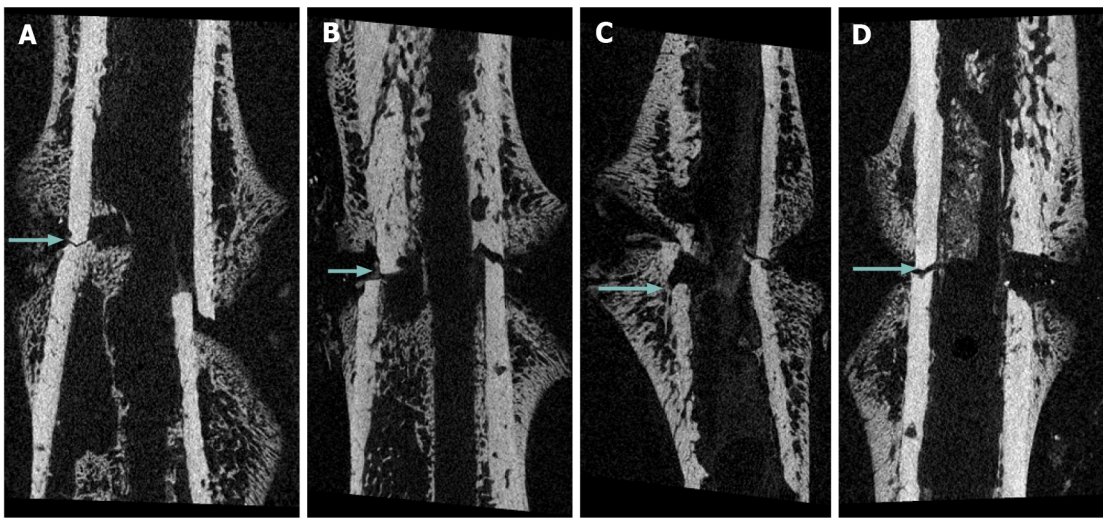

DOI: 10.4252/wjsc.v14.i12.839

Figure 1 Micro-computed tomography imaging at 2 wk post-fracture. A: Rats were injected with normal saline; B: Rats were injected with 2.5 × 10^6 mesenchymal stem cells (MSCs); C: Rats were injected with 5.0 × 10^6 MSCs; D: Rats were injected with 10.0 × 10^6 MSCs. Callus formation was observed in all groups; however, fracture lines (arrows) were clearly observed, indicating that union had not yet occurred.

5.0 × 10^6 cells, which has been used in several previous studies, maximizes fracture healing.

The nonunion of long bone fractures results in a high socioeconomic burden and long treatment duration[7]. Studies aimed at enhancing fracture healing through bone regeneration[25,26] and those

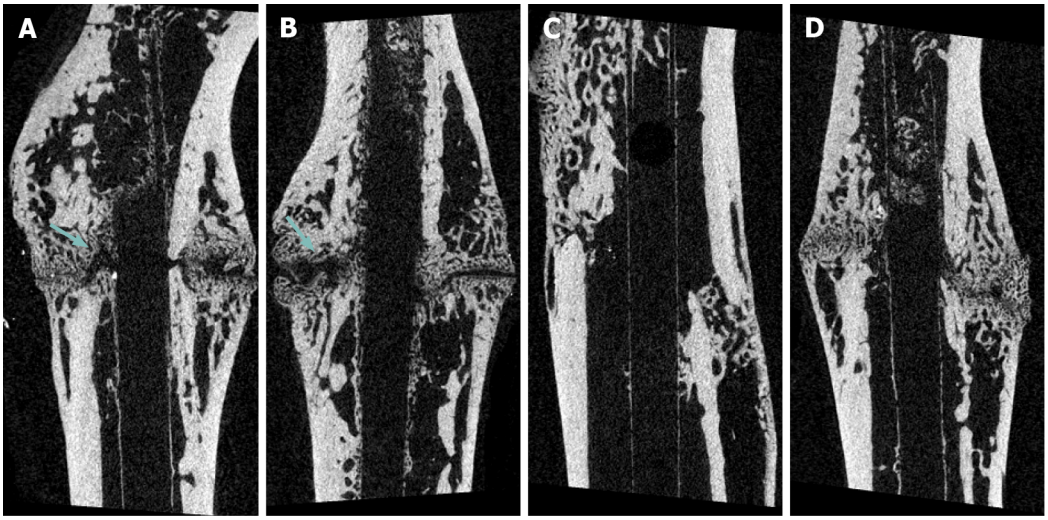

DOI: 10.4252/wjsc.v14.i12.839 **Copyright** ©The Author(s) 2022.

Figure 2 Micro-computed tomography imaging at 6 wk post-fracture. A: Rats were injected with normal saline; B: Rats were injected with 2.5 × 10^6 adipose-derived-mesenchymal stem cells (AD-MSCs); C: Rats were injected with 5.0 × 10^6 AD-MSCs; D: Rats were injected with 10.0 × 10^6 AD-MSCs. In the group injected with normal saline and 2.5 × 10^6 AD-MSCs, fracture lines (arrows) were clearly observed, indicating that union had not yet occurred.

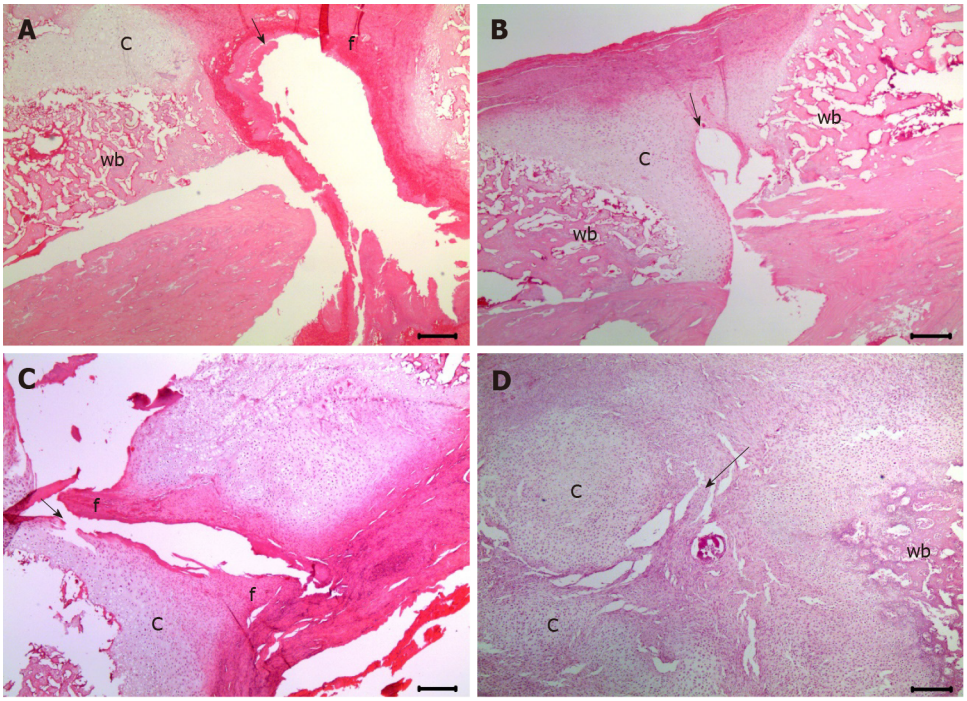

DOI: 10.4252/wjsc.v14.i12.839 **Copyright** ©The Author(s) 2022.

Figure 3 Assessment of histological scores for fracture healing at 2 wk post-fracture using hematoxylin and eosin staining (200 × magnification). A: The histological score was 2 in the group injected with normal saline; B: The histological score was 3 in the group injected with 2.5 × 10^6 mesenchymal stem cells (MSCs); C: The histological score was 4 in the groups injected with 5.0 × 10^6 MSCs; D: The histological score was 4 in the groups injected with 10.0 × 10^6 MSCs. The black arrows indicate the fracture lines. c: Cartilage in the fracture area; f: Fibrous tissue; wb: Woven bone.

that used MSCs as a cell therapy have been conducted[12,13,27]. Obermeyer *et al*[13] compared fracture healing after the injection of MSCs and saline in an animal model of impaired fracture healing. They reported that significantly more callus formation was observed in the group injected with MSCs and that MSCs migrated and homed to the fracture site, contributing to fracture healing. However, they evaluated only the migration of labeled MSCs to the fracture site *via* immunofluorescence staining; they did not quantitatively evaluate the levels of factors related to MSC homing.

The homing of MSCs to the fracture site is a key mechanism during the early stages of fracture healing. After MSCs are recruited to a fracture site, they differentiate into osteogenic cells to enhance healing[28]. In addition, Caplan[29] reported that directly injected MSCs did not differentiate in the

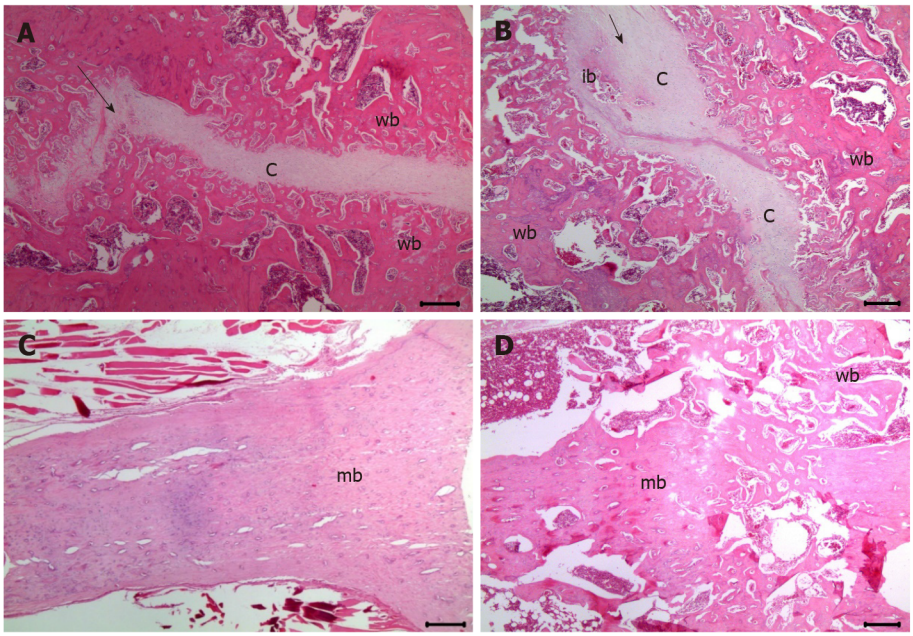

DOI: 10.4252/wjsc.v14.i12.839 **Copyright** ©The Author(s) 2022.

Figure 4 Assessment of histological scores for fracture healing at 6 wk post-fracture using hematoxylin and eosin staining (200 × magnification). A: The histological score was 5 in the groups injected with normal saline; B: The histological score was 5 in the groups injected with 2.5 × 10^6 mesenchymal stem cells (MSCs); C: The histological score was 9 in the group injected with 5.0 × 10^6 MSCs; D: The histological score was 10 in the group injected with 10.0 × 10^6 MSCs. The black arrows indicate the fracture lines. c: Cartilage in the fracture area; wb: Woven bone; ib: Immature bone; mb: Mature bone.

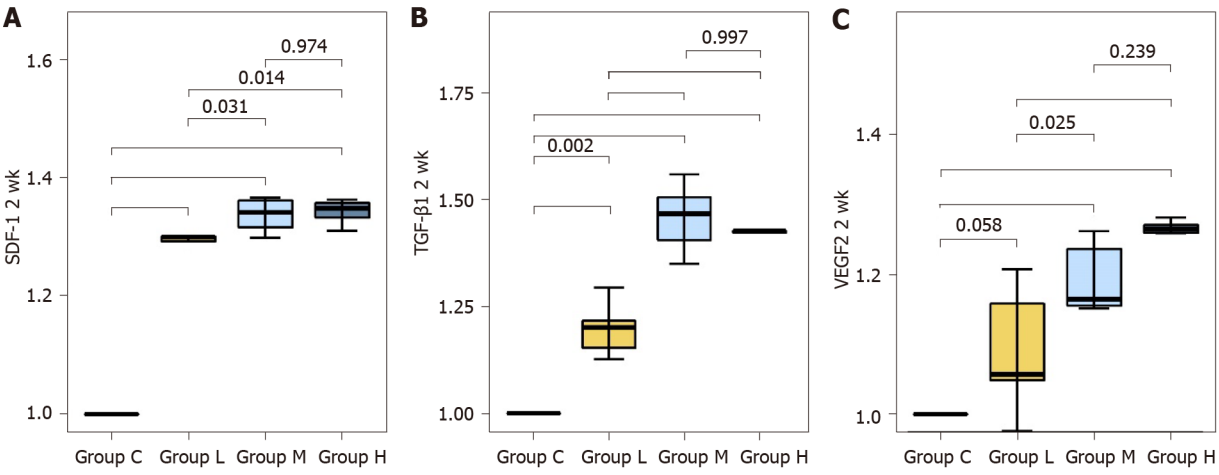

DOI: 10.4252/wjsc.v14.i12.839 **Copyright** ©The Author(s) 2022.

Figure 5 Relative protein expression levels of chemokines related to mesenchymal stem cell migration and angiogenesis at 2 wk post-fracture. SDF-1: Stromal cell-derived factor 1; TGF-β1: Transforming growth factor-beta 1; VEGF: Vascular endothelial growth factor.

injured tissue, but homed to the injury site to secrete bioactive factors, thereby resulting in therapeutic effects. Therefore, in this study, we evaluated the homing effect by quantitatively analyzing the expression of SDF-1, which is known to be an important chemokine for the recruitment of MSCs to fracture sites[20], and TGF-β1, which is known to enhance MSC proliferation[30], using western blotting at 2 wk post-fracture. The expression of factors related to MSC homing to the fracture site was higher in the groups injected with 5.0 × 10^6 and 10.0 × 10^6 MSCs than in the control group injected with normal saline.

Known methods of injecting MSCs for fracture healing include systemic intravenous and direct injections[20,31]. Systemic MSC injection is convenient and minimally invasive[15], and repeated administration is possible[20]. Therefore, it has been used in many animal studies. Ra *et al*[15] evaluated the safety of systemic MSC injection in animals and humans and reported no serious side effects in any animal or patient. However, other than this study, no studies have analyzed the stability, toxicity, and possible adverse effects of systemic MSC injection. On the other hand, Galindo *et al*[32] suggested that systemic injection of MSCs may be associated with a high risk of side effects, and the number of cells

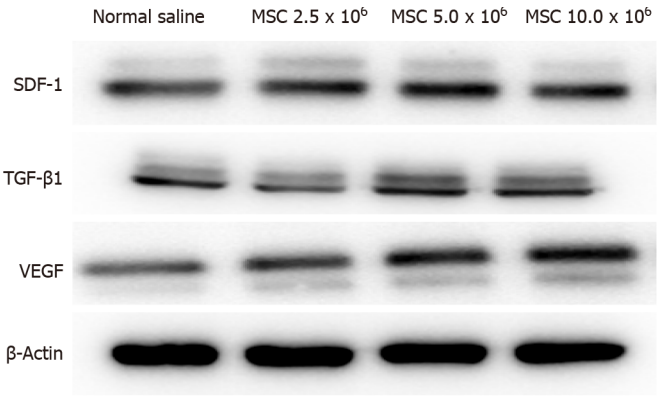

DOI: 10.4252/wjsc.v14.i12.839 **Copyright** ©The Author(s) 2022.

Figure 6 Western blot analysis of factors related to mesenchymal stem cell homing and angiogenesis. At 2 wk post-fracture, the protein expressions of stromal cell-derived factor 1 (SDF-1), transforming growth factor-beta 1 (TGF-β1) and vascular endothelial growth factor (VEGF) were significantly higher in the groups injected with 5.0 × 10^6 and 10.0 × 10^6 mesenchymal stem cells (MSCs) compared to the group injected with normal saline. No significant difference in SDF-1, TGF-β1 and VEGF protein expression was found in the groups injected with 5.0 × 10^6 and 10.0 × 10^6 MSCs. MSCs: Mesenchymal stem cells; SDF-1: Stromal cell-derived factor 1; TGF-β1: Transforming growth factor-beta 1; VEGF: Vascular endothelial growth factor.

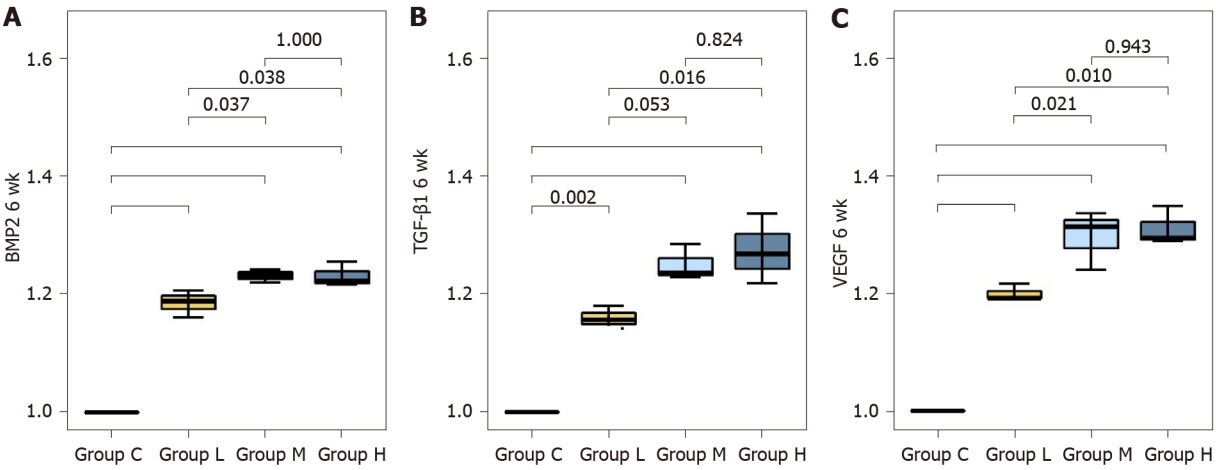

DOI: 10.4252/wjsc.v14.i12.839 **Copyright** ©The Author(s) 2022.

Figure 7 Relative mRNA expression levels of osteogenesis-related factors and chemokines related to angiogenesis at 6 wk post-fracture. BMP: Bone morphogenetic protein; TGF-β1: Transforming growth factor-beta 1; VEGF: Vascular endothelial growth factor.

reaching the target area may be small. The treatment of fractures often requires opening of the fracture site to fix the injured area. Therefore, in this study, the above-mentioned disadvantage of systemic injection was reflected, and direct injection of MSCs into the fracture site was performed instead.

Hou *et al*[18] reported that MSCs at a concentration higher than 3.0 × 10^6 should be administered in mice. Dreger *et al*[27] evaluated bone regeneration in a mouse femur shaft fracture model after the injection of 2.0 × 10^6 MSCs, which was less than that reported by Hou *et al*[27]. Dreger *et al*[27] reported that injected MSCs significantly accumulate at the fracture site and enhance bone regeneration. However, there is still no consensus on the optimal number of MSCs to be injected to enhance fracture healing. Janko *et al*[19] injected MSCs using scaffolds in a large-sized bone defect rat model and reported that a range of (2.0-10.0) × 10^6 MSCs was an effective dose window for fracture healing. However, they evaluated only healing at 8 wk post-fracture and did not analyze the effect of MSC concentration on fracture healing in the early phase. In addition, they analyzed only callus formation *via* histological analysis, not *via* radiologic evaluation, such as micro-CT. Furthermore, the expression of factors related to osteogenesis and angiogenesis, which are important in evaluating fracture healing, was not analyzed. In this study, fracture healing was analyzed at 2 and 6 wk post-fracture, that is, in both the early and late phases. Histological analysis, micro-CT, and the expression of factors related to MSC migration, osteogenesis, and angiogenesis were analyzed. Our results showed that fracture healing was enhanced in the groups injected with 5.0 × 10^6 and 10 × 10^6 MSCs compared to the groups injected with normal saline and 2.5 × 10^6 MSCs. There was no significant difference between the groups injected with 5.0 × 10^6 and 10 × 10^6 MSCs.

This study has several limitations. First, although previous reports have shown that human MSCs are safe when injected into animals[15], MSCs cultured in rats were not used in this study. However, because conventionally prepared MSCs are used, purity can be guaranteed. Second, in this study, fracture healing was compared by administering MSCs at different concentrations of 2.5×10^6, 5.0×10^6, and 10×10^6 cells; however, the criterion for determining the concentrations was ambiguous. Third, in cases of direct injection of MSCs mixed with normal saline, it may be difficult to retain MSCs at the fracture site for the long time. Additionally, we did not evaluate retention of the implanted MSC at the fracture site using fluorescence imaging analysis. Despite these limitations, this study is meaningful because it is the first animal study to analyze the optimal concentration of MSCs that maximizes the effect on fracture healing. In addition, this study could help to set the standard concentration of MSCs for evaluating fracture healing in an rat model of long bone fracture.

CONCLUSION

Direct injection of various concentrations of MSCs enhances fracture healing in a rat model of long bone fractures. Among the various concentrations used, 5.0×10^6 MSCs was optimal to promote fracture healing. Therefore, in order to evaluate the therapeutic effect on fracture healing of MSCs in a rat model of fractures, administration of at least 5.0×10^6 MSCs is suggested.

ARTICLE HIGHLIGHTS

Research background

Previous studies have reported that injection of mesenchymal stem cells (MSCs) improves fracture healing. However, no studies have specifically reported the most effective concentration of MSC.

Research motivation

There is no consensus on which concentration of MSCs to use for promoting fracture healing in a rat model of long bone fracture.

Research objectives

The present study aimed to assess the optimal concentration of MSCs for promoting fracture healing in a rat model.

Research methods

Wistar rats were divided into four groups according to MSC concentrations: Normal saline (C), 2.5×10^6 (L), 5.0×10^6 (M), and 10.0×10^6 (H) groups. New bone formation was evaluated using micro-computed tomography (micro-CT). Histological analysis was performed to evaluate fracture healing score. The protein expression of factors related to MSC migration and angiogenesis was evaluated using western blot analysis. The expression of cytokines associated with osteogenesis was evaluated using real-time polymerase chain reaction.

Research results

Micro-CT showed that new bone formation was significantly increased in groups M and H compared to that in group C at 6 wk post-fracture. Significantly more cartilaginous tissue and immature bone were formed in groups M and H than in group C at 2 and 6 wk post-fracture. At 2 post-fracture, the protein expression levels of factors related to MSC migration and angiogenesis were significantly higher in groups M and H than in group L. The mRNA levels of cytokines associated with osteogenesis and angiogenesis were significantly higher in groups M and H than in group C at 6 wk post-fracture. There were no significant differences between M and H groups.

Research conclusions

Among the various concentrations used, 5.0×10^6 MSCs was the optimal concentration that promoted healing of long bone shaft fractures.

Research perspectives

This study could help to set the standard concentration of MSCs for evaluating fracture healing in an animal model of fracture.

FOOTNOTES

Author contributions: Kim MS collected and assembled the data and performed data analysis and interpretation, manuscript writing; Chung HJ analyzed the data and performed interpretation; Kim KI provided the study material and designed the research study and performed final approval of manuscript; and all authors have read and approve the final manuscript.

Supported by the Korea Health Technology R&D Project through the Korea Health Industry Development Institute (KHIDI), funded by the Ministry of Health & Welfare, Republic of Korea, No. HI20C1405.

Institutional review board statement: The study was reviewed and approved by the Institutional Review Board at Kyung Hee University Hospital at Gangdong (KHNMC 2022-11-017).

Institutional animal care and use committee statement: All procedures and treatments involving animals in this study followed the requirements of the Institutional Animal Care and Use Committee of the Clinical Research Institute, and the final approval was obtained from the ethics committee of Kyung Hee University Hospital at Gangdong (KHNMC AP 2020-018).

Conflict-of-interest statement: All the authors report no relevant conflicts of interest for this article.

Data sharing statement: Data underlying this article are available in the article and in its online supplementary material.

ARRIVE guidelines statement: The authors have read the ARRIVE guidelines, and the manuscript was prepared and revised according to the ARRIVE guidelines.

Country/Territory of origin: South Korea

ORCID number: Myung-Seo Kim 0000-0003-2916-0131; Hyun-Ju Chung 0000-0002-2312-3199; Kang-Il Kim 0000-0002-4010-1063.

S-Editor: Wang JJ
L-Editor: A
P-Editor: Wang JJ

REFERENCES

1 **Bucholz RW**, Jones A. Fractures of the shaft of the femur. *J Bone Joint Surg Am* 1991; **73**: 1561-1566 [PMID: 1748704]
2 **Wu KJ**, Li SH, Yeh KT, Chen IH, Lee RP, Yu TC, Peng CH, Liu KL, Yao TK, Wang JH, Wu WT. The risk factors of nonunion after intramedullary nailing fixation of femur shaft fracture in middle age patients. *Medicine (Baltimore)* 2019; **98**: e16559 [PMID: 31335740 DOI: 10.1097/MD.0000000000016559]
3 **Ekegren CL**, Edwards ER, de Steiger R, Gabbe BJ. Incidence, Costs and Predictors of Non-Union, Delayed Union and Mal-Union Following Long Bone Fracture. *Int J Environ Res Public Health* 2018; **15** [PMID: 30551632 DOI: 10.3390/ijerph15122845]
4 **Ricci WM**, Gallagher B, Haidukewych GJ. Intramedullary nailing of femoral shaft fractures: current concepts. *J Am Acad Orthop Surg* 2009; **17**: 296-305 [PMID: 19411641 DOI: 10.5435/00124635-200905000-00004]
5 **Song SH**. Radiologic Outcomes of Intramedullary Nailing in Infraisthmal Femur-Shaft Fracture with or without Poller Screws. *Biomed Res Int* 2019; **2019**: 9412379 [PMID: 31205948 DOI: 10.1155/2019/9412379]
6 **Bell A**, Templeman D, Weinlein JC. Nonunion of the Femur and Tibia: An Update. *Orthop Clin North Am* 2016; **47**: 365-375 [PMID: 26772945 DOI: 10.1016/j.ocl.2015.09.010]
7 **Rupp M**, Biehl C, Budak M, Thormann U, Heiss C, Alt V. Diaphyseal long bone nonunions - types, aetiology, economics, and treatment recommendations. *Int Orthop* 2018; **42**: 247-258 [PMID: 29273837 DOI: 10.1007/s00264-017-3734-5]
8 **Henrich D**. Focus on bone healing: new strategies for improvement of bone healing. *Eur J Trauma Emerg Surg* 2020; **46**: 229-230 [PMID: 32239240 DOI: 10.1007/s00068-020-01344-x]
9 **Giuliani N**, Lisignoli G, Magnani M, Racano C, Bolzoni M, Dalla Palma B, Spolzino A, Manferdini C, Abati C, Toscani D, Facchini A, Aversa F. New insights into osteogenic and chondrogenic differentiation of human bone marrow mesenchymal stem cells and their potential clinical applications for bone regeneration in pediatric orthopaedics. *Stem Cells Int* 2013; **2013**: 312501 [PMID: 23766767 DOI: 10.1155/2013/312501]
10 **Oryan A**, Kamali A, Moshiri A, Baghaban Eslaminejad M. Role of Mesenchymal Stem Cells in Bone Regenerative Medicine: What Is the Evidence? *Cells Tissues Organs* 2017; **204**: 59-83 [PMID: 28647733 DOI: 10.1159/000469704]

11 **Bajada S**, Harrison PE, Ashton BA, Cassar-Pullicino VN, Ashammakhi N, Richardson JB. Successful treatment of refractory tibial nonunion using calcium sulphate and bone marrow stromal cell implantation. *J Bone Joint Surg Br* 2007; **89**: 1382-1386 [PMID: 17957083 DOI: 10.1302/0301-620X.89B10.19103]

12 **Wilson SM**, Goldwasser MS, Clark SG, Monaco E, Bionaz M, Hurley WL, Rodriguez-Zas S, Feng L, Dymon Z, Wheeler MB. Adipose-derived mesenchymal stem cells enhance healing of mandibular defects in the ramus of swine. *J Oral Maxillofac Surg* 2012; **70**: e193-e203 [PMID: 22374062 DOI: 10.1016/j.joms.2011.10.029]

13 **Obermeyer TS**, Yonick D, Lauing K, Stock SR, Nauer R, Strotman P, Shankar R, Gamelli R, Stover M, Callaci JJ. Mesenchymal stem cells facilitate fracture repair in an alcohol-induced impaired healing model. *J Orthop Trauma* 2012; **26**: 712-718 [PMID: 23010646 DOI: 10.1097/BOT.0b013e3182724298]

14 **Furuta T**, Miyaki S, Ishitobi H, Ogura T, Kato Y, Kamei N, Miyado K, Higashi Y, Ochi M. Mesenchymal Stem Cell-Derived Exosomes Promote Fracture Healing in a Mouse Model. *Stem Cells Transl Med* 2016; **5**: 1620-1630 [PMID: 27460850 DOI: 10.5966/sctm.2015-0285]

15 **Ra JC**, Shin IS, Kim SH, Kang SK, Kang BC, Lee HY, Kim YJ, Jo JY, Yoon EJ, Choi HJ, Kwon E. Safety of intravenous infusion of human adipose tissue-derived mesenchymal stem cells in animals and humans. *Stem Cells Dev* 2011; **20**: 1297-1308 [PMID: 21303266 DOI: 10.1089/scd.2010.0466]

16 **Lee WS**, Kim HJ, Kim KI, Kim GB, Jin W. Intra-Articular Injection of Autologous Adipose Tissue-Derived Mesenchymal Stem Cells for the Treatment of Knee Osteoarthritis: A Phase IIb, Randomized, Placebo-Controlled Clinical Trial. *Stem Cells Transl Med* 2019; **8**: 504-511 [PMID: 30835956 DOI: 10.1002/sctm.18-0122]

17 **Green MR**, Sambrook J. Estimation of Cell Number by Hemocytometry Counting. *Cold Spring Harb Protoc* 2019; **2019** [PMID: 31676576 DOI: 10.1101/pdb.prot097980]

18 **Hou Z**, Nguyen Q, Frenkel B, Nilsson SK, Milne M, van Wijnen AJ, Stein JL, Quesenberry P, Lian JB, Stein GS. Osteoblast-specific gene expression after transplantation of marrow cells: implications for skeletal gene therapy. *Proc Natl Acad Sci U S A* 1999; **96**: 7294-7299 [PMID: 10377408 DOI: 10.1073/pnas.96.13.7294]

19 **Janko M**, Pöllinger S, Schaible A, Bellen M, Schröder K, Heilani M, Fremdling C, Marzi I, Nau C, Henrich D, Verboket RD. Determination of the effective dose of bone marrow mononuclear cell therapy for bone healing in vivo. *Eur J Trauma Emerg Surg* 2020; **46**: 265-276 [PMID: 32112259 DOI: 10.1007/s00068-020-01331-2]

20 **Wang X**, Wang C, Gou W, Xu X, Wang Y, Wang A, Xu W, Guo Q, Liu S, Lu Q, Meng H, Yuan M, Peng J, Lu S. The optimal time to inject bone mesenchymal stem cells for fracture healing in a murine model. *Stem Cell Res Ther* 2018; **9**: 272 [PMID: 30359311 DOI: 10.1186/s13287-018-1034-7]

21 **Gorter EA**, Hamdy NA, Appelman-Dijkstra NM, Schipper IB. The role of vitamin D in human fracture healing: a systematic review of the literature. *Bone* 2014; **64**: 288-297 [PMID: 24792958 DOI: 10.1016/j.bone.2014.04.026]

22 **Einhorn TA**, Gerstenfeld LC. Fracture healing: mechanisms and interventions. *Nat Rev Rheumatol* 2015; **11**: 45-54 [PMID: 25266456 DOI: 10.1038/nrrheum.2014.164]

23 **Majidinia M**, Sadeghpour A, Yousefi B. The roles of signaling pathways in bone repair and regeneration. *J Cell Physiol* 2018; **233**: 2937-2948 [PMID: 28590066 DOI: 10.1002/jcp.26042]

24 **Oetgen ME**, Merrell GA, Troiano NW, Horowitz MC, Kacena MA. Development of a femoral non-union model in the mouse. *Injury* 2008; **39**: 1119-1126 [PMID: 18656866 DOI: 10.1016/j.injury.2008.04.008]

25 **Gómez-Barrena E**, Rosset P, Müller I, Giordano R, Bunu C, Layrolle P, Konttinen YT, Luyten FP. Bone regeneration: stem cell therapies and clinical studies in orthopaedics and traumatology. *J Cell Mol Med* 2011; **15**: 1266-1286 [PMID: 21251219 DOI: 10.1111/j.1582-4934.2011.01265.x]

26 **Gómez-Barrena E**, Padilla-Eguiluz N, Rosset P, Gebhard F, Hernigou P, Baldini N, Rouard H, Sensebé L, Gonzalo-Daganzo RM, Giordano R, García-Rey E, Cordero-Ampuero J, Rubio-Suárez JC, García-Simón MD, Stanovici J, Ehrnthaller C, Huber-Lang M, Flouzat-Lachaniette CH, Chevallier N, Donati DM, Spazzoli B, Ciapetti G, Fleury S, Fernandez MN, Cabrera JR, Avendaño-Solá C, Montemurro T, Panaitescu C, Veronesi E, Rojewski MT, Lotfi R, Dominici M, Schrezenmeier H, Layrolle P. Early efficacy evaluation of mesenchymal stromal cells (MSC) combined to biomaterials to treat long bone non-unions. *Injury* 2020; **51** Suppl 1: S63-S73 [PMID: 32139130 DOI: 10.1016/j.injury.2020.02.070]

27 **Dreger T**, Watson JT, Akers W, Molligan J, Achilefu S, Schon LC, Zhang Z. Intravenous application of CD271-selected mesenchymal stem cells during fracture healing. *J Orthop Trauma* 2014; **28** Suppl 1: S15-S19 [PMID: 24378433 DOI: 10.1097/BOT.0000000000000063]

28 **Li WY**, Xiong H. [Study on MSCs homing and its research on osteodiseases]. *Zhongguo Gu Shang* 2020; **33**: 689-692 [PMID: 32700498 DOI: 10.12200/j.issn.1003-0034.2020.07.020]

29 **Caplan AI**. Mesenchymal Stem Cells: Time to Change the Name! *Stem Cells Transl Med* 2017; **6**: 1445-1451 [PMID: 28452204 DOI: 10.1002/sctm.17-0051]

30 **Sarahrudi K**, Thomas A, Mousavi M, Kaiser G, Köttstorfer J, Kecht M, Hajdu S, Aharinejad S. Elevated transforming growth factor-beta 1 (TGF-β1) levels in human fracture healing. *Injury* 2011; **42**: 833-837 [PMID: 21529804 DOI: 10.1016/j.injury.2011.03.055]

31 **Zhang Y**, Hao Z, Wang P, Xia Y, Wu J, Xia D, Fang S, Xu S. Exosomes from human umbilical cord mesenchymal stem cells enhance fracture healing through HIF-1α-mediated promotion of angiogenesis in a rat model of stabilized fracture. *Cell Prolif* 2019; **52**: e12570 [PMID: 30663158 DOI: 10.1111/cpr.12570]

32 **Galindo S**, de la Mata A, López-Paniagua M, Herreras JM, Pérez I, Calonge M, Nieto-Miguel T. Subconjunctival injection of mesenchymal stem cells for corneal failure due to limbal stem cell deficiency: state of the art. *Stem Cell Res Ther* 2021; **12**: 60 [PMID: 33441175 DOI: 10.1186/s13287-020-02129-0]

World Journal of Stem Cells

Submit a Manuscript: https://www.f6publishing.com

World J Stem Cells 2022 December 26; 14(12): 851-867

DOI: 10.4252/wjsc.v14.i12.851

ISSN 1948-0210 (online)

SYSTEMATIC REVIEWS

Biomaterial application strategies to enhance stem cell-based therapy for ischemic stroke

Asmaa' Mohd Satar, Farah Amna Othman, Suat Cheng Tan

Specialty type: Cell biology

Provenance and peer review: Invited article; Externally peer reviewed.

Peer-review model: Single blind

Peer-review report's scientific quality classification

Grade A (Excellent): A
Grade B (Very good): 0
Grade C (Good): C
Grade D (Fair): D
Grade E (Poor): 0

P-Reviewer: Liu J, China; Shao A, China; Ye Y, China

Received: September 11, 2022
Peer-review started: September 11, 2022
First decision: October 20, 2022
Revised: October 29, 2022
Accepted: December 6, 2022
Article in press: December 6, 2022
Published online: December 26, 2022

Asmaa' Mohd Satar, Farah Amna Othman, Suat Cheng Tan, School of Health Sciences, Health Campus, Universiti Sains Malaysia, Kubang Kerian, Kelantan 16150, Malaysia

Corresponding author: Suat Cheng Tan, PhD, Lecturer, School of Health Sciences, Health Campus, Universiti Sains Malaysia, Kubang Kerian, Kelantan 16150, Malaysia. tansc@usm.my

Abstract

BACKGROUND

Ischemic stroke is a condition in which an occluded blood vessel interrupts blood flow to the brain and causes irreversible neuronal cell death. Transplantation of regenerative stem cells has been proposed as a novel therapy to restore damaged neural circuitry after ischemic stroke attack. However, limitations such as low cell survival rates after transplantation remain significant challenges to stem cell-based therapy for ischemic stroke in the clinical setting. In order to enhance the therapeutic efficacy of transplanted stem cells, several biomaterials have been developed to provide a supportable cellular microenvironment or functional modification on the stem cells to optimize their reparative roles in injured tissues or organs.

AIM

To discuss state-of-the-art functional biomaterials that could enhance the therapeutic potential of stem cell-based treatment for ischemic stroke and provide detailed insights into the mechanisms underlying these biomaterial approaches.

METHODS

The PubMed, Science Direct and Scopus literature databases were searched using the keywords of "biomaterial" and "ischemic stroke". All topically-relevant articles were then screened to identify those with focused relevance to *in vivo*, *in vitro* and clinical studies related to "stem cells" OR "progenitor cells" OR "undifferentiated cells" published in English during the years of 2011 to 2022. The systematic search was conducted up to September 30, 2022.

RESULTS

A total of 19 articles matched all the inclusion criteria. The data contained within this collection of papers comprehensively represented 19 types of biomaterials applied on seven different types of stem/progenitor cells, namely mesenchymal stem cells, neural stem cells, induced pluripotent stem cells, neural progenitor cells, endothelial progenitor cells, neuroepithelial progenitor cells, and neuroblasts. The potential major benefits gained from the application of

biomaterials in stem cell-based therapy were noted as induction of structural and functional modifications, increased stem cell retention rate in the hostile ischemic microenvironment, and promoting the secretion of important cytokines for reparative mechanisms.

CONCLUSION

Biomaterials have a relatively high potential for enhancing stem cell therapy. Nonetheless, there is a scarcity of evidence from human clinical studies for the efficacy of this bioengineered cell therapy, highlighting that it is still too early to draw a definitive conclusion on efficacy and safety for patient usage. Future in-depth clinical investigations are necessary to realize translation of this therapy into a more conscientious and judicious evidence-based therapy for clinical application.

Key Words: Biomaterial; Stroke; Stem/progenitor cell therapy; Tissue bioengineering; Combined treatment

Core Tip: Ischemic stroke is becoming a significant health issue globally. An increasing number of studies have proposed the applications of regenerative stem cells for the treatment of this neurodegenerative disease. We critically reviewed the literature on biomaterial application to enhance the therapeutic potential of stem/progenitor cell therapy for ischemic stroke. Despite the limited evidence collected to translate this evidence into clinical practice, it is postulated that application of stem cells as regenerative treatment for stroke is practicable and beneficial for stroke patients, especially those in the chronic phase of stroke which could not be cured by any other established means.

Citation: Mohd Satar A, Othman FA, Tan SC. Biomaterial application strategies to enhance stem cell-based therapy for ischemic stroke. *World J Stem Cells* 2022; 14(12): 851-867
URL: https://www.wjgnet.com/1948-0210/full/v14/i12/851.htm
DOI: https://dx.doi.org/10.4252/wjsc.v14.i12.851

INTRODUCTION

Ischemic stroke is a cerebrovascular disease that occurs when blood supply to part of a brain is interrupted, causing the affected brain portion to be deprived of oxygen and nutrients and subsequently leading to irreversible brain cell death. There are three major types of ischemic stroke, namely thrombotic stroke (Figure 1A), embolic stroke (Figure 1B), and lacunar stroke (Figure 1C). Thrombotic stroke occurs when a thrombus (blood clot) develops in the brain arteries and disrupts normal blood flow to the brain tissue that are supplied by those arteries. The thrombus normally develops due to atherosclerosis (deposit of a fatty substance called 'plaque' on the artery lining), which halts the flow of blood and causes the blood clumps to form blood clots[1]. On the other hand, embolic stroke is caused by an embolus (blood clot) being formed elsewhere in the body (*e.g.*, heart or carotid arteries) and then traveling in the bloodstream until it reaches a blood vessel where its passage is blocked. Embolic stroke is usually associated with atrial fibrillation (*i.e.* abnormal heart rhythm, in which the atria does not beat effectively), itself eventually facilitating clot formation. It could also be caused by a clot dislodging from the atherosclerotic plaque formed in the aorta and carotid artery[2]. Last but not least, lacunar stroke happens when an occlusion occurs in a small artery in the brain that penetrates deep into the organ. Lacunar stroke is often associated with chronic hypertension, itself facilitating a small arteriole to become abnormal and susceptible to occlusion from micro-thrombi[3].

Human brain cells are permanent cells, being incapable of regeneration once matured. Brain cells also require a continuous supply of glucose and oxygen to support their heavy workload. These characteristics make brain cells vulnerable to any type of the ischemic stroke since any disruption of the blood supply to the brain, even within a few minutes, is sufficient to cause brain cell death and trigger permanent brain damage. Brain damage itself can lead to many devastating effects such as paralysis on one side of or the whole body, difficulty in speaking, inability to understand speech, and many other cognitive and neurological deficits. The adverse effect of stroke depends on which part of the brain is affected, whilst the severity of deficits depends on the extent of damage caused by the stroke.

Ischemic cell death could happen within minutes after a blood vessel occlusion. Due to acute onset and rapid deterioration, repairing ischemic damage in the brain has remained the most crucial, yet daunting, challenge of medical science. Immediate treatment is required in order to reduce complications from an ischemic stroke. Currently, clinical treatment for ischemic stroke disease mainly aims to restore blood flow to the ischemic penumbra in order to minimize the mortality and morbidity caused by brain damage and prevent recurrence or secondary complications. Nonetheless, such treatments

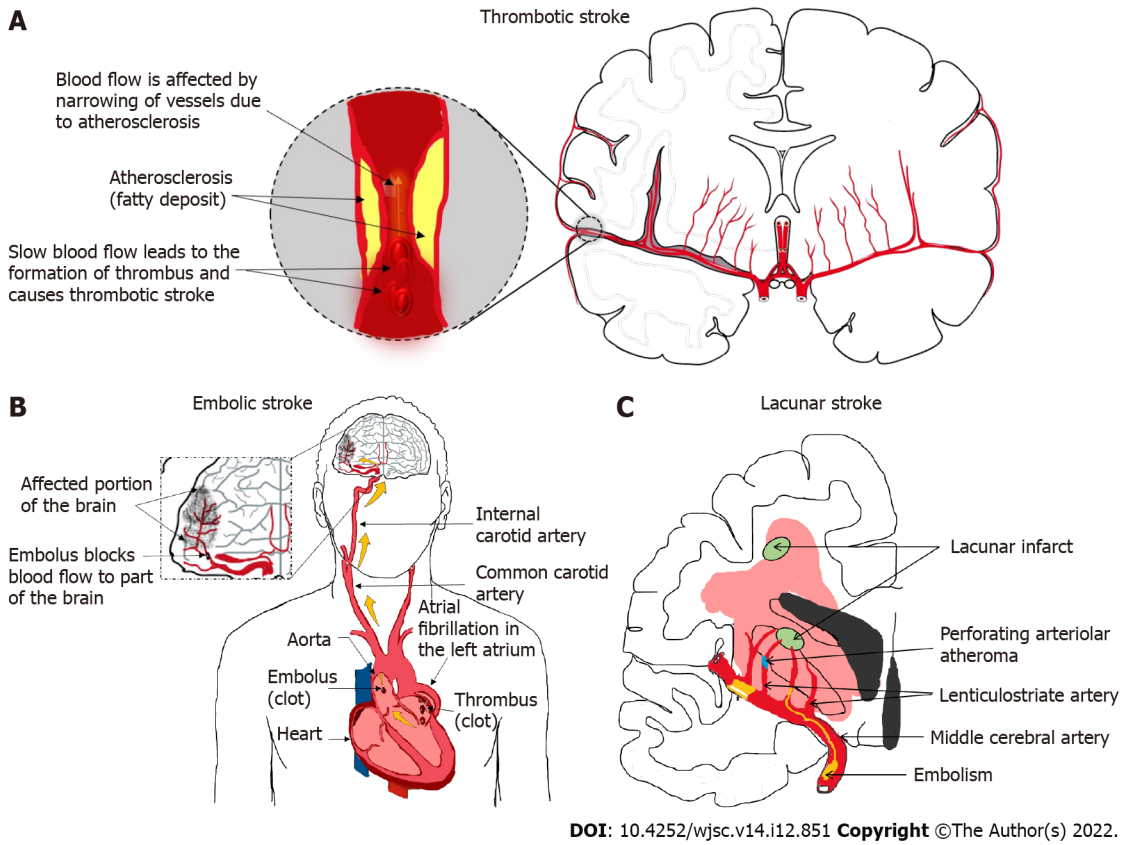

DOI: 10.4252/wjsc.v14.i12.851

Figure 1 Types of ischemic stroke. A: Thrombotic stroke occurs when thrombus formed from atherosclerosis blocks the blood flow; B: Embolic stroke occurs when a blood clot dislodges from a distant site and then travels to and lodges in an artery in the brain; C: Lacunar stroke occurs when a blood clot obstructs the normal blood flow in one of the small arteries found deep within the brain.

cannot regenerate the brain tissues that have died. Therefore, the prognosis after current stroke treatments is very limited. According to the National Stroke Association, only 10% of stroke survivors exhibit full recovery, with an additional 25% showing mild disabilities and 50% showing moderate-to-severe disabilities which require special care[4]. This indicates that the current stroke treatments are not fully effective and are very limited according to their abilities to only minimize damage and reduce risk of stroke recurrence. Therefore, there is an urgent need for alternative treatments that will facilitate regeneration of damaged brain tissue for full recovery.

Recently, stem cells have emerged as a promising therapeutic agent for stroke patients due to their self-renewal and differentiation potentials[5]. Stem cells are present in many organs of the human body. These undifferentiated cells are capable of self-renewal and differentiate into specific functional cells depending on their lineages, in response to body conditions and requirements. Furthermore, under suitable stimulation *in vitro*, stem cells can also be induced to differentiate across cell type lineages. Using stem cells as regenerative treatment for stroke is, therefore, a practicable approach for ischemic stroke patients in the chronic phase of stroke.

Many stem cell types have been investigated to determine their feasibility, safety and efficacy in stem cell replacement therapy, for example, embryonic stem cells (ESCs), induced pluripotent stem cells (iPSCs), bone marrow stem cells, umbilical cord blood stem cells, and neural stem cells (NSCs)[6,7]. On top of these, an emerging strategy was developed to enhance the potential of stem cells for ischemic stroke treatment by incorporating biomaterial application[8]. A biomaterial is a substance that has been engineered to interact with biological systems for a medical purpose. A carefully designed biomaterial could serve its purpose in the environment of the living body without causing toxicity to other bodily organs. Typically, a tissue engineering approach using a combination of biomaterial and stem cells involves growing stem cells on a three-dimensional scaffold material which could provide a supportable microenvironment for the stem cells to optimize their growth without affecting their therapeutic efficacy for regenerative treatments.

Due to the continuous research and progress in biomaterial sciences, there has been a rapid growth in applications of a vast variety of novel biomaterials in tissue engineering and regenerative medicine. However, there is no comprehensive report in the up-to-date literature that reviews the potential of all these biomaterials to enhance stem cell-based therapy. Therefore, we performed a systematic review of the literature databases to provide a comprehensive summarization of the recent findings regarding the efficacy of biomaterial strategies to enhance stem cell therapeutic potential for ischemic stroke

treatment. The findings from this literature review will be beneficial due to its provision of collated updated information regarding the different types of biomaterials currently used by researchers, along with detailed descriptions of their key mechanisms, advantages and limitations, with an additional focus on stem cell-based ischemic stroke therapy.

MATERIALS AND METHODS

Search strategy

A literature search was performed based on the Preferred Reporting Items for Systematic Reviews and Meta-Analyses (PRISMA) guidelines to identify research documentation on application of biomaterials utilizing stem cell-based therapy for ischemic stroke diseases. Three carefully selected databases, namely PubMed, ScienceDirect, and Scopus, were used for the literature search using the keywords "biomaterial" and "ischemic stroke". The resultant literature collection was further screened to identify all the articles relevant to *in vivo*, *in vitro* and clinical studies using "stem cell" OR "progenitor cells" OR "undifferentiated cells published in English during the years of 2011 to 2022. The systematic search was conducted up to September 30, 2022. When revising the manuscript, we applied the Reference Citation Analysis (https://www.referencecitationanalysis.com/) to supplement high quality research results.

Research article selection and evaluation

Search results were limited to articles following the inclusion and exclusion criteria.

Inclusion criteria: (1) Full-text articles; (2) *In vitro* studies related to biomaterial application in stem cell-based therapy for ischemic stroke; (3) *In vivo* studies related to biomaterial application in stem cell-based therapy for ischemic stroke; and (4) Clinical studies related to biomaterial application in stem cell-based therapy for ischemic stroke.

Exclusion criteria: (1) Irrelevant titles and abstracts; (2) Duplicated studies; (3) Review articles/meta-analyses; (4) News/editorials/letters; (5) Case reports; and (6) Non-English language.

Three independent reviewers screened the databases and selected articles with potential relevance based on the inclusion and exclusion criteria stated above. For the first screening, the related articles were screened based on their titles and abstracts. Next, the remaining papers were checked for duplications. Finally, the selected full-text articles were checked by another reviewer according to the inclusion criteria for final validation.

RESULTS

Selected studies for analysis

The primary search identified 459 articles, including 161 from PubMed, 257 from ScienceDirect and 41 from Scopus. Following the preliminary screening of the titles and abstracts, a total of 383 articles were excluded accordingly. Out of the 76 articles remaining, 12 were found to be present in two or more of the databases, and thus the duplicates were excluded, resulting in 64 articles eligible for further assessment. After a careful full-text analysis and validation of the content, a total of 19 articles that met all the screening criteria were selected for inclusion in the systematic review. A PRISMA diagram illustrating the flow of this systematic literature review search is shown in Figure 2.

Key findings

Our systematic literature review analysis identified 19 articles that matched all the inclusion criteria. The selected articles were carefully read and analyzed. Based on the collected literature data, we identified a total of 19 different major types of materials applied on seven major types of stem cells, namely mesenchymal stem cells (MSCs), NSCs, iPSCs, neural progenitor cells (NPCs), endothelial progenitor cells (EPCs), neuroepithelial progenitor cells (NEPCs), and neuroblasts, respectively, to enhance their therapeutic potential for ischemic stroke treatment (Figure 3). The key findings reported in each article are presented in Table 1. Elaboration of the therapeutic benefits gained from each of these biomaterial engineered-stem cells for *in vitro* and *in vivo* stroke studies and detailed insights on the mechanisms underlying these cell-based therapies are provided in the Discussion section.

DISCUSSION

MSCs

MSCs are undifferentiated non-hematopoietic stromal cells present in almost all tissues such as bone

Table 1 Biomaterial applications to enhance the therapeutic potential of stem/progenitor cells for ischemic stroke treatment

Ref.	Type and source of stem cells	Type of biomaterials used	Biomaterial-based optimization strategy	Type of ischemic stroke model	Beneficial outcomes
Yang *et al*[12], 2015	MSCs from human adipose tissue	PβAE	Genetically engineered hMSCs to overexpress GDNF using PβAE	Hypoxic-ischemic mice brains	Enhanced neurobehavioral functions of animals after transplantation in ischemic stroke model
Lin *et al*[22], 2017	MSCs from SD rat bone marrow	ASP-SPION nanocomplex	Conjugation of cationic amylose and SPIONs to produce cationic nanoparticles	MCAO SD rats	A rapid and highly efficient approach for MSCs magnetic labelling, with no destructive effects on cells
Huang *et al*[24], 2017	MSCs from bone marrow of 3 wk male SD rat	PA-CLEVSRKNC peptide	MSCs co-modified with PA-CLEVSRKNC peptide	MCAO SD rats	Effectively guide and homing a large amount of MSCs to the ischemic brain directly and enhanced miR-133b expression level
Tian *et al*[26], 2018	MSC-derived exosomes from mouse	cRGD-Exo	[c(RGDyK)] peptide conjugated to MSCs exosome and loaded with curcumin	MCAO mice	Successfully targeted ischemic area, with inflammatory response and cellular apoptosis were suppressed effectively in the lesion region
Kim *et al*[34], 2020	MSC-derived exosomes from rat	MNV	MNV derived from IONP-harboring MSCs	MCAO rats	Ischemic lesion targeting, and the therapeutic outcome improved
Zamproni *et al* [40], 2019	MSCs from bone marrow from adult C57/BI6 mouse	PLA-PRM scaffolds	PRM microspheres produced by RJS and conjugated with the MSCs in the scaffold	MCAO mice	Retention time of MSCs in the injury site increased, possibly through upregulation of α6-integrin and CXCL12
Hsu *et al*[43], 2021	MSCs from mouse HUVEC and umbilical cord blood	3D MSCs/ECs spheroids	Preassembled 3D spheroids with MSCs and vascular ECs	MCAO mice	Cell retention, structural and motor function recovery significantly improved in the ischemic stroke brain
Ghuman *et al* [49], 2021	NSCs from SVZ of 2-mo-old mouse	PEG microspheres	PEG microsphere encapsulated the NSCs and ECs with suspension in ECM hydrogel	Photothrombotic and MCAO rats	Provision of ideal microenvironment, with highly efficient cell delivery to the damaged area
Ge *et al*[53], 2022	NSCs from neocortices of day 14.5 mouse embryo	LbL-NSCs	LbL assembly of NSCs using gelatin and HA	Distal MCAO mice	LbL-NSCs engraftment enhanced NSC survival and neurogenesis; promotion of endogenous neuroblasts migration to the ischemic region
Shabani *et al*[56], 2022	NSCs from 14-d-old murine embryo	PLGA-PEG	NSC encapsulation within PLGA-PEG and loaded with Reelin	Photothrombotic mice	PLGA-PEG with Reelin enhanced the NSCs proliferation, survival and differentiation
Li *et al*[59], 2022	NSCs from hippocampus of fetal rat	MNBs	MNBs were fabricated through self-assembly of PSCE-modified (γ-Fe_2O_3SPIONPs) and internalized within NSCs in the ratio of 1:10	Photothrombotic mice	MNBs activate Plezo1-Ca^{2+}-BMP2/Smad signaling pathway, inducing NSCs differentiation; efficiently tracking and imaging the MNBs-labelled NSCs using MRI and ultrasound
Zhang *et al*[67], 2021	Mouse iPSC cell line	3D microscaffold culture using AATS medium	Simplified and chemically defined AATS medium for robust production of iPSCs-derived ECs and SMCs	Permanent MCAO mice	ECs and SMCs successfully grown in simple, cost effective AATS medium, allowing GMP large scale production of these cells
McCrary *et al* [68], 2022	Mouse iPSC cell line	CS-A + iPSCs-NPCs	iPSCs-derived NPCs were encapsulated in CS-A hydrogel	MCAO mice	Promote regenerative microglia/macrophage response *via* IL-10 accumulation; improvements of post-stroke neuropsychiatric deficits
Zhang *et al*[72], 2013	NPCs from cerebellum of neonatal mouse	fmSiO4@SPION	SPIONs were modified with fmSiO4 to label and track the NPCs	MCAO mice	Labelled cells successfully migrating to the lesion with highly effective cell imaging and cell tracking
Somaa *et al*[73],	NPCs from human	SAP hydrogel scaffold	SAP hydrogel scaffold	MCAO rats	Embedding in a self-assembling

2017	ESC		was synthesized using laminin-derived epitope (IKVAV)		scaffold formed *de novo* "bio-bridges" between the lesions for prolonged survival, therapeutic efficacy and integration of neural grafts
Li *et al*[78], 2013	EPCs from human umbilical cord blood	SiO4@ SPIONs	EPCs were labelled with SiO4@SPIONs and magnetic exterior to guide the cell migration to ischemic area	Transient MCAO mice	Dual benefit of cell homing and cell tracking were achieved; Atrophic volume of brain was reduced while the microvessel density and VEGF expression were increased
Wang *et al*[80], 2019	EPCs from human umbilical cord blood	Alkyl-PEI encapsulated SPIONs	Alkyl-PEI/SPIONs were used to direct delivery of siRNA to EPCs	Photothrombotic mice	PHD2 silencing in EPCs improved the migration and survival of the cells through elevation of CXCR4 and HIF-1α expression
Payne *et al*[82], 2019	NEPCs from human fibroblasts	HAMC hydrogel	HAMC as co-delivery agent to deliver cortically specified-NEPCs into a specific ischemic area	MCAO SD rats	HAMC led to cell survival along the migration process for more mature cells formation and increased host tissue repairs
Fujioka *et al*[86], 2017	Neuroblasts	Laminin-rich hydrogel	Laminin-rich scaffold was developed with β1 integrins to facilitate neuronal migration toward an injured area	MCAO mice	Able to mimic the vasculature and increased neuroblasts chain formation and migration toward the infarct area of brain tissue

ASP: Spermine-modified amylose; cRGD-Exo: Cyclo (Arg-Gly-Asp-D-Tyr-Lys) peptide-exosome; c(RGDyK): Cyclo (Arg-Gly-Asp-D-Tyr-Lys) peptide; CS-A: Chondroitin sulfate-A; CXCL12: C-X-C motif chemokine ligand 12; CXCR4: C-X-C chemokine receptor type 4; EC: Endothelial cell; ECM: Extracellular matrix; EPC: Endothelial progenitor cell; ESC: Embryonic stem cell; fmSiO4@SPION: Fluorescent mesoporous silica-coated superparamagnetic iron 1 oxide nanoparticle; GDNF: Glial cell-derived neurotrophic factor; GMP: Good manufacturing practice; HA: Hyaluronic acid; HAMC: Hyaluronan methylcellulose; HIF-1α: Hypoxia-inducible factor 1-alpha; HUVEC: Human umbilical vein epithelial cell; ; IL-10: Interleukin-10; iPSCs: Induced pluripotent stem cells; IKVAV: Ile-lys-Val-ala-Val; IONP: Iron-oxide nanoparticle; LbL-NSCs: Layer-by-layer assembly of NSCs; MNV: Magnetic nanovesicles; MCAO: Middle cerebral artery occlusion; miR-133b: MicroRNA 133b; MSC: Mesenchymal stem cell; MNBs: Magnetic nanobubbles; MRI: Magnetic resonance imaging; NEPC: Neuroepithelial progenitor cell; NPC: Neural progenitor cell; NSC: Neural stem cell; PA: Palmitic acid; PβAE: Poly (β-amino esters); PEG: Polyethylene glycol; PEI: Polyethylenimine; PHD2: Prolyl hydroxylase 2; PLA-PRM; Polylactic acid polymeric rough microfibers; PSCE: Poly-glucose sorbitol carboxymethyl ether; RJS: Rotary jet spinning; SAP: Self-assembling peptide; SD: Sprague-Dawley; SiO4@SPION: Silica-coated superparamagnetic iron 1 oxide nanoparticle; SMCs: Smooth muscle cells; SPION: Superparamagnetic iron oxide nanoparticle; SVZ: Subventricular zone.

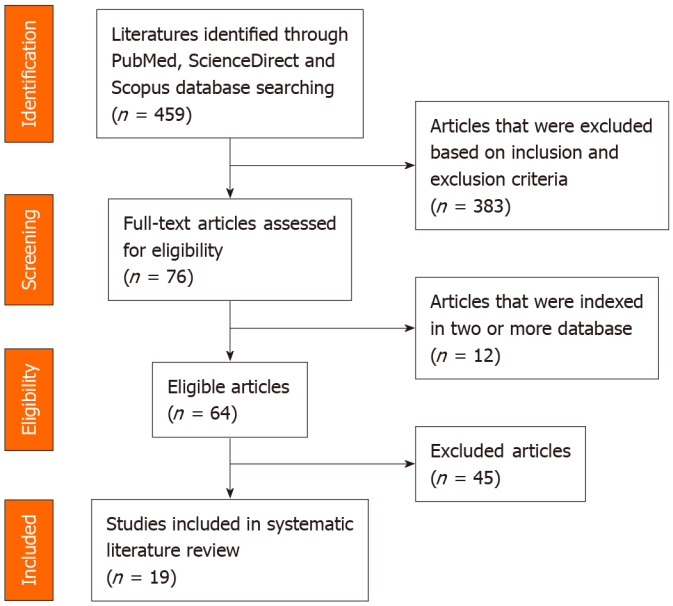

DOI: 10.4252/wjsc.v14.i12.851

Figure 2 Progressive study selection performed according to the PRISMA flow diagram search strategy.

marrow, adipose tissue, cartilage, trabecular bone, and arterial wall. MSCs from different tissues might exhibit different biological activities and cell markers depending on their tissue of origin. However, most MSCs share many common characteristics; for example, they have multilineage differentiation

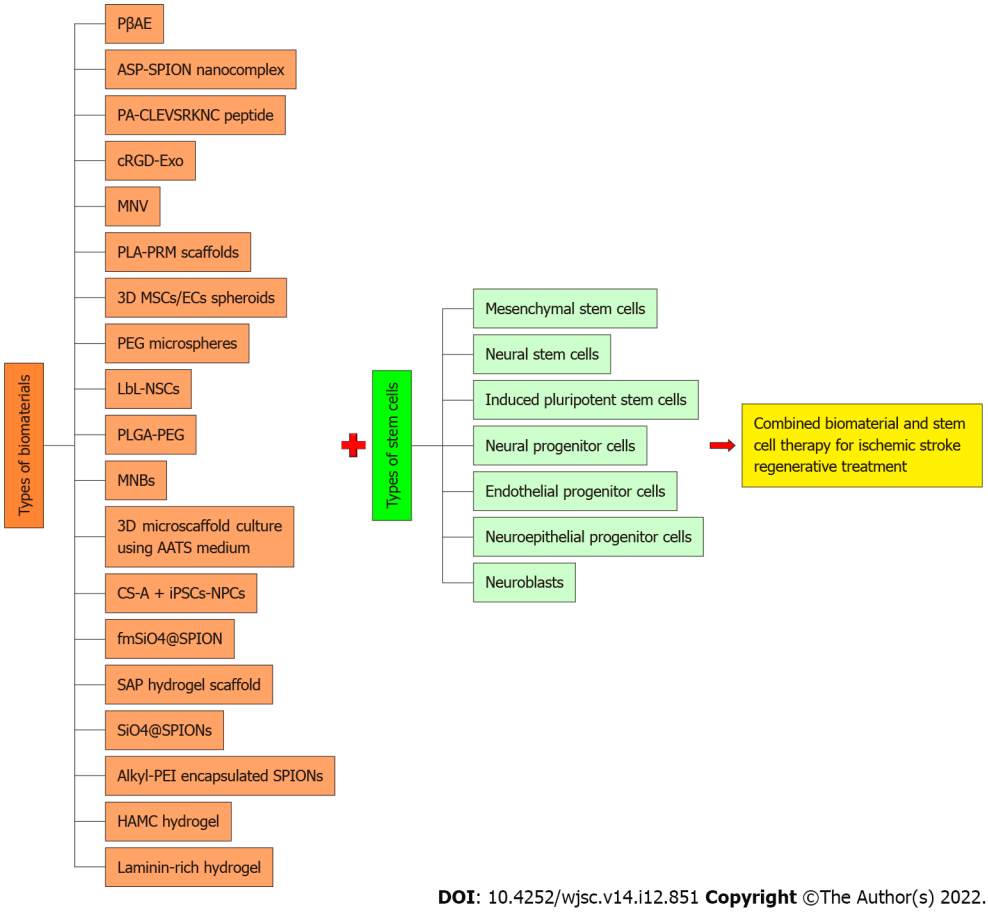

DOI: 10.4252/wjsc.v14.i12.851

Figure 3 Summary of the collective literature data for a total of 19 different major types of material applied on seven different major types of stem/progenitor cells to enhance their therapeutic potential for ischemic stroke treatment. AATS: Recombinant human albumin, L-ascorbic acid 2-phosphate, human apo-transferrin, sodium selenite medium; ASP: Spermine-modified amylose; cRGD-Exo: Cyclo (Arg-Gly-Asp-D-Tyr-Lys) peptide-exosome; CS-A: Chondroitin sulfate-A; fmSiO4@SPION: Fluorescent mesoporous silica-coated superparamagnetic iron 1 oxide nanoparticle; HAMC: Hyaluronan methylcellulose; iPSCs-NPCs: Induced pluripotent stem cells/neural progenitor cells; LbL-NSCs: Layer-by-layer assembly of neural stem cells; MNBs: Magnetic nanobubbles; MNV: Magnetic nanovesicle; MSCs/ECs: Mesenchymal stem cells/endothelial cells; PβAE: Poly (β-amino esters); PA-CLEVSRKNC: Palmitic acid-peptide; PEG: Polyethylene glycol; PEI: Polyethylenimine; PLA-PRM; Polylactic acid polymeric rough microfibers; PLGA-PEG: Polylactic coglycolic acidpolyethylene glycol; SAP: Self-assembling peptide; SiO4@SPION: Silica-coated superparamagnetic iron 1 oxide nanoparticle; SPION: Superparamagnetic iron 1 oxide nanoparticle.

potential and thus are considered as a reservoir of reparative cells for numerous degenerative disorders including myocardial infarction, liver cirrhosis, limb ischemia and spinal cord injury[9]. The main features of this cell type is their ability to proliferate and differentiate into committed cell types and to mobilize to the site of injured tissues following specific signals in order to support the overall regeneration process[10]. Moreover, the protocols to isolate and expand MSCs *in vitro* are simple and do not pose ethical or tumorigenic concerns, unlike those for pluripotent ESCs[11]. Thus, the potential of MSCs have been explored over the last few decades extensively for tissue regeneration therapies in musculoskeletal, cardiovascular, liver, autoimmune, neurodegenerative and cancer-related diseases.

In biological cell-based therapeutic strategies for ischemic stroke, MSCs have been regarded as an ideal candidate due to their migratory capacity and expansive capabilities to regenerate neural cells after being grafted into the central nervous system (CNS). In recent years, the potential of MSCs for ischemic stroke treatment has been further enhanced by employing biomaterial tissue/cell engineering approaches. For example, in 2015, Yang *et al*[12] reported a method for genetically engineered human MSCs to overexpress glial cell-derived neurotrophic factor (GDNF) using a potent biodegradable cationic polymer known as poly (β-amino ester) (PβAE). PβAE is a synthetic polymer that has demonstrated extraordinary efficiency to overcome distinct cellular barriers for site-specific delivery [13]. PβAE is also widely used for gene transfer due to its demonstrated higher transfection efficiency and lower cytotoxicity in various cell and tissue types compared to several commercially available transfection reagents, including polyethylenimine and Lipofectamine 2000[14]. In that study[14], a GDNF plasmid was transfected into human MSCs (hMSCs) efficiently using PβAE nanoparticles and was found to successfully induce over-expression of GDNF protein in hMSCs. GDNF is a specific neurotrophic factor that is responsible for neuronal survival, differentiation and neurogenesis[15]. Transplantation of the GDNF-overexpressed hMSCs into a hypoxic-ischemic stroke animal model significantly improved the neurobehavioral functions of animals after the transplantation, indicating the

potential of PβAE biomaterial in enhancing the MSC-based therapy for ischemic stroke.

Furthermore, tracking of transplanted MSCs in biological cell-based tissue therapy is essential in order to provide better understanding of the cellular proliferation dynamics, biodistribution, migrational dynamics, differentiation process and participation in the mechanisms of tissue repair[16]. Commonly used non-invasive imaging known as magnetic resonance imaging (MRI) is the right fit for a long-term imaging purpose, as this technology is clinically safe compared to ionizing radiation and capable of providing high three-dimensional (3D) resolution with deep tissue penetration[17]. In order to detect the cells of interest against the host tissue background using MRI, the cells need to be labelled with a substance to produce a strong contrast against the background tissue before transplantation. For *in vivo* MRI, this has been achieved mostly with superparamagnetic iron oxide nanoparticles (SPIONs) which could be incorporated into the cells to produce a strong signal loss in T2-weighted MRI by virtue of susceptibility differences to the adjacent environment[18]. However, most of the paramagnetic substances used for MRI contrast agents are composed of gadolinium (Gd^{3+}) and manganese (Mn^{2+}) which are cytotoxic, thus limiting their application *in vivo*[19]. Recent research by Lin and colleagues[20] developed a novel biocompatible nanocomplex known as spermine-modified amylose (ASP) to generate ASP-SPIONs. Amylose, present in starch along with amylopectin, is a linear polysaccharide, in which repeated glucose units are joined by α-1,4 glycosidic linkage. This naturally-occurring polysaccharide has been the subject of intense scientific investigation in the biomaterial field due to absence of toxic effects, biodegradability, biocompatibility, low-cost production, high tensile strength, and better flexibility. On the other hand, spermine, a natural polyamine required for cell physiology, has also been scientifically investigated in cationization of polymers for its potential action as a gene vector[21]. Lin *et al*[22] found that MSCs labelled with ASP-SPIONs have no detrimental toxicity effects on the cell and the labelled cells also retain the magnetic labels and remain viable up to 6 wk (when tested *in vivo*), suggesting the efficiency of this nanomaterial in stem cell tracking after transplantation.

MSCs have been demonstrated to exert therapeutic benefits for brain diseases. However, as previously reported, the percentage of homing cells is relatively low, and only a limited number of MSCs survive and engraft into the ischemic lesion because some cells die once exposed to unfavorable conditions[23]. Hence, improving the engraftment efficiency of MSCs into ischemic lesions is important. In a study done by Huang *et al*[24], a brain-targeting peptide known as palmitic acid (PA)-CLEVSRKNC was selected and coated onto the MSC surface *via* a lipid raft to induce the migration of MSCs to the ischemic lesion specifically. The CLEVSRKNC peptide could be generated from a phage peptide library based on T7 415-1b phage vector displaying CX7C[25]. This peptide has been shown to be able to guide cells to ischemic regions, making it an ideal stroke-homing peptide. Huang *et al*[24] reported that the PA-CLEVSRKNC peptide coating onto MSCs did not impose any cytotoxicity nor detrimental influence on cell differentiation. On the other hand, engraftment of PA-CLEVSRKNC-modified MSCs into the injured brain tissue was significantly enhanced. Moreover, with enhanced targeted cell homing, the number of cells trapped in other non-targeted organs (such as lung and liver) was reduced. This could decrease the risk of toxicity in other non-targeted organs.

The same strategy has also been applied by Tian *et al*[26], where a cyclo (Arg-Gly-Asp-D-Tyr-Lys) peptide [c(RGDyK)] was conjugated to the MSC exosome surface, namely as cRGD-Exo to enhance the targeting capability of the exosomes. c(RGDyK) is a type of peptide sequence with an arginine-glycine-aspartic acid motif, where it possesses strong affinity for $\alpha_v\beta_3$ integrin. $\alpha_v\beta_3$ integrin is a transmembrane glycoprotein that plays an important role in angiogenesis, tumor metastasis and leucocyte migration, making it a suitable target for various inflammatory-related disease including ischemic stroke[27]. In addition, curcumin, a natural compound with antioxidant and anti-inflammatory properties[28] was also loaded onto the cRGD-Exo (cRGD-Exo-cur) to enhance the efficiency of this therapy. The data from this research revealed that the extents of suppression of inflammation and cellular apoptosis were higher than those of the therapy using exosomes or curcumin alone, demonstrating the promising potential of this strategy for ischemic stroke treatment.

Exosomes are extracellular vesicles secreted from various types of cells with diameter range of 40-150 nm[29]. It plays an important role for intercellular communication, facilitating crosstalk between cells located in a distant location *via* transfer of bioactive proteins, lipid and genetic material (*i.e.* RNA). This form of communication may affect many cellular processes such as immune response, antigen presentation and signal transduction[30,31]. Collective lines of evidence have highlighted the possibility of the MSC-derived exosomes as a potential substitute for biological MSC activity, as exosomes are not live cells and thus can overcome the poor survival limitation otherwise associated with MSC therapy [32]. While holding much promise, the use of exosomes for therapy has been hampered by their limited production yield, and thus require some modifications before they can be used efficiently as a therapeutic agent for stroke disease[33]. Based on a study reported by Kim *et al*[34] in the year 2020, the authors had managed to derive exosome-mimicking nanovesicles from MSCs, namely magnetic nanovesicles, *via* serial extrusion through 10 μm, 5 μm, 1 μm, and 400 nm pore-sized membrane filters. The nanovesicles produced were uniform in size (between 168.3 ± 48.3 nm and 194.2 ± 44.5 nm), spherical in shape and possessed lipid bilayers, mimicking the structure of exosomes. Furthermore, they also reported on having fabricated the localization of iron-oxide nanoparticles (IONPs) into the nanovesicles *via* the MSCs. An IONP is a chemical compound at nanoscale size that possesses unique properties including high specific surface area, super paramagnetism and biocompatibility. Therefore,

the IONP is an ideal material for surface functionalization and modification[35]. Kim *et al*[34] also demonstrated that the transplantation of nanovesicles derived from IONP-incorporated MSCs displayed an attenuation in infarction volume and significantly improved motor function in ischemic stroke animal models.

Biomaterial scaffolds have been widely applied in regeneration therapy, as they can mimic the native microenvironment of a healthy brain region to support the regeneration of injured nervous system tissues. In a previous study, the incorporation of this biomaterial demonstrated promising results in CNS regeneration, specifically for tissue repair and functional recovery[36]. A 3D polymer scaffold made by either natural or synthetic material has also been shown to facilitate cell infiltration and proliferation, and aid in the regulation of cell behavior when combined with cell therapy[37]. Among the methods to fabricate the porous structure of 3D scaffolds are microfluidic fabrication, freeze drying, thermoforming, 3D printing, water emulsion, and electrospinning[38,39]. An alternative scaffold material using polylactic acid polymeric rough microfiber (PLA-PRM) scaffolding produced by rotary jet spinning (RJS) was designed by Zamproni *et al*[40] and reported in 2018. The novel RJS engineering strategy was designed without conventional electrospinning; the new method boasts a simple controlling rotation and may produce the functional rough and porous 3D structural support for MSCs to grow on it. In addition, the PLA-PRM 3D scaffold generated using the RJS technique was found to upregulate α6-integrin and C-X-C motif chemokine ligand 12 production of MSCs, which may underlie the mechanism for greater cell retention at the lesion site and may provide additional benefits to MSC transplantation procedures. Indeed, this was demonstrated by the survival and proliferation of MSCs being increased when the cells were transplanted into the ischemic brain region with the aid of a PLA-RPM scaffold, compared to direct injection of MSCs without a scaffold.

Increasing documented evidence has demonstrated the assembly of stem cells into 3D multicellular spheroids, which has many advantages over a traditional 2D monolayer cell culture. This is because the conventional 2D cell culture has losses of cell-cell contact, cell-matrix interaction as well as chemical and mechanical cues due to the lack of exposure to the extracellular matrix (ECM) environment, which may cause alteration in cell metabolism and protein expression[41]. A 3D multicellular spheroid overcomes these limitations by mimicking the *in vivo* cell-matrix interaction and physiological environment[42]. In addition, the bulky size of the spheroid configuration could also reduce the potential of cell leakage from the site of injection. In a study by Hsu and colleagues[43], the potential of this approach was investigated by preassembling the MSCs with vascular endothelial cells (ECs) into a 3D spherical configuration (to generate a MSC/EC spheroid). Using this approach, the transplanted 3D MSC/EC spheroid successfully displayed upregulation of neurotrophic factor, enhanced promotion of neovascularization, higher post-engraftment cell retention, and improved functional recovery in an ischemic stroke animal model.

NSCs

Besides MSCs, NSCs are another potential stem cell type important for regenerative treatment. NSCs are multipotent cells that were first isolated from the CNS of embryonic and adult mice by Reynold, Weiss and colleagues[44], as reported in 1992. These cells have the capacity to self-renew and proliferate for extensive periods of time without limit, while maintaining a stable differentiation capacity. They are able to produce progeny cells that give rise to more specialized cells such as neurons, oligodendrocytes and astrocytes[45]. Endogenous adult NSCs reside in specific niches in the brain including the subventricular zone (SVZ), dentate gyrus of the hippocampus, and the olfactory bulb[45]. However, the turnover rate of endogenous NSCs for neurogenesis at the ischemic-injured area is extremely low, hampered by the harsh ischemic environment and its surrounding high concentration of pro-inflammatory cytokines[46]. Therefore, transplantation of exogenous NSCs has been proposed as an alternative strategy to obviate this issue[47].

Exogenous NSCs can be modified *in vitro* to enhance their therapeutic potential for ischemic stroke therapy prior to transplantation[48]. In a study reported by Ghuman *et al*[49], a combination therapy involving NSCs encapsulated in polyethylene glycol (PEG) microspheres was applied. The encapsulation of these cells into microspheres allowed for the avoidance of a cell mass that would otherwise hamper the stem cell-based therapeutic strategy, as the microsphere could maintain close cell-cell proximity[50]. Results of the study indicated that packaging of NSCs into a microsphere enhanced survival as well as migration after implantation into a stroke cavity. Furthermore, in order to achieve higher efficiency of NSC therapy and confer an effective cellular shield against host enzymatic degradation, the microspheres were packaged into ECM hydrogel. ECM is an essential non-cellular component of the tissue microenvironment, comprised of a complex and highly organized network of macromolecules and is a conglomerate of proteins[51] while hydrogel is a material commonly used in regenerative medicine because it could maintain its structural integrity by physically and chemically crosslinking the polymer chains[52]. As part of the strategy to enhance NSC-based therapy, ECM hydrogel is not only able to provide stability and structural strength to the cells but it can also mimic and provide an ideal microenvironment for cell adhesion, migration, proliferation, differentiation, and maturation. Moreover, the probable reason for use of hydrogel to construct the ECM in the study was its high water absorbing property and dimensional stability which could aid the NSC microsphere for better retention in the ischemic brain region.

Ge *et al*[53] also applied a feasible method to encapsulate NSCs as a layered structure composed of gelatin and hyaluronic acid (HA) biomaterials in order to enhance the therapeutic potential of the NSCs for ischemic stroke. HA is a widely used polyanion that can easily bind to gelatin *via* electrospinning. Moreover, HA can stabilize the components of ECM and trigger its reorganization and consequent remodeling of its original structure after CNS injury[54,55]. Simultaneously, HA facilitates NSCs' direction into neurons, suppresses local excessive inflammation, and reduces cell necrosis and apoptosis at the injured site. The multiple neuroprotective effects demonstrated by HA indicate that layer-by-layer assembly of NSCs (LbL-NSCs) using gelatin and HA is a promising therapeutic strategy to increase the potential benefits of NSCs for ischemic stroke treatment. The researchers also showed that transplantation of LbL-NSCs into a distal middle cerebral artery occlusion (MCAO) mouse model availed functional recovery and reduced infarct volume through promoting the survival of transplanted NSCs, reinforcing neurogenesis in the penumbra area, activating migration of neuroblasts from the lateral ventricle to the penumbra area, and repairing the damaged blood-brain barrier in a hostile niche, after ischemic stroke in mice.

On the other hand, Shabani *et al*[56] encapsulated NSCs with bioengineered Reelin-loaded polylactic coglycolic acidpolyethylene glycol (PLGA/PEG) micelles to retain the NSCs within the ischemic infarct cavity and accelerate the differentiation of these cells to generate *de novo* neuronal tissue after transplantation into a photothrombotic stroke model of mice[56]. Reelin, encoded by the *RELN* gene, is a large secreted ECM glycoprotein that regulates dendritic growth, dendritic spine development, synapse formation, and plasticity[57]. This protein is touted as a key player in the formation of the cerebral cortex and maintenance of adult synaptogenesis. Therefore, it was suggested that Reelin can reduce pathologies related to cerebral ischemia-reperfusion injury. In line with this claim, the researchers enriched the NSCs with Reelin and packaged the modified NSCs into PLGA, a United States Food and Drug Administration-approved biomaterial that can be injected directly into the injured sites. Due to the unique physicochemical features of PLGA, it is commonly used as a carrier to support stem cell delivery for the treatment of brain disorders[58]. In the study, the researchers further functionalized PLGA micelles using PEG polymer chains *via* the biochemical modification process known as PEGylation. The combination of PLGA copolymer with the non-cytotoxic and hydrophilic PEG substrate offers the desired microenvironment for the optimal growth of NSCs. The co-administration of NSCs with the Reelin-loaded PLGA/PEG micelles successfully promoted the commitment of NSCs toward a neural lineage and adult neurogenesis, resulting in reduction of the cavity size and alleviation of the functional behavior disorders after ischemic conditions.

Nanomaterial-assisted NSC therapy has led to significant progress in the treatment for ischemic stroke disease. A recent finding reported by Li *et al*[59] showed that a type of magnetic nanobubbles (MNBs) fabricated through the self-assembly of poly-glucose sorbitol carboxymethyl ether-modified (γ-Fe_2O_3)-SPIONPs can guide NSC differentiation fate by activation of the bone morphogenetic protein 2 (BMP2)/Smad biochemical signaling pathway. BMP signaling plays a pivotal role in brain development and NSC behavior, and it has been associated with a large number of related biological processes such as cell growth and cell differentiation[60]. Implantation of MNB-labeled NSCs into photothrombotic ischemic stroke mice also demonstrated that the MNB structure can direct NSC differentiation *in vivo* and in particular it can increase the efficiency of neuronal lineage differentiation.

iPSCs

iPSCs are a type of pluripotent stem cell derived from adult somatic cells that have been genetically reprogrammed to ESC-like state through the forced expression of pluripotency genes[61]. iPSCs are similar to ESCs in many aspects, including the expression of ESC markers, chromatin methylation patterns, embryoid body formation, and most importantly the pluripotency and the ability to differentiate into many different types of tissues *in vitro*. iPSCs were first generated from mouse fibroblasts by the Yamanaka lab at Kyoto University in 2006[62]. Shortly thereafter, in late 2007, human iPSCs were produced for the first time by Yamanaka's and Thomson's groups[63,64], both labs working independently and starting with human fibroblasts; these studies provided an invaluable reservoir of human pluripotent cells that could be genetically engineered and differentiated into target cells to treat various human genetic and degenerative diseases once transplanted. However, a major obstacle for using human iPSCs for cell therapy is the lack of simple, cost-saving, and scalable methods for cell production[65]. Moreover, the biological activity of the differentiated cells may be variable due to line-to-line variation (batch effect)[66].

In order to overcome this obstacle, Zhang *et al*[67] described a simplified 3D microscaffold culture using chemically defined medium composed of only four main ingredients, namely recombinant human albumin, L-ascorbic acid 2-phosphate, human apo-transferrin, and sodium selenite (AATS), for rapid, stable and highly efficient differentiation of human iPSCs into ECs and smooth muscle cells (SMCs). The researchers found that the ECs and SMCs generated in the AATS medium were similar to their counterpart primary cells. Moreover, the ECs and SMCs exhibit a strong revascularization ability upon transplantation to the permanent MCAO mouse model, which confirmed their therapeutic value in regenerative medicine. Such a simplified and robust design may facilitate a cost-effective and efficient system to create good manufacturing practices for the large-scale bioproduction of ECs and SMCs for human vascular diseases including the ischemic stroke.

On the other hand, McCarry *et al*[68] described the optimization of mouse iPSC- derived NPCs by encapsulating the cells in a chondroitin sulfate-A hydrogel (to generate CS-A + iPSC-NPCs) that can confer protection to the iPSC-NPCs and enhance their survival rate in ischemic brain. Treatment with CS-A + iPSC-NPCs were found to increase vascular density, improve angiogenesis, promote large vessel remodeling, augment cerebral blood flow recovery, and improve post-stroke sensorimotor deficits after transplantation into an ischemic mouse brain. CS-A was also found to interact with iPSC-NPCs synergically to increase the level of macrophage expression factors associated with tissue regeneration, such as monocyte chemo-attractant protein-1 which had been shown to recruit specific subsets of macrophages that participate in regeneration processes, including angiogenesis, arteriogenesis, and even neurogenesis[69,70].

NPCs

NPCs are mostly present in the CNS of a developing embryo, but they are also found in the neonatal and mature adult brain. Initially, the NPCs were referred to as ''spongioblasts'' and ''fetal glia'' due to their non-neuronal nature and non-mature glial cell morphology[71]. In general, progenitor cells are multipotent precursor cells that have the capacity to differentiate into a subset of cell types. The difference between stem cells and progenitor cells is that the former are self-renewing and can replicate indefinitely to produce daughter cells, while the latter only divide a limited number of times. There are many types of progenitor cells throughout the human body with the capability to differentiate into cells that belong to the same tissue or organ. NPCs are descendants of NSCs that are destined to further differentiate into specialized brain cell types. Thus, the NPCs are postulated to play important roles in facilitating neuronal and functional recovery post-stroke.

Therapeutic strategies based on transplanted progenitor cells have strong promise for the treatment of diseases by implementing tissue regeneration and repair. However, one of the crucial points in this approach is the need to carry out long-term and noninvasive imaging of the transplanted cells in the host organ and to track their migration and distribution *in vivo*. Zhang *et al*[72] reported on a successful NPC labeling and tracking method using SPIONs that had been fabricated with template growth of silica on the surface to fluorescent mesoporous silica-coated superparamagnetic iron 1 oxide nanoparticles (fmSiO_4@SPIONs) which were discrete and uniform in size, and had clear core-shell structure. The magnetic core size was about 10 nm and the fluorescent mesoporous silica coating layer was around 20 nm. The fmSiO_4@SPIONs showed improved cell labeling efficiency, and hence increased MRI sensitivity to track the NPCs after transplantation. In the future, a useful innovation of this biomaterial will be resiliency for cell imaging, which will provide greater promise for cell tracking by MRI.

The long-term survival and integration of grafted NPCs remain challenges in a stroke-affected hostile environment, due to the ischemic condition and highly pro-inflammatory cues. A variety of natural and synthetic polymers such as collagen, chitosan, and poly (lactic acid) as well as decellularized scaffolds have been employed to support neural grafts in the ischemic brain. In a recent study reported by Somaa *et al*[73], a self-assembling peptide (SAP) scaffold was developed to provide physical and trophic support for long-term survival and functional maturation of NPCs generated from pluripotent stem cells. The SAP is a tissue (brain)-specific peptide and it was made using solid phase peptide synthesis. According to the results reported, the functionalized SAP scaffold was capable of restoring tissue structure within the lesion cavity, thereby reducing atrophy and cell loss within the damaged area after the stroke attack. Moreover, they also found that the SAP scaffold-supported cells were capable of prolonged restoration of motor function, providing evidence of sustained benefits of human stem cells and biomaterials in repair of the ischemic brain.

EPCs

Recently, EPCs, the precursor of the mature endothelial blood vessel, have been studied extensively in the tissue regeneration and repair field. Isolation of EPCs was first reported by Asahara *et al*[74] in 1997, from peripheral blood circulation. These mononuclear cells are a subtype of progenitor cells originated from bone marrow. In general, EPCs could be identified by cell surface expression of hematopoietic marker proteins CD34 and CD133 and the endothelial marker vascular endothelial growth factor receptor 2. EPCs are able to promote and facilitate angiogenesis, vascular homeostasis, vascular repair, neovascularization and endothelial regeneration of ischemic tissues[75] because they express several angiogenic and vasculogenic factors such as platelet-derived growth factor BB, fibroblast growth factor, hepatocyte growth factor, vascular endothelial growth factor (VEGF) and angiopoietin-1[76,77]. Despite the potential of these cells to be applied in ischemic stroke treatment, however, similar to the other types of cell-based therapies, their low rates of migration and survival after engraftment are key limiting factors. Therefore, strategic modifications are required to enhance the migration and survival rates of this therapy.

Research efforts by Li *et al*[78] to enhance the migration of EPCs to an ischemic affected area in the brain involved labelling the EPCs with silica-coated SPIONs (SiO_4@SPIONs-EPCs). Subsequently, an exterior magnetic field was applied to guide these cells directly to the targeted area. Silica was added to the unmodified SPION because this material has higher intracellular labelling efficiency and therefore was anticipated to have higher MRI sensitivity[17]. Moreover, silica has also been recognized in

previous studies as a superior choice of coating material for SPIONs due to its biocompatibility, stability, and functionality[79]. SiO_4@SPIONs-EPCs homing was found to be increased greatly in this study, with further promising findings of enhanced neurobehavioral activity, reduced infract volume, higher VEGF expression, and increased microvessel density. Besides its effect on homing to the infarcted region, silica also acts as a cell tracking agent, supporting its role as a tool to provide better understanding of cellular migration and survival after cell transplantation.

Another study carried out by Wang *et al*[80] involved the utilization of small interfering RNA (siRNA) to silence the hypoxia-inducible factor (HIF)-prolyl hydroxylase 2 (*PHD2*) gene in EPCs. The silencing was expected to stabilize the HIF-1 transcriptional factor, which is the key regulator of multiple genes that promote cell survival in a hypoxic environment such as glycolytic enzymes, erythropoietin, and VEGF[81]. Nonetheless, direct delivery of siRNA to EPCs may trigger rapid enzymatic digestion and poor cellular intake, representing a potential limitation of this strategy. Therefore, a delivery system using polyethylenimine (Alkyl-PEI)-encapsulated SPIONs was designed by this team to ensure effective delivery of the siRNA to the EPCs. Ultimately, this study demonstrated the effectiveness of PHD2 silencing in EPCs, with an elevation of CXCR4 and HIF-1α expression, which are important in homing, migration and survival of cells in an ischemic region. Furthermore, the observed reduction in infarct area and increases in functional activity and fractional anisotropy values suggested the potential of this strategy to enhance the effectiveness of EPCs for stroke treatment.

NEPCs

NEPCs are stem cells that differentiate into neurons and glia, essential components of the human CNS, following the process of neurogenesis. In a study reported by Payne *et al*[82], a biocompatible and bioresorbable hydrogel composed of hyaluronan and methylcellulose (HAMC) was used to deliver human cortically-specified NEPCs into stroke-injured rat brain. The authors then examined the survival and proliferation of the transplanted cells based on the expression of a specific NEPC marker, the human nuclear antigen (HuNu). They successfully found $HuNu^+$ nuclei at the injected location 50 d after transplantation and that approximately 80% of animals that received transplants contained surviving cells, which was similar across all experimental groups. Their findings were similar to those of other studies in which HAMC hydrogel was found to improve cell survival and distribution in several CNS preclinical models of disease[83-85]. In conclusion, the HAMC hydrogel delivery vehicle used could co-deliver pro-survival or differentiation factors to promote the survival of NEPCs and/or direct their differentiation.

Neuroblasts

Neuroblasts, also known as immature neurons, are the precursors of neurons, which can be found in the neurogenic niche of the ventricular-SVZ in brain. Recent studies on implantation of neuroblasts have suggested their potential as an alternative therapy for ischemic stroke. Neuroblasts are capable of homing to an injured site and differentiating into a matured neuron; however, the molecular mechanism that regulates this migration process is unknown. Fujioka *et al*[86] suggested a role for β1-class integrins, transmembrane receptors for ECM proteins, in the neuroblast migration activity. They also developed an artificial laminin-containing scaffold to promote neuroblast chain formation and migration toward an injured area. To do this, they injected hydrogel with or without laminin (designated as laminin-hydrogel and control-hydrogel, respectively), which self-assembles from a soluble state into hydrated nanofibers, into the striatum of 10-d post-stroke brains. The migration of neuroblasts along the hydrogel toward the injured area was examined 8 d later. More migrating neuroblasts were observed on the laminin-hydrogel than on the control-hydrogel; additionally, chains were only formed on the laminin-hydrogel group, suggesting that the artificial laminin scaffold can efficiently mimic vasculature and facilitate neuronal migration toward an injured area. Thus, for the regeneration of brain tissue, artificial scaffolds containing laminin would be useful to promote neuroblast migration.

CONCLUSION

This review article provides new insights into the novel biomaterial applications that have been developed to enhance stem/progenitor cell-based therapy for ischemic stroke. According to the previously published data collected in this review, we can reasonably conclude that biomaterials could modify these cells to enhance their migration capacity to a targeted area of injury, increase their retention rate in the hostile ischemic microenvironment, and promote the secretion of importance cytokines for reparative mechanisms, such as neurogenic factors and angiogenic factors. In addition, biomaterials can be used also to track the cells *in vivo*, providing for a clearer understanding of the fate of the cells after transplantation. Some of these effects are direct and some are indirect, but each mechanism of action must be clearly understood in order to improve the efficacy of this therapy for stroke. There is currently a scarcity of published evidence on the efficacy of biomaterial-modified cell-based therapy in clinical studies. Therefore, more evidence-based clinical studies are required to verify the efficacy and safety of the combination of biomaterials and stem/progenitor cells as potential

therapeutic agents for various human diseases such as ischemic stroke.

ARTICLE HIGHLIGHTS

Research background

Low cell survival after transplantation has emerged as the biggest challenge of stem cell-based therapies for ischemic stroke in the clinical setting. Thus, biomaterials have been explored as a potential approach to provide a supportable cellular microenvironment or functional modification on the stem cells to optimize their reparative roles in injured tissues or organs.

Research motivation

Ischemic stroke remains a significant health issue globally. Stem/progenitor cells as regenerative treatment for stroke is practicable and beneficial for stroke patients, especially those in the chronic phase who could not be cured by any other means of currently available treatments.

Research objectives

This systematic review aimed to collect and present the current knowledge on state-of-art functional biomaterials that have been developed to enhance the therapeutic potential of stem cell-based treatments for ischemic stroke and to provide detailed insights of the mechanisms underlying these biomaterial-based approaches.

Research methods

Publications indexed in the PubMed, Science Direct and Scopus literature databases were searched using the keywords "biomaterial" AND "ischemic stroke" AND "stem cells" OR "progenitor cells" OR "undifferentiated cells" to identify topically-relevant articles published in English during the years of 2011 to 2022. The systematic search was conducted up to September 30, 2022.

Research results

Ultimately, 19 types of biomaterials were identified that modify seven major stem/progenitor cell types to enhance their therapeutic potential for ischemic stroke.

Research conclusions

Biomaterials can modify stem cells to enhance their migration capacity to a targeted area of injury, increase their retention rate, promote the secretion of important cytokines to support a reparative mechanism, and provide clearer understanding of the fate of transplanted cells *via in vivo* tracking. Biomaterials can enhance stem cell-based therapy for ischemic stroke.

Research perspectives

It is crucial to study and define the mechanisms of state-of-art functional biomaterial-based approaches to maximize the therapeutic potential of stem cell-based treatments for ischemic stroke. Findings from future in-depth clinical investigations are expected to support the translation of this therapy into clinical application. Meta-analyses can be performed to generate a quantitative estimate of the effectiveness of the intervention.

ACKNOWLEDGEMENTS

The authors would like to thank the Universiti Sains Malaysia libraries, particularly Perpustakaan Hamdan Tahir and Perpustakaan Hamzah Sendut, for providing the resources to write this systematic review. Finally, the authors would like to express their appreciation to all the scientists whose previous work contributed to this review article.

FOOTNOTES

Author contributions: Tan SC designed the research; Mohd Satar A and Othman FA performed the literature review and analysis; All authors contributed to writing of the paper and gave approval of the final version.

Supported by the Universiti Sains Malaysia Research University Individual Grant, No. 1001/PPSK/8012273.

Conflict-of-interest statement: All the authors declare having no conflicts of interest.

PRISMA 2009 Checklist statement: The authors have read the PRISMA 2009 Checklist, and the manuscript was prepared and revised according to the PRISMA 2009 Checklist.

Country/Territory of origin: Malaysia

ORCID number: Suat Cheng Tan 0000-0001-5869-6096.

S-Editor: Zhang H
L-Editor: Filipodia
P-Editor: Zhang H

REFERENCES

1 **Rojsanga W**, Sawanyawisuth K, Chotmongkol V, Tiamkao S, Kongbonkiat K, Kasemsap N. Clinical risk factors predictive of thrombotic stroke with large cerebral infarction. *Neurol Int* 2019; **11**: 7941 [PMID: 31281599 DOI: 10.4081/ni.2019.7941]
2 **Ntaios G**, Papavasileiou V, Milionis H, Makaritsis K, Vemmou A, Koroboki E, Manios E, Spengos K, Michel P, Vemmos K. Embolic Strokes of Undetermined Source in the Athens Stroke Registry: An Outcome Analysis. *Stroke* 2015; **46**: 2087-2093 [PMID: 26159795 DOI: 10.1161/STROKEAHA.115.009334]
3 **Regenhardt RW**, Das AS, Lo EH, Caplan LR. Advances in Understanding the Pathophysiology of Lacunar Stroke: A Review. *JAMA Neurol* 2018; **75**: 1273-1281 [PMID: 30167649 DOI: 10.1001/jamaneurol.2018.1073]
4 **Kwon S**, Hartzema AG, Duncan PW, Min-Lai S. Disability measures in stroke: relationship among the Barthel Index, the Functional Independence Measure, and the Modified Rankin Scale. *Stroke* 2004; **35**: 918-923 [PMID: 14976324 DOI: 10.1161/01.STR.0000119385.56094.32]
5 **Baker EW**, Kinder HA, West FD. Neural stem cell therapy for stroke: A multimechanistic approach to restoring neurological function. *Brain Behav* 2019; 9: e01214 [PMID: 30747485 DOI: 10.1002/brb3.1214]
6 **Li Z**, Dong X, Tian M, Liu C, Wang K, Li L, Liu Z, Liu J. Stem cell-based therapies for ischemic stroke: a systematic review and meta-analysis of clinical trials. *Stem Cell Res Ther* 2020; **11**: 252 [PMID: 32586371 DOI: 10.1186/s13287-020-01762-z]
7 **Singh M**, Pandey PK, Bhasin A, Padma MV, Mohanty S. Application of Stem Cells in Stroke: A Multifactorial Approach. *Front Neurosci* 2020; **14**: 473 [PMID: 32581669 DOI: 10.3389/fnins.2020.00473]
8 **Lin X**, Li N, Tang H. Recent Advances in Nanomaterials for Diagnosis, Treatments, and Neurorestoration in Ischemic Stroke. *Front Cell Neurosci* 2022; **16**: 885190 [PMID: 35836741 DOI: 10.3389/fncel.2022.885190]
9 **Wang Y**, Yi H, Song Y. The safety of MSC therapy over the past 15 years: a meta-analysis. *Stem Cell Res Ther* 2021; **12**: 545 [PMID: 34663461 DOI: 10.1186/s13287-021-02609-x]
10 **Pountos I**. Mesenchymal Stem Cells. In: Adult Stem Cells: Recent Advances. SM Group, 2017: 1-15
11 **Sandhaanam SD**, Pathalam G, Dorairaj S, Savariar V. Mesenchymal stem cells (MSC): Identification, Proliferation and Differentiation-A review article. *PeerJ PrePrints* 2013; **1**: 1-13 [DOI: 10.7287/peerj.preprints.148v1]
12 **Yang K**, Park HJ, Han S, Lee J, Ko E, Kim J, Lee JS, Yu JH, Song KY, Cheong E, Cho SR, Chung S, Cho SW. Recapitulation of in vivo-like paracrine signals of human mesenchymal stem cells for functional neuronal differentiation of human neural stem cells in a 3D microfluidic system. *Biomaterials* 2015; **63**: 177-188 [PMID: 26113074 DOI: 10.1016/j.biomaterials.2015.06.011]
13 **Iqbal S**, Zhao Z. Poly (β amino esters) copolymers: Novel potential vectors for delivery of genes and related therapeutics. *Int J Pharm* 2022; **611**: 121289 [PMID: 34775041 DOI: 10.1016/j.ijpharm.2021.121289]
14 **Park HJ**, Lee J, Kim MJ, Kang TJ, Jeong Y, Um SH, Cho SW. Sonic hedgehog intradermal gene therapy using a biodegradable poly(β-amino esters) nanoparticle to enhance wound healing. *Biomaterials* 2012; **33**: 9148-9156 [PMID: 23018131 DOI: 10.1016/j.biomaterials.2012.09.005]
15 **Zhang Z**, Zhang N, Ding S. Glial cell line derived neurotrophic factor in brain repair after focal ischemic stroke. *Neural Regen Res* 2022; **17**: 1735-1736 [PMID: 35017424 DOI: 10.4103/1673-5374.332141]
16 **Kircher MF**, Gambhir SS, Grimm J. Noninvasive cell-tracking methods. *Nat Rev Clin Oncol* 2011; **8**: 677-688 [PMID: 21946842 DOI: 10.1038/nrclinonc.2011.141]
17 **Gera A**, Steinberg GK, Guzman R. In vivo neural stem cell imaging: current modalities and future directions. *Regen Med* 2010; **5**: 73-86 [PMID: 20017696 DOI: 10.2217/rme.09.79]
18 **Li L**, Jiang W, Luo K, Song H, Lan F, Wu Y, Gu Z. Superparamagnetic iron oxide nanoparticles as MRI contrast agents for non-invasive stem cell labeling and tracking. *Theranostics* 2013; **3**: 595-615 [PMID: 23946825 DOI: 10.7150/thno.5366]
19 **Yang X**, Tian DC, He W, Lv W, Fan J, Li H, Jin WN, Meng X. Cellular and molecular imaging for stem cell tracking in neurological diseases. *Stroke Vasc Neurol* 2021; **6**: 121-127 [PMID: 33122254 DOI: 10.1136/svn-2020-000408]
20 **Clifton P**, Keogh J. Starch. In: Benjamin Caballero, Paul M. Finglas FT. Encyclopedia of Food and Health. Academic Press, 2016: 146-151

21 **Pegg AE**. The function of spermine. *IUBMB Life* 2014; **66**: 8-18 [PMID: 24395705 DOI: 10.1002/iub.1237]
22 **Lin BL**, Zhang JZ, Lu LJ, Mao JJ, Cao MH, Mao XH, Zhang F, Duan XH, Zheng CS, Zhang LM, Shen J. Superparamagnetic Iron Oxide Nanoparticles-Complexed Cationic Amylose for In Vivo Magnetic Resonance Imaging Tracking of Transplanted Stem Cells in Stroke. *Nanomaterials (Basel)* 2017; **7** [PMID: 28489049 DOI: 10.3390/nano7050107]
23 **Ullah M**, Liu DD, Thakor AS. Mesenchymal Stromal Cell Homing: Mechanisms and Strategies for Improvement. *iScience* 2019; **15**: 421-438 [PMID: 31121468 DOI: 10.1016/j.isci.2019.05.004]
24 **Huang B**, Jiang XC, Zhang TY, Hu YL, Tabata Y, Chen Z, Pluchino S, Gao JQ. Peptide modified mesenchymal stem cells as targeting delivery system transfected with miR-133b for the treatment of cerebral ischemia. *Int J Pharm* 2017; **531**: 90-100 [PMID: 28827201 DOI: 10.1016/j.ijpharm.2017.08.073]
25 **Hong HY**, Choi JS, Kim YJ, Lee HY, Kwak W, Yoo J, Lee JT, Kwon TH, Kim IS, Han HS, Lee BH. Detection of apoptosis in a rat model of focal cerebral ischemia using a homing peptide selected from in vivo phage display. *J Control Release* 2008; **131**: 167-172 [PMID: 18692101 DOI: 10.1016/j.jconrel.2008.07.020]
26 **Tian T**, Zhang HX, He CP, Fan S, Zhu YL, Qi C, Huang NP, Xiao ZD, Lu ZH, Tannous BA, Gao J. Surface functionalized exosomes as targeted drug delivery vehicles for cerebral ischemia therapy. *Biomaterials* 2018; **150**: 137-149 [PMID: 29040874 DOI: 10.1016/j.biomaterials.2017.10.012]
27 **Vhora I**, Bhatt SPPB, Misra A. Protein- and Peptide-Drug Conjugates: An Emerging Drug Delivery Technology. In: Donev R. Advances in Protein Chemistry and Structural Biology. Academic Press, 2015: 1-55
28 **Hewlings SJ**, Kalman DS. Curcumin: A Review of Its Effects on Human Health. *Foods* 2017; **6** [PMID: 29065496 DOI: 10.3390/foods6100092]
29 **Heldring N**, Mäger I, Wood MJ, Le Blanc K, Andaloussi SE. Therapeutic Potential of Multipotent Mesenchymal Stromal Cells and Their Extracellular Vesicles. *Hum Gene Ther* 2015; **26**: 506-517 [PMID: 26153722 DOI: 10.1089/hum.2015.072]
30 **Greening DW**, Gopal SK, Xu R, Simpson RJ, Chen W. Exosomes and their roles in immune regulation and cancer. *Semin Cell Dev Biol* 2015; **40**: 72-81 [PMID: 25724562 DOI: 10.1016/j.semcdb.2015.02.009]
31 **Gangoda L**, Boukouris S, Liem M, Kalra H, Mathivanan S. Extracellular vesicles including exosomes are mediators of signal transduction: are they protective or pathogenic? *Proteomics* 2015; **15**: 260-271 [PMID: 25307053 DOI: 10.1002/pmic.201400234]
32 **Mendt M**, Rezvani K, Shpall E. Mesenchymal stem cell-derived exosomes for clinical use. *Bone Marrow Transplant* 2019; **54**: 789-792 [PMID: 31431712 DOI: 10.1038/s41409-019-0616-z]
33 **Wiklander OP**, Nordin JZ, O'Loughlin A, Gustafsson Y, Corso G, Mäger I, Vader P, Lee Y, Sork H, Seow Y, Heldring N, Alvarez-Erviti L, Smith CI, Le Blanc K, Macchiarini P, Jungebluth P, Wood MJ, Andaloussi SE. Extracellular vesicle in vivo biodistribution is determined by cell source, route of administration and targeting. *J Extracell Vesicles* 2015; **4**: 26316 [PMID: 25899407 DOI: 10.3402/jev.v4.26316]
34 **Kim HY**, Kim TJ, Kang L, Kim YJ, Kang MK, Kim J, Ryu JH, Hyeon T, Yoon BW, Ko SB, Kim BS. Mesenchymal stem cell-derived magnetic extracellular nanovesicles for targeting and treatment of ischemic stroke. *Biomaterials* 2020; **243**: 119942 [PMID: 32179302 DOI: 10.1016/j.biomaterials.2020.119942]
35 **Ajinkya N**, Yu X, Kaithal P, Luo H, Somani P, Ramakrishna S. Magnetic Iron Oxide Nanoparticle (IONP) Synthesis to Applications: Present and Future. *Materials (Basel)* 2020; **13** [PMID: 33080937 DOI: 10.3390/ma13204644]
36 **Wang Y**, Tan H, Hui X. Biomaterial Scaffolds in Regenerative Therapy of the Central Nervous System. *Biomed Res Int* 2018; **2018**: 7848901 [PMID: 29805977 DOI: 10.1155/2018/7848901]
37 **Ellis-Behnke RG**, Teather LA, Schneider GE, So KF. Using nanotechnology to design potential therapies for CNS regeneration. *Curr Pharm Des* 2007; **13**: 2519-2528 [PMID: 17692020 DOI: 10.2174/138161207781368648]
38 **Tan Y**, Richards DJ, Trusk TC, Visconti RP, Yost MJ, Kindy MS, Drake CJ, Argraves WS, Markwald RR, Mei Y. 3D printing facilitated scaffold-free tissue unit fabrication. *Biofabrication* 2014; **6**: 024111 [PMID: 24717646 DOI: 10.1088/1758-5082/6/2/024111]
39 **Wu X**, Liu Y, Li X, Wen P, Zhang Y, Long Y, Wang X, Guo Y, Xing F, Gao J. Preparation of aligned porous gelatin scaffolds by unidirectional freeze-drying method. *Acta Biomater* 2010; **6**: 1167-1177 [PMID: 19733699 DOI: 10.1016/j.actbio.2009.08.041]
40 **Zamproni LN**, Grinet MAVM, Mundim MTVV, Reis MBC, Galindo LT, Marciano FR, Lobo AO, Porcionatto M. Rotary jet-spun porous microfibers as scaffolds for stem cells delivery to central nervous system injury. *Nanomedicine* 2019; **15**: 98-107 [PMID: 30244084 DOI: 10.1016/j.nano.2018.08.014]
41 **Nath S**, Devi GR. Three-dimensional culture systems in cancer research: Focus on tumor spheroid model. *Pharmacol Ther* 2016; **163**: 94-108 [PMID: 27063403 DOI: 10.1016/j.pharmthera.2016.03.013]
42 **Cui X**, Hartanto Y, Zhang H. Advances in multicellular spheroids formation. *J R Soc Interface* 2017; **14** [PMID: 28202590 DOI: 10.1098/rsif.2016.0877]
43 **Hsu TW**, Lu YJ, Lin YJ, Huang YT, Hsieh LH, Wu BH, Lin YC, Chen LC, Wang HW, Chuang JC, Fang YQ, Huang CC. Transplantation of 3D MSC/HUVEC spheroids with neuroprotective and proangiogenic potentials ameliorates ischemic stroke brain injury. *Biomaterials* 2021; **272**: 120765 [PMID: 33780686 DOI: 10.1016/j.biomaterials.2021.120765]
44 **Reynolds BA**, Weiss S. Generation of neurons and astrocytes from isolated cells of the adult mammalian central nervous system. *Science* 1992; **255**: 1707-1710 [PMID: 1553558 DOI: 10.1126/science.1553558]
45 **Lee VM**, Louis SA, Reynolds BA. Neural Stem Cells. Stem Cell Technologies 2015; 1-6
46 **Hao L**, Zou Z, Tian H, Zhang Y, Zhou H, Liu L. Stem cell-based therapies for ischemic stroke. *Biomed Res Int* 2014; **2014**: 468748 [PMID: 24719869 DOI: 10.1155/2014/468748]
47 **Garzón-Muvdi T**, Quiñones-Hinojosa A. Neural stem cell niches and homing: recruitment and integration into functional tissues. *ILAR J* 2009; **51**: 3-23 [PMID: 20075495 DOI: 10.1093/ilar.51.1.3]
48 **Kornblum HI**. Introduction to neural stem cells. *Stroke***38**: 810-816 [PMID: 17261745 DOI: 10.1161/01.STR.0000255757.12198.0f]
49 **Ghuman H**, Matta R, Tompkins A, Nitzsche F, Badylak SF, Gonzalez AL, Modo M. ECM hydrogel improves the delivery of PEG microsphere-encapsulated neural stem cells and endothelial cells into tissue cavities caused by stroke. *Brain Res*

Bull 2021; **168**: 120-137 [PMID: 33373665 DOI: 10.1016/j.brainresbull.2020.12.004]
50 **Matta R**, Gonzalez AL. Stroke repair *via* biomimicry of subventricular zone. *Fornt Mater* 2018; **5** [DOI: 10.3389/fmats.2018.00015]
51 **Assunção M**, Dehghan-Baniani D, Yiu CHK, Später T, Beyer S, Blocki A. Cell-Derived Extracellular Matrix for Tissue Engineering and Regenerative Medicine. *Front Bioeng Biotechnol* 2020; **8**: 602009 [PMID: 33344434 DOI: 10.3389/fbioe.2020.602009]
52 **Sackett SD**, Tremmel DM, Ma F, Feeney AK, Maguire RM, Brown ME, Zhou Y, Li X, O'Brien C, Li L, Burlingham WJ, Odorico JS. Extracellular matrix scaffold and hydrogel derived from decellularized and delipidized human pancreas. *Sci Rep* 2018; **8**: 10452 [PMID: 29993013 DOI: 10.1038/s41598-018-28857-1]
53 **Ge H**, Hu Q, Chen T, Yang Y, Zhang C, Zhong J, Yin Y, Jiang X, Zhou X, Wang S, Hu R, Li W, Feng H. Transplantation of layer-by-layer assembled neural stem cells tethered with vascular endothelial growth factor reservoir promotes neurogenesis and angiogenesis after ischemic stroke in mice. *Appl Mater Today* 2022; **28**: 101548 [DOI: 10.1016/j.apmt.2022.101548]
54 **Shuborna NS**, Chaiyasamut T, Sakdajeyont W, Vorakulpipat C, Rojvanakarn M, Wongsirichat N. Generation of novel hyaluronic acid biomaterials for study of pain in third molar intervention: a review. *J Dent Anesth Pain Med* 2019; **19**: 11-19 [PMID: 30859129 DOI: 10.17245/jdapm.2019.19.1.11]
55 **Dovedytis M**, Liu ZJ, Bartlett S. Hyaluronic acid and its biomedical applications: A review. *Engineered Regeneration* 2020; **1**: 102-113 [DOI: 10.1016/j.engreg.2020.10.001]
56 **Shabani Z**, Rahbarghazi R, Karimipour M, Ghadiri T, Salehi R, Sadigh-Eteghad S, Farhoudi M. Transplantation of bioengineered Reelin-loaded PLGA/PEG micelles can accelerate neural tissue regeneration in photothrombotic stroke model of mouse. *Bioeng Transl Med* 2022; **7**: e10264 [PMID: 35111956 DOI: 10.1002/btm2.10264]
57 **Jossin Y**. Reelin Functions, Mechanisms of Action and Signaling Pathways During Brain Development and Maturation. *Biomolecules* 2020; **10** [PMID: 32604886 DOI: 10.3390/biom10060964]
58 **Essa D**, Kondiah PPD, Choonara YE, Pillay V. The Design of Poly(lactide-co-glycolide) Nanocarriers for Medical Applications. *Front Bioeng Biotechnol* 2020; **8**: 48 [PMID: 32117928 DOI: 10.3389/fbioe.2020.00048]
59 **Li J**, Zhang Y, Lou Z, Li M, Cui L, Yang Z, Zhang L, Gu N, Yang F. Magnetic Nanobubble Mechanical Stress Induces the Piezo1-Ca^{2+}-BMP2/Smad Pathway to Modulate Neural Stem Cell Fate and MRI/Ultrasound Dual Imaging Surveillance for Ischemic Stroke. *Small* 2022; **18**: e2201123 [PMID: 35555970 DOI: 10.1002/smll.202201123]
60 **Yan W**, Chen ZY, Chen JQ, Chen HM. BMP2 promotes the differentiation of neural stem cells into dopaminergic neurons *in vitro* via miR-145-mediated upregulation of Nurr1 expression. *Am J Transl Res* 2016; **8**: 3689-3699 [PMID: 27725851]
61 **Al Abbar A**, Ngai SC, Nograles N, Alhaji SY, Abdullah S. Induced Pluripotent Stem Cells: Reprogramming Platforms and Applications in Cell Replacement Therapy. *Biores Open Access* 2020; **9**: 121-136 [PMID: 32368414 DOI: 10.1089/biores.2019.0046]
62 **Takahashi K**, Yamanaka S. Induction of pluripotent stem cells from mouse embryonic and adult fibroblast cultures by defined factors. *Cell* 2006; **126**: 663-676 [PMID: 16904174 DOI: 10.1016/j.cell.2006.07.024]
63 **Takahashi K**, Tanabe K, Ohnuki M, Narita M, Ichisaka T, Tomoda K, Yamanaka S. Induction of pluripotent stem cells from adult human fibroblasts by defined factors. *Cell* 2007; **131**: 861-872 [PMID: 18035408 DOI: 10.1016/j.cell.2007.11.019]
64 **Yu J**, Vodyanik MA, Smuga-Otto K, Antosiewicz-Bourget J, Frane JL, Tian S, Nie J, Jonsdottir GA, Ruotti V, Stewart R, Slukvin II, Thomson JA. Induced pluripotent stem cell lines derived from human somatic cells. *Science* 2007; **318**: 1917-1920 [PMID: 18029452 DOI: 10.1126/science.1151526]
65 **Youssef AA**, Ross EG, Bolli R, Pepine CJ, Leeper NJ, Yang PC. The Promise and Challenge of Induced Pluripotent Stem Cells for Cardiovascular Applications. *JACC Basic Transl Sci* 2016; **1**: 510-523 [PMID: 28580434 DOI: 10.1016/j.jacbts.2016.06.010]
66 **Shi Y**, Inoue H, Wu JC, Yamanaka S. Induced pluripotent stem cell technology: a decade of progress. *Nat Rev Drug Discov* 2017; **16**: 115-130 [PMID: 27980341 DOI: 10.1038/nrd.2016.245]
67 **Zhang F**, Zhu Y, Chen J, Kuang W, Huang R, Duan F, Li Y, Wang L, Qiu H, Chen X, Ming J, Liu P, Du Y, Chang SC, Chen L, Na J. Efficient endothelial and smooth muscle cell differentiation from human pluripotent stem cells through a simplified insulin-free culture system. *Biomaterials* 2021; **271**: 120713 [PMID: 33618219 DOI: 10.1016/j.biomaterials.2021.120713]
68 **McCrary MR**, Jiang MQ, Jesson K, Gu X, Logun MT, Wu A, Gonsalves N, Karumbaiah L, Yu SP, Wei L. Glycosaminoglycan scaffolding and neural progenitor cell transplantation promotes regenerative immunomodulation in the mouse ischemic brain. *Exp Neurol* 2022; **357**: 114177 [PMID: 35868359 DOI: 10.1016/j.expneurol.2022.114177]
69 **Deshmane SL**, Kremlev S, Amini S, Sawaya BE. Monocyte chemoattractant protein-1 (MCP-1): an overview. *J Interferon Cytokine Res* 2009; **29**: 313-326 [PMID: 19441883 DOI: 10.1089/jir.2008.0027]
70 **Singh S**, Anshita D, Ravichandiran V. MCP-1: Function, regulation, and involvement in disease. *Int Immunopharmacol* 2021; **101**: 107598 [PMID: 34233864 DOI: 10.1016/j.intimp.2021.107598]
71 **Martínez-Cerdeño V**, Noctor SC. Neural Progenitor Cell Terminology. *Front Neuroanat* 2018; **12**: 104 [PMID: 30574073 DOI: 10.3389/fnana.2018.00104]
72 **Zhang L**, Wang Y, Tang Y, Jiao Z, Xie C, Zhang H, Gu P, Wei X, Yang GY, Gu H, Zhang C. High MRI performance fluorescent mesoporous silica-coated magnetic nanoparticles for tracking neural progenitor cells in an ischemic mouse model. *Nanoscale* 2013; **5**: 4506-4516 [PMID: 23591936 DOI: 10.1039/c3nr00119a]
73 **Somaa FA**, Wang TY, Niclis JC, Bruggeman KF, Kauhausen JA, Guo H, McDougall S, Williams RJ, Nisbet DR, Thompson LH, Parish CL. Peptide-Based Scaffolds Support Human Cortical Progenitor Graft Integration to Reduce Atrophy and Promote Functional Repair in a Model of Stroke. *Cell Rep* 2017; **20**: 1964-1977 [PMID: 28834757 DOI: 10.1016/j.celrep.2017.07.069]
74 **Asahara T**, Murohara T, Sullivan A, Silver M, van der Zee R, Li T, Witzenbichler B, Schatteman G, Isner JM. Isolation of putative progenitor endothelial cells for angiogenesis. *Science* 1997; **275**: 964-967 [PMID: 9020076 DOI: 10.1126/science.275.5302.964]

75 **Kalka C**, Masuda H, Takahashi T, Kalka-Moll WM, Silver M, Kearney M, Li T, Isner JM, Asahara T. Transplantation of ex vivo expanded endothelial progenitor cells for therapeutic neovascularization. *Proc Natl Acad Sci U S A* 2000; **97**: 3422-3427 [PMID: 10725398 DOI: 10.1073/pnas.97.7.3422]

76 **Park SJ**, Moon SH, Lee HJ, Lim JJ, Kim JM, Seo J, Yoo JW, Kim OJ, Kang SW, Chung HM. A comparison of human cord blood- and embryonic stem cell-derived endothelial progenitor cells in the treatment of chronic wounds. *Biomaterials* 2013; **34**: 995-1003 [PMID: 23127335 DOI: 10.1016/j.biomaterials.2012.10.039]

77 **Navarro-Sobrino M**, Rosell A, Hernandez-Guillamon M, Penalba A, Ribó M, Alvarez-Sabín J, Montaner J. Mobilization, endothelial differentiation and functional capacity of endothelial progenitor cells after ischemic stroke. *Microvasc Res* 2010; **80**: 317-323 [PMID: 20594997 DOI: 10.1016/j.mvr.2010.05.008]

78 **Li Q**, Tang G, Xue S, He X, Miao P, Li Y, Wang J, Xiong L, Wang Y, Zhang C, Yang GY. Silica-coated superparamagnetic iron oxide nanoparticles targeting of EPCs in ischemic brain injury. *Biomaterials* 2013; **34**: 4982-4992 [PMID: 23566799 DOI: 10.1016/j.biomaterials.2013.03.030]

79 **Jana NR**, Earhart C, Ying JY. Synthesis of water-soluble and functionalized nanoparticles by silica coating. *Chem Mater* 2007; **19**: 5074-5082 [DOI: 10.1021/cm071368z]

80 **Wang C**, Lin G, Luan Y, Ding J, Li PC, Zhao Z, Qian C, Liu G, Ju S, Teng GJ. HIF-prolyl hydroxylase 2 silencing using siRNA delivered by MRI-visible nanoparticles improves therapy efficacy of transplanted EPCs for ischemic stroke. *Biomaterials* 2019; **197**: 229-243 [PMID: 30677555 DOI: 10.1016/j.biomaterials.2018.05.053]

81 **Giusti S**, Fiszer de Plazas S. Neuroprotection by hypoxic preconditioning involves upregulation of hypoxia-inducible factor-1 in a prenatal model of acute hypoxia. *J Neurosci Res* 2012; **90**: 468-478 [PMID: 21953610 DOI: 10.1002/jnr.22766]

82 **Payne SL**, Tuladhar A, Obermeyer JM, Varga BV, Teal CJ, Morshead CM, Nagy A, Shoichet MS. Initial cell maturity changes following transplantation in a hyaluronan-based hydrogel and impacts therapeutic success in the stroke-injured rodent brain. *Biomaterials* 2019; **192**: 309-322 [PMID: 30468998 DOI: 10.1016/j.biomaterials.2018.11.020]

83 **Ballios BG**, Cooke MJ, Donaldson L, Coles BL, Morshead CM, van der Kooy D, Shoichet MS. A Hyaluronan-Based Injectable Hydrogel Improves the Survival and Integration of Stem Cell Progeny following Transplantation. *Stem Cell Reports* 2015; **4**: 1031-1045 [PMID: 25981414 DOI: 10.1016/j.stemcr.2015.04.008]

84 **Ballios BG**, Cooke MJ, van der Kooy D, Shoichet MS. A hydrogel-based stem cell delivery system to treat retinal degenerative diseases. *Biomaterials* 2010; **31**: 2555-2564 [PMID: 20056272 DOI: 10.1016/j.biomaterials.2009.12.004]

85 **Führmann T**, Tam RY, Ballarin B, Coles B, Elliott Donaghue I, van der Kooy D, Nagy A, Tator CH, Morshead CM, Shoichet MS. Injectable hydrogel promotes early survival of induced pluripotent stem cell-derived oligodendrocytes and attenuates longterm teratoma formation in a spinal cord injury model. *Biomaterials* 2016; **83**: 23-36 [PMID: 26773663 DOI: 10.1016/j.biomaterials.2015.12.032]

86 **Fujioka T**, Kaneko N, Ajioka I, Nakaguchi K, Omata T, Ohba H, Fässler R, García-Verdugo JM, Sekiguchi K, Matsukawa N, Sawamoto K. β1 integrin signaling promotes neuronal migration along vascular scaffolds in the post-stroke brain. *EBioMedicine* 2017; **16**: 195-203 [PMID: 28153772 DOI: 10.1016/j.ebiom.2017.01.005]

Published by **Baishideng Publishing Group Inc**
7041 Koll Center Parkway, Suite 160, Pleasanton, CA 94566, USA
Telephone: +1-925-3991568
E-mail: bpgoffice@wjgnet.com
Help Desk: https://www.f6publishing.com/helpdesk
https://www.wjgnet.com